



Ana Maria Gomes Oliveira

Bachelor of Science in Biomedical Engineering

**Development of a Body-powered Hand
Prosthesis with Flexible Materials by Additive
Manufacturing**

Dissertation submitted in partial fulfillment
of the requirements for the degree of

Master of Science in
Biomedical Engineering

Adviser: Bruno Alexandre Rodrigues Simões Soares
Assistant Professor, NOVA University Lisbon

Co-adviser: Cláudia Regina Pereira Quaresma
Assistant Professor, NOVA University Lisbon



FACULDADE DE
CIÊNCIAS E TECNOLOGIA
UNIVERSIDADE NOVA DE LISBOA

September, 2021

Development of a Body-powered Hand Prosthesis with Flexible Materials by Additive Manufacturing

Copyright © Ana Maria Gomes Oliveira, NOVA School of Science and Technology, NOVA University Lisbon.

The NOVA School of Science and Technology and the NOVA University Lisbon have the right, perpetual and without geographical boundaries, to file and publish this dissertation through printed copies reproduced on paper or on digital form, or by any other means known or that may be invented, and to disseminate through scientific repositories and admit its copying and distribution for non-commercial, educational or research purposes, as long as credit is given to the author and editor.

This document was created using the (pdf/Xe/Lua)LaTeX processor, based on the [NOVAtesis](#) template, developed at the [Dep. Informática of FCT-NOVA](#) by João M. Lourenço. [1]

Para os meus.

ACKNOWLEDGEMENTS

Sempre ouvi a frase cliché que diz que sozinhos vamos mais rápido, mas que juntos de alguém vamos mais longe. Quero acreditar que ao longo destes meses fui mais longe. No entanto, se o fui, o mérito não é só meu.

Em primeiro lugar quero agradecer ao Professor Bruno Soares, com o qual tive o enorme prazer de poder trabalhar durante estes longos meses e sem o qual este trabalho não seria possível. Quero agradecer o conhecimento transmitido, os conselhos, os telefonemas, e-mails e mensagens fora de horas, mas sobretudo pela paciência para aturar esta aluna picuinhas de Engenharia Biomédica. Ainda bem que há alguém que goste tanto desta área como eu!

À Professora Cláudia Quaresma quero agradecer a grande oportunidade que foi poder trabalhar nesta área que tanto me cativa. A si devo o entusiasmo, a palavra amiga e os avisos para não me esquecer de nada. O meu sincero obrigada!

À D. Sandra e ao Eduardo devo o mundo, pois foram essenciais em todo o processo. Obrigada por toda a amabilidade, hospitalidade e disponibilidade. As palavras são poucas para descrever a minha gratidão para convosco.

À Patient Innovation, que de certa forma tornou este estudo possível. Obrigada à Catarina por toda a ajuda e disponibilidade. Obrigada à Salomé por me ter criado este bichinho há quatro anos atrás, pela motivação e pelo sermão de duas horas no estágio. Acredito que sem ele não me teria tornado na quase-engenheira que sou hoje.

Aos meus. À grande rede de apoio que fez de mim aquilo que sou hoje. Aos meus pais, que se esforçam dia após dia para me proporcionar o melhor deste mundo. Espero não vos ter desiludido e que tenham orgulho na filha que criaram. Obrigada por tudo! Estarei para sempre em dívida para convosco. Ao meu mano, que mesmo sem saber, me inspira dia após dia, desde o dia zero, só por existir. Mesmo a quilómetros de distância foste, és e serás sempre essencial para o meu crescimento. Obrigada pela palavra amiga no momento certo.

Ao Diogo Tecelão por caminhar a meu lado ao longo destes últimos anos. Obrigada por acreditares em mim, por ti e por mim. Obrigada pelos ensinamentos, pelos conselhos, pelo carinho e até pelos ralhetes, mas sobretudo pelos abraços certos nos momentos

certos.

À Francisca, a minha psicóloga de serviço, por nunca me largar e por nunca me deixar cair. Não teria chegado aqui sem ti.

À família que Biomédica me deu e que tornou todo este percurso ainda mais especial. Sem vocês, o fim não seria tão incrível.

Podia continuar, mas uma dissertação não chegaria para agradecer a todos aqueles que me querem bem, que sempre aqui estiveram, cada um à sua maneira e que sei que continuarão a estar. Se sou o que sou hoje, a vocês o devo. Convosco, cheguei mais longe. Obrigada.

“... the real way to get happiness is by giving out happiness to other people.” (Robert Baden-Powell)

ABSTRACT

The research on prostheses made by [Additive Manufacturing \(AM\)](#) has been increasing, as they solve some of the issues of the most common prostheses. However, despite their growth, these prostheses have a high rejection rate, especially in children, due to their low level of anthropomorphism. The main goal of this study was to develop an aesthetically appealing [three-dimensional \(3D\)](#) printed body-powered prosthesis for a four-year-old child with a transverse metacarpal total deficiency.

The development of the prosthesis started through an assessment of the anatomical features of the extremities of patient's both upper limbs, performed with body casting, simple measurements and 3D-scanning of the cast. The whole prosthesis was designed using the *Fusion 360 CAD* software and produced using *The Original Prusa i3 MK3S* and [polylactic acid \(PLA\)](#) and *Filaflex* filaments. The prosthesis was designed through an iterative process, whereby the prosthesis' appearance and functionality were optimised. During the design stages, several design configurations and printing settings were tested. Some printed models were evaluated using pull tests.

The developed prosthesis possessed a high level of anthropomorphism, consisting of a solution that is quite similar to a human hand. Despite all the generated concepts focused on increasing the performance of 3D-printed body-powered prostheses, the developed prosthesis presented a low functionality. However, the device was cheaper and lighter than the existing 3D-printed body-powered prostheses. Moreover, the performed tests revealed that a better printing quality implied higher forces to flex the prosthesis and consequently, lower functionality.

The final prototype was presented to the child and his family, which provided their feedback using the *System Usability Survey* and a custom-made assessment questionnaire. The resulting scores classified the device as "Excellent". Despite being promising, further work is still required for this device to be used by children with upper limb defects.

Keywords: Additive Manufacturing, upper limb prosthesis, body-powered prosthesis, flexible materials

RESUMO

A investigação em próteses feitas através de Manufatura Aditiva tem aumentado, uma vez que as mesmas solucionam alguns dos problemas das próteses mais comuns. Porém, apesar deste crescimento, estas próteses apresentam uma elevada taxa de rejeição, principalmente em crianças, devido ao seu baixo nível de antropomorfismo. O objetivo principal deste estudo consistiu no desenvolvimento de uma prótese *body-powered* esteticamente apelativa, impressa a três dimensões, para uma criança de quatro anos com uma deficiência total transversal do metacarpo.

O desenvolvimento da prótese começou com uma avaliação das características anatómicas das extremidades de ambos os membros superiores do paciente, realizada através de extração de moldes, medições simples e *scanning* tridimensional dos moldes. Toda a prótese foi desenhada com o *software Fusion 360 CAD* e produzida através da impressora *The Original Prusa i3 MK3S* com filamentos de ácido polilático (PLA) e *Filaflex*. A prótese foi desenvolvida através de um processo iterativo, em que a aparência e a funcionalidade da prótese foram otimizadas. Durante as fases de design, foram testadas várias configurações de design e impressão. Alguns modelos impressos foram avaliados através de testes de tração.

A prótese desenvolvida possui um elevado nível de antropomorfismo, consistindo numa solução bastante semelhante a uma mão humana. Apesar de todos os conceitos gerados com o objetivo de aumentar o desempenho das próteses *body-powered* impressas a três dimensões, a prótese desenvolvida apresentou uma baixa funcionalidade. No entanto, o dispositivo é mais barato e mais leve do que outras próteses *body-powered* impressas a três dimensões. Além disso, os testes realizados revelaram que uma melhor qualidade de impressão implica maiores forças para flexionar a prótese e, conseqüentemente, uma menor funcionalidade.

O protótipo final foi apresentado à criança e sua família, os quais forneceram *feedback* através do questionário de usabilidade "*System Usability Survey*" e de um questionário personalizado. As pontuações resultantes classificaram o dispositivo como "Excelente". Apesar de promissor, é necessário trabalho futuro para que este dispositivo seja utilizado por crianças com deficiências dos membros superiores.

Palavras-chave: Manufactura Aditiva, prótese do membro superior, prótese *body-powered*, materiais flexíveis

CONTENTS

List of Figures	xix
List of Tables	xxiii
Abbreviations	xxv
1 Introduction	1
1.1 Study goals	2
1.2 Document Outline	3
2 Clinical Background	5
2.1 Upper Limb Deficiencies	5
2.1.1 Acquired limb deficiencies	5
2.1.2 Congenital limb deficiencies	6
2.1.3 Upper limb deficiencies classification	6
2.2 Upper Limb Prostheses	7
2.2.1 Cosmetic prostheses	8
2.2.2 Body-powered prostheses	8
2.2.3 Electronic prostheses	10
2.3 Upper Limb Prosthetic Rehabilitation	11
2.3.1 Prosthetic rehabilitation of acquired deficiencies	11
2.3.2 Prosthetic rehabilitation of congenital deficiencies	12
2.3.3 User's needs	13
3 Additive Manufacturing	17
3.1 Additive Manufacturing Methods	18
3.2 Fused Deposition Modeling	18
3.2.1 Working principles of Fused Deposition Modeling	20
3.2.2 Prostheses made with Fused Deposition Modeling	21
3.3 Design for Additive Manufacturing Principles	22

4	Present and Future Trends	25
4.1	Overall technological progresses	25
4.2	3D-printed prostheses	26
5	Concept Development	33
5.1	Introduction to the Clinical Case	33
5.2	Methodology	34
5.2.1	Anatomical and functional features assessment	34
5.2.2	3D scanning	36
5.2.3	Design and printing	37
5.2.4	Tuning of the printing parameters	46
5.2.5	Prosthesis assembly	50
5.2.6	Prosthesis evaluation	59
6	Results and Discussion	61
6.1	Anatomical and Functional Features Assessment	61
6.1.1	Measurements	62
6.1.2	Body casting	63
6.2	3D Scanning	65
6.3	Prosthesis Design	66
6.3.1	Fingers design	67
6.3.2	Metacarpal region design	84
6.3.3	Wrist design	95
6.4	Tuning of the Printing Parameters	96
6.4.1	First printing approaches	97
6.4.2	Printing tests	100
6.4.3	Printing overview	106
6.5	Prosthesis Assembly	107
6.6	Prosthesis Evaluation	108
6.6.1	Prosthesis characteristics	113
6.6.2	System Usability Scale assessment	114
7	Conclusion	115
7.1	Summary of the Study Achievements	115
7.2	Future Work	118
	References	121
	Appendices	
A	Thorough description of Additive Manufacturing Methods	131
B	Additional details on the Concept Development	133

C Documentation of the Anatomical and Functional Features Assessment	135
D Phalanges Measurements	149
E Printing Parameters Tests	153
F Pull Tests	157
G Prostheses Costs	171
H System Usability Scale	173

LIST OF FIGURES

2.1	Upper limb congenital defects classification	7
2.2	©Ottobock’s custom silicone hand prosthesis	8
2.3	<i>X-Finger</i> body-powered prosthesis	10
2.4	<i>bebionic hand</i> prosthesis	11
3.1	Additive Manufacturing techniques	19
3.2	Anatomy of <i>The Original Prusa i3 MK3S+</i>	20
4.1	<i>Raptor Reloaded</i> prosthesis	27
4.2	<i>Phoenix Hand v2</i> prosthesis	28
4.3	<i>Nazree’s Prosthetic Hand</i>	28
4.4	V. Lopes’ cosmetic hand prosthesis	29
4.5	Design details of the components of the body-powered hand prosthesis developed by F. Pinheiro	30
4.6	F. Pinheiro’s body-powered prosthesis	30
4.7	Examples of other prostheses with components made of flexible materials	31
5.1	Methodology flowchart	35
5.2	The <i>Ein Scan-SE</i> by SHINNING 3D®	36
5.3	Modification process of the design file	37
5.4	Representation of the extension and flexion angles of the interphalangeal joints	38
5.5	Design of the proximal interphalangeal phalanx joint of the index finger	39
5.6	Inner mechanisms of the index finger	40
5.7	Fitting mechanism design	41
5.8	Left limb extremity modification process	42
5.9	Metacarpal region design	43
5.10	Design of the metacarpal region modifier	44
5.11	Thumb’s design	44
5.12	Components from <i>e-NABLE</i> ’s prostheses used in the designed prosthesis	45
5.13	Gauntlet modification process	45

LIST OF FIGURES

5.14	Tested printing settings of <i>PrusaSlicer</i> software	47
5.15	Tested filament settings of <i>PrusaSlicer</i> software	48
5.16	Tested printer settings of <i>PrusaSlicer</i> software	49
5.17	Pull tests setup	50
5.18	Prosthesis' components and needed tools for its assembly	51
5.19	Marks for moulding the gauntlet in hot water	52
5.20	Stages of the placement of the self-adhesive foam	52
5.21	Connection between the gauntlet and the metacarpal region structure	53
5.22	Assembly of the tensioner system	53
5.23	Assembly of the fingers	54
5.24	Insertion of the PET-G rings	55
5.25	Dimensions of the Grosgrain ribbons and Velcro tape	55
5.26	Assembly of the straps	56
5.27	Third prosthesis' components and needed tools for its assembly	56
5.28	Design of the metacarpal region and thermo pins of the third prosthesis	57
5.29	Fitting of the pins in the metacarpal region of the third prosthesis	57
5.30	Connection of the fingers to the metacarpal region	58
5.31	Assembly of the tensioning system of the third prosthesis	59
6.1	Results of the positions' reproduction	63
6.2	Body casting failures	64
6.3	Upper limb's extremities of the child replicas made with plaster	64
6.4	Comparison between the plaster replicas and <i>.stl</i> files resulting from the 3D scanning procedure	66
6.5	Number of faces reduction process	67
6.6	First prototypes of the index finger	68
6.7	External design of the second prototypes	69
6.8	Inner design of the second prototypes	70
6.9	Comparison between the inner mechanisms of the first and second prototypes	71
6.10	Location of the pausing layers of the start-stop method	72
6.11	Parallelism between flexing an index model with smaller chambers and bigger chambers	73
6.12	Flexion of the third prototype	74
6.13	Slicing of the of the original second prototype and its replica scaled to 140%	74
6.14	Comparison between the second and fourth prototypes	75
6.15	Design of the fifth prototype	76
6.16	Comparison between the fifth and sixth prototypes	77
6.17	Inner design of the seventh prototype	78
6.18	Results of the pull tests used to select the opening angles of the chambers	79
6.19	Design resulting from removing the phalanges structures	79
6.20	Flexing of the finger prototype with no phalanges	80

6.21 Comparison of the inner design of the seventh prototypes and the models with thicker chambers' walls	80
6.22 Printing results of the finger prototypes with thinner chambers' external walls	81
6.23 First prototype of the fitting mechanism	82
6.24 Second prototype of the fitting mechanism	83
6.25 Test cube to simulate the fitting hole of the metacarpal region	83
6.26 First draft of the metacarpal region structure	85
6.27 Design of the first prototype of the metacarpal region	86
6.28 Flexion of the first prototype of the metacarpal region.	86
6.29 External design of the second and third prototypes	87
6.30 Inner design of the second and third prototypes	88
6.31 Flexion of the second prototype of the metacarpal region.	88
6.32 Flexion of the third prototype of the metacarpal region.	89
6.33 Design of the fourth prototype of the metacarpal region	90
6.34 Printing results of the fourth prototype of the metacarpal region	91
6.35 Comparison between the external design of the fourth and fifth prototypes of the metacarpal region	92
6.36 Printing results of the fifth prototype of the metacarpal region	93
6.37 Printing results of the sixth prototype of the metacarpal region	94
6.38 Results of the first printing approaches	97
6.39 Testing of the start-stop method	99
6.40 Printing results of the finger models printed with the start-stop method . .	99
6.41 Results of the pull tests of the fingers printed by modifying the set A of printing parameters	101
6.42 Results of the pull tests of the fingers printed by modifying the set B of printing parameters	102
6.43 Results of the pull tests of the fingers printed by modifying the printing speed of the set B	103
6.44 Fingers printed horizontally	104
6.45 Pull tests results	105
6.46 Results of the pull tests of the fingers printed with <i>Filaflex 70A</i>	106
6.47 First developed prosthesis	109
6.48 Child wearing the prosthesis	110
6.49 Second developed prosthesis	112
6.50 Third developed prosthesis	112
6.51 Flexion of the third developed prosthesis	113
B.1 Extended methodology flowchart	134
D.1 Antero-posterior X-ray of a human hand	150

LIST OF TABLES

2.1	Mean rejection rates of the three types of prostheses	14
4.1	Advantages and disadvantages of 3D-printed upper limb prostheses	26
5.1	Interphalangeal joints' extension and flexion angles for each finger	38
5.2	Phalanges' design values	41
6.1	Results of the measures of both upper limbs of the child	62
6.2	<i>Phoenix Hand v2</i> Sizing Guide	96
6.3	<i>Raptor Reloaded</i> Sizing Guide	96
6.4	Materials cost, mass and total printing time of each developed prosthesis	113
D.1	Phalanges measurements	151
E.1	Print settings of the main printing tests	154
E.2	Printer settings of the main printing tests	155
E.3	Filament settings of the main printing tests	156
F.1	Pull tests results of the model with 55° chambers	166
F.2	Pull tests results of the model with 60° chambers	166
F.3	Pull tests results of the model with 65° chambers	166
F.4	Pull tests results of the model printed with the set A parameters	167
F.5	Pull tests results of the model printed with the set A1 parameters	167
F.6	Pull tests results of the model printed with the set A2 parameters	167
F.7	Pull tests results of the model printed with the set B parameters	168
F.8	Pull tests results of the model printed with the set B1 parameters	168
F.9	Pull tests results of the model printed with the set B2 parameters	168
F.10	Pull tests results of the model printed with the set B3 parameters	169
F.11	Pull tests results of the model printed with the set B4 parameters	169
F.12	Pull tests results of the model printed with the set B5 parameters	169
F.13	Pull tests results of the model printed with the set B6 parameters	170

LIST OF TABLES

F.14	Pull tests results of the model printed with <i>Filaflex</i> 70A and the set A parameters	170
F.15	Pull tests results of the model printed with <i>Filaflex</i> 70A and the set B parameters	170
G.1	Discriminated cost of the first and second prostheses	171
G.2	Discriminated cost of the third prosthesis	172

ABBREVIATIONS

2D	two-dimensional
3D	three-dimensional
ABS	acrylonitrile butadiene styrene
ACPOC	Association of Children’s Prosthetic and Orthotic Clinics
AM	Additive Manufacturing
CAD	computer-aided design
CT	computed tomography
DfAM	Design for Additive Manufacturing
DIP	distal interphalangeal
EM	extrusion multiplier
FDM	Fused Deposition Modeling
ISPO	International Society for Prosthetics and Orthotics
LMICs	lower-middle income countries
MVP	minimum viable product
PC	polycarbonate
PET-G	polyethylene terephthalate glycol
PIP	proximal interphalangeal
PLA	polylactic acid

ABBREVIATIONS

SD	standard deviation
STL	Standard Tessellation Language
SUS	System Usability Scale
TPE	thermoplastic elastomer
TPU	thermoplastic polyurethane
UV	ultraviolet
VC	voluntary closing
VO	voluntary opening

INTRODUCTION

Hands are one of the most important anatomical structures in the human body, as they are used in most day-to-day activities. Hands allow the identification of objects through the sense of touch, extracting a multitude of information such as shape, size, weight and texture, among others. The upper limb extremity is responsible for activities like grasping, manipulating objects and even communicating through gestures [2–4]. Thus, the absence of this anatomical structure, either partial or complete, decreases the quality of life of patients, since it impairs their level of autonomy and limits their ability to perform a wide range of activities [5]. Additionally, this condition may also have a huge psychological impact [6].

Prosthetic rehabilitation can help to reestablish function and consequently improve the quality of life of upper limb amputees [7]. However, as of 2016, prosthetic innovation was not a very appealing field due to the high development costs that contrasted with a low market demand. As such, more sophisticated prostheses were very expensive and unaffordable to most subjects with prosthetic needs. Nevertheless, the growth of AM techniques has opened doors to the prosthetic field as it can be used to develop functional low-cost prostheses [8].

The *e-NABLE* project is an online worldwide community of volunteers who collaborate in the development of low-cost body-powered upper limb prosthetic devices for children and adults in need. These prostheses are developed by a multidisciplinary team composed of engineers, 3D printing enthusiasts, occupational therapists, university professors and students, designers, families, artists and teachers from all over the world. Anyone can have access to these devices as they are free and open-source [9, 10]. However, biocompatibility, durability, risk of injury and the suitability to the user's daily activities are responsibility of the user since there is no medical control of these devices [8].

Despite the huge growth of 3D-printed body-powered upper limb prostheses, especially through the efforts of the *e-NABLE* community, these devices seem to have a high rejection rate, especially by children. These prostheses are similar to hero hands, which was expected to improve the acceptance rates for children. However, this similarity seems

to contribute to their rejection after a few hours, as many children consider them toys. Adults, on the other hand, do not find this type of prostheses very appealing due to its childish appearance, which makes them commonly choose to build their prostheses using a skin-coloured filament [10]. Moreover, the stiffness of these prostheses also promotes rejection. Therefore, it is important to invest in more flexible and realistic prostheses that also ensure the other essential features such as comfort, low-cost and optimised functionality.

Although some prostheses with flexible materials have already been proposed, their function is mainly cosmetic. Functional prostheses built with flexible materials only use this type of materials in some specific parts. Moreover, there is no complete body-powered solution that combines stiff and flexible materials. Therefore, there is a need for developing a body-powered prosthesis that take advantage of the combination of these materials in order to ensure comfort as well as all the other user's needs.

1.1 Study goals

The main goal of this study is to design a 3D-printed body-powered upper limb prosthesis with flexible materials and improved cosmetic appearance. The hypothesis of this study is that a more realistic, functional and tailored hand prosthesis can be developed by using Additive Manufacturing and flexible materials. Replacing the stiff material, that composes the common 3D-printed prostheses, with flexible materials, makes these devices more comfortable. In addition, by giving them a more natural shape, these devices become more aesthetically appealing, without compromising other features such as functionality, lightweightness, ease of repair and low-cost.

For this purpose, it was necessary to perform a state of the art analysis on the existent prostheses and to determine the optimal combination of materials. The identification of the user's needs was crucial to determine prosthesis specifications and therefore create some concepts in order to identify the best model to develop. Concerning concepts generation and selection, it was desired a high level of customisation, especially regarding to the size of the printed hand when compared to the sound hand. Establishing sensory feedback was also a concern.

As a result of the created concepts, several prototypes for testing and concept validation were designed, according to Product Design and Development methodology [11].

This study is the first developing a 3D-printed body-powered hand prosthesis that presents a high level of anthropomorphism and customisation. By taking advantage of the properties of flexible materials, it is possible to mimic the human hands features and design a more comfortable and appealing solution for the user, while preserving other essential features such as low-cost and lightweight. In addition, this study presents a thorough analysis of the challenges faced while printing with flexible materials, which is specially important since the prosthesis' functionality depends on the materials behaviour.

1.2 Document Outline

The present study is structured in seven chapters:

- Chapter 1 presents the motivation behind this study, as well as its goals.
- Chapter 2 presents the background regarding the prosthetic field and is divided in three parts. The first part focuses on the etiology of upper limb lesions and presents the standard classification methodology for these deficiencies. The second part presents the types of prostheses and the third part describes the prosthetic rehabilitation process with focus on the patients' needs.
- Chapter 3 describes the progresses achieved in the prosthetic field with special focus on Additive Manufacturing, 3D-printed devices with flexible materials.
- Chapter 4 presents the state of the art on prostheses developed with Additive Manufacturing, introducing a parallelism between the progress of technology and medicine. It also presents the literature review of the most relevant 3D-printed body-powered prostheses that use flexible materials and are aesthetically enhanced.
- Chapter 5 presents the clinical case in which this study was based on, as well the methodology used to develop a customised 3D-printed body-powered prosthesis with Additive Manufacturing.
- Chapter 6 presents and discusses the results of the development process of this study's prosthesis, in which several prototypes and created concepts are analysed. This chapter also presents suggestions on further improvements of the developed prosthesis.
- Chapter 7 contains the final considerations of the developed work, namely the major conclusions and suggestions for future work.

CLINICAL BACKGROUND

This chapter presents the background on prosthetics. The first section introduces the etiology of upper limb lesions as well as the standard classification methodology for these deficiencies. In the second section, the three types of prostheses are explored together with currently available examples. Finally, the last section describes the prosthetic rehabilitation process with focus on the patients' needs.

2.1 Upper Limb Deficiencies

Worldwide, it is estimated that in 10 000 people, 4 to 5 suffer from upper limb deficiencies [12]. An upper limb deficiency may have two possible origins: acquired or congenital. Congenital deficiencies primarily affect children, especially up to 10 years old. On the other hand, acquired deficiencies are more frequent in individuals older than 10 years old [13, 14]. Both acquired and congenital deficiencies are an overwhelming situation for the individual and its family [15].

2.1.1 Acquired limb deficiencies

Acquired limb deficiencies, also known as amputations [16], are limb absences that occur during a person's lifetime due to trauma amputation surgeries caused by trauma or disease [17].

About 90% of acquired deficiencies involve only one limb and 60% of these cases correspond to lower limb. About 70% to 80% of the cases correspond to trauma. The main causes are usually road and work injuries, natural disasters or consequences of violence. Accidents with fireworks are the most common cause of children's amputations. The remaining cases result from diseases such as tumors, infections or vascular problems. However, the causes of this type of deficiency may vary from country to country [14, 16, 18]. For example, in [lower-middle income countries \(LMICs\)](#), besides work injuries, amputations are mostly caused by war and diseases like diabetes and polio [19].

2.1.2 Congenital limb deficiencies

A congenital deficiency is an abnormality which occurs during the gestation period and is characterized as the absence of bones or hypoplasia, which must be significant enough in appearance to be identified by the medical team in the first five days of child's life. These deficiencies vary greatly in etiology and anatomic characteristics [20].

Congenital limb malformations occur between the third and eighth gestation week. After this period of embryogenesis, all the limb structures should be present [21, 22]. Upper limb congenital malformations are twice as frequent than lower limb deficiencies [21, 23]. These deficiencies may have origin on primary structural defects due to localized development failures or on later changes during normal development. Congenital limb anomalies may be isolated or part of a malformation syndrome that affects different organ systems with several congenital defects [22].

The [Association of Children's Prosthetic and Orthotic Clinics \(ACPOC\)](#) estimates that 60% of children's limb deficiencies are from congenital causes such as genetics, vascular problems and teratogenic agents [21]. However, little is known about the precise etiology of congenital upper limb defects. Indeed, in 60% to 70% of the cases, the causes of congenital limb deficiencies are unknown [14]. Regarding genetics, these defects may be autosomal recessive, gender-linked or simply sporadic and non-hereditary. Teratogenic agents like thalidomide, misoprostol, ergotamine or retinoic acid may be responsible for these sporadic errors during embryogenesis. Vascular disruption could be caused by chorionic villous sampling, dilation, curettage or trauma to the abdomen and placenta. Vascular disruption can result in amniotic band syndrome due to hypoxia, followed by endothelial cell damage, hemorrhage, tissue loss and finally reperfusion. Despite the great advances in prenatal care and technology, currently it is not easy to detect these defects through ultrasound scans [21–24].

2.1.3 Upper limb deficiencies classification

According to the [International Society for Prosthetics and Orthotics \(ISPO\)](#), congenital upper limb defects may be classified as transverse or longitudinal [25].

In transverse deformities the limb has a normal development up to the existing skeletal structures. These structures can be proximal structures such as nerves, arteries and tendons and there is the possibility of existing digital buds. The classification of this type of lesions is given by the name of the segment in which the limb finishes followed by the indication of the lesion's level [22, 25].

In longitudinal deformities, there is a deficiency or absence of one or more structures along the limb axis. In these cases, there is the possibility of existing normal distal elements. In order to classify these lesions, it is referred the name of the compromised bones, in proximo-distal order. Then, it is stated the absence level of each bone, whether it is total or partial. In partial cases, the absence fraction should be referred. When referring to metacarpal structures or phalanges, the digit number should be indicated from the

radial side. Finally, to refer to metacarpal structures and its corresponding phalanges, the term “Ray” may be used [22, 25].

The most common upper limb congenital deficiency is the below elbow unilateral transverse deformity. This condition is more predominant in females and in the left limb [16]. Figure 2.1 schematizes the description of upper limb’s longitudinal and transverse deformities.

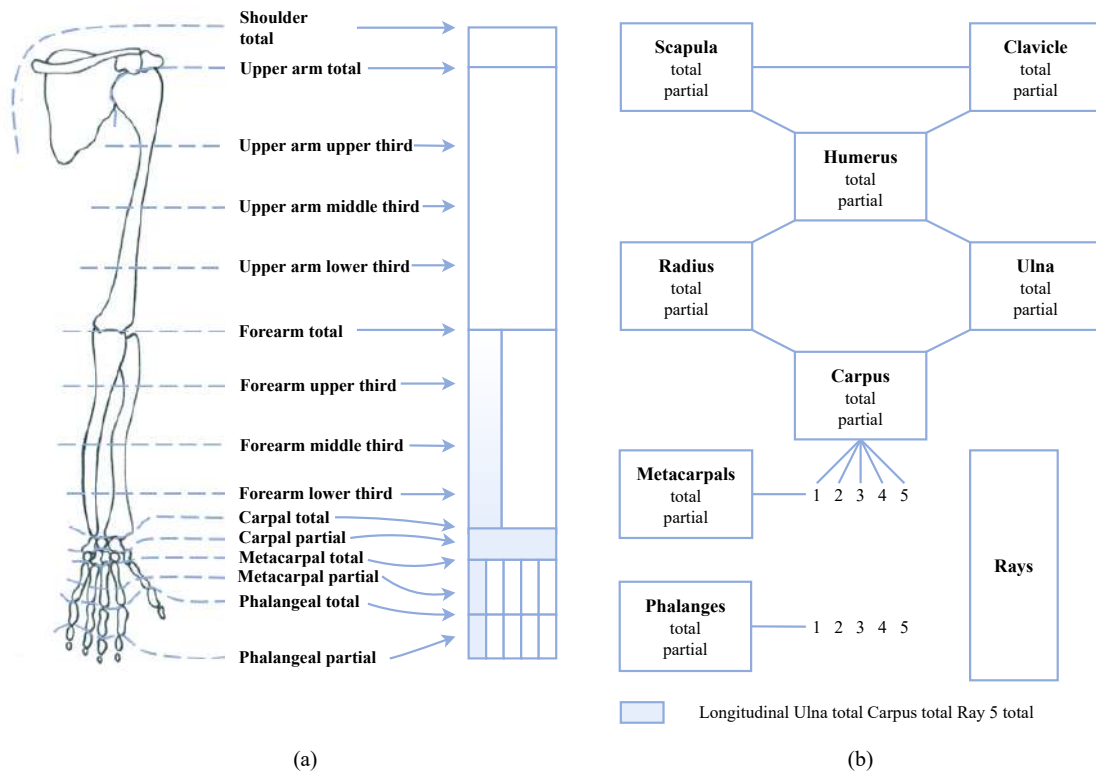


Figure 2.1: Upper limb congenital defects classification according to ISPO: (a) description of transverse deficiencies; (b) description of longitudinal deficiencies. Adapted from H. Day [25].

2.2 Upper Limb Prostheses

A prosthesis is an artificial body-part that helps disabled people living a normal life by replacing the function of the missing part [26]. The main goal of an upper limb prosthetic device is to reestablish the functional capacity of the lost extremity in a natural, comfortable and aesthetical way for the user, resulting in a psycho-spiritual sense of wholeness [19, 27].

There are three main types of prostheses: cosmetic, body-powered and electronic [28]. Electronic and body-powered ones are active prostheses, while cosmetic ones are passive prostheses. In active prostheses, the grasping force is controlled by an internal mechanism. Passive prostheses may be divided into static prostheses and adjustable prostheses.

While static prostheses do not move at all, adjustable prostheses contain mechanisms to control the grasping force externally through the sound hand or by pushing the prostheses against the objects [29].

2.2.1 Cosmetic prostheses

Cosmetic prostheses are non-functional prosthetic devices developed solely for appearance purposes. These are usually skin coloured prostheses, shaped to match the unaffected arm. This type of prostheses is usually lighter as they don't have additional components and they can also assist the sound arm in bimanual activities [18, 28].

Passive prostheses have improved over time [30]. However, the current existing prostheses seem to have not evolved as much as active prostheses [29]. Nevertheless, cosmetic prostheses that have a high realistic appearance can cost from 3000 to 5000 \$ [30, 31]. Companies like ©Ottobock [32] have several solutions for those who search for this and other types of prostheses. Examples of ©Ottobock's cosmetic solutions include custom silicone prostheses for hand or fingers replacement, passive arm prostheses and even silicone covers for arms prostheses. All these devices can be highly customised by skin colour and shape definition and include other details such as freckles, veins and even hair. Thanks to their realistic designs, these devices are hardly noticed by others, allowing the patients to feel more confident and comfortable with their prostheses. Figure 2.2 shows a custom silicone hand prosthesis for an adult [33].



Figure 2.2: ©Ottobock's custom silicone hand prosthesis [34].

2.2.2 Body-powered prostheses

Body-powered upper limb prostheses are functional devices composed by an active hand that opens and closes by operating cables through body movements [28]. The cable control system uses the flexion of the remaining limb to generate forces that enable the movement of the prosthesis' joints. However, the generated forces have only one direction, allowing for a single degree of freedom and limiting the user to voluntarily close or open the prosthetic hand [19, 35]. The increasing tension in the cables allows the prosthetic hand to close or open. When the tension is released, the prosthetic hand returns to its default state [36]. Commercial body-powered prostheses can cost about 4,000 to 20,000\$, depending on the complexity of the controlling system [10, 37, 38].

There is a large diversity of hand replacement tools, known as terminal devices, that can be changed depending on user's daily activities. Terminal devices offer improved accuracy, functionality and extended physiological perception. These prosthetic components provide an efficient interaction between the user and the environment by reducing user's mental and physical effort that is required while using body-powered prostheses. These accessories can be tailored according the patient's daily tasks [35, 39]. Depending on the task, the user may prefer a **voluntary opening (VO)** or a **voluntary closing (VC)** terminal device, or one that can switch between the two modes of operation [35].

Voluntary opening terminal devices are the most widely used. This operating mode allows the user to hold the object without sustaining the force during the task. Once the object is grasped, there is no need to exert more force and the user can relax. The grasp force is determined by the tension of a spring, which is unique and chosen according to the user's daily activities. However, the spring force may or may be not enough to perform a certain task. Furthermore, the user must overcome the spring force in each performed task and sometimes spend more energy than the necessary. To avoid these limitations, some VO terminal devices allow to adjust the spring tension but only over a limited range [35, 36].

In voluntary closing terminal devices, the grasping force is generated by the user. Therefore, the exerted force is only the necessary to perform the user's specific tasks, but the user has to exert it during the whole task, which can lead to fatigue. However, there are some VC devices that enable to hold the objects without exerting force during the task's performance due to an incorporated clutch system. Even still, the clutch needs to be disengaged at the end of the task, which implies an additional action, and often wears out before the prehension [35, 36]. These devices are more suitable for children and are very important for the improvement of their gross motor development [38].

Some terminal devices provide both modes: VO and VC. The transitioning between the two modes can be done over the range of cable excursion or through a switch system [35, 36].

Figure 2.3 shows the *X-Finger*, a body-powered prosthesis for patients with partial finger amputations developed by Didrick Medical. It is a customisable prosthesis that enables the flexion and extension of the prosthetic finger through the movement of the residual fingers. When the residual finger do not exist, the movement can be obtained using the hand. The device is held around the wrist with a strap similar to a watch and is composed by stainless steel and plastic parts in the fingertips, covered by a soft thermoplastic skin. The *X-Finger* has several versions and can replace up to four fingers. The replacing fingers move as quickly as the prior fingers and enable restoring the dexterity of the patient. Due to its considerable strength, the *X-finger* has been used namely by militars, machinists, musicians and doctors [39–41].



Figure 2.3: *X-Finger*, a body-powered prosthesis for partial finger amputations [41].

2.2.3 Electronic prostheses

Electronic prostheses are functional prosthetic devices composed by an external power source that can cost from 25.000 to 75.000 \$. The prostheses' movement is achieved by a electric motor which is controlled by a microcontroller, which can be activated through a switch or through electromiography [10, 14, 19, 37]. Prostheses controlled by electromiographic signals are called myoelectric prostheses.

Myoelectric prostheses monitor muscle activity through electrodes placed on skin of the residual limb, near agonist and antagonist muscles. This signal is read by a transducer and amplified, leading to hand opening and closing. The success of these prostheses depends on careful evaluation, patient mobility, accurate fitting and proper training [28, 42]. The level of lesion is also important as it necessary enough muscle bulk to generate a readable signal [22].

When there are few myoelectric accesses, it is possible to use a hybrid device that combines myoelectric activity with a switch control. Some myoelectric prostheses enable the speed controlling, by varying the contraction force or the degree of movement [39]. This is called servo control. In general, electronic prostheses are typically used by adolescents and adults. Nevertheless, microelectronics has allowed the use of these prostheses by younger children [15].

©OttoBock company [32] has also developed myoelectric upper limb devices, such as *bebionic hand*, displayed in Figure 2.4. This prosthesis has fourteen different grip patterns and hand positions that allow users to perform their daily tasks. Each finger of the *bebionic hand* moves individually which allows the hand to have a precise, natural and coordinated movement. Therefore, the *bebionic hand* is a comfortable and intuitive device which restores the user's confidence. This device is available in three different sizes and has multiple wrist options that can change according to the user's requirements [43].



Figure 2.4: *bebionic hand* prosthesis by ©OttoBock [43].

2.3 Upper Limb Prosthetic Rehabilitation

The absence of the upper limb is more life-changing than losing a lower limb and involves a more challenging adaptation. Therefore, proper prosthetic prescription and rehabilitation has to be done in order to improve the lives of those who suffer from this condition [18, 39]. The rehabilitation process aims to help patients restoring their functionality in the daily activities by teaching them how to use their prostheses [4, 28]. The success of this process in patients with upper limb defects is reliant on many factors. The rehabilitation team plays an important role in this process as some of these factors are under their control [39]. However, K. Soyer *et al.* performed a systematic literature research that concludes that prosthetic rehabilitation of the upper limb amputees has shown itself to be promising [4].

2.3.1 Prosthetic rehabilitation of acquired deficiencies

For people with acquired deficiencies, it is recommended early prosthetic fitting and post-traumatic counselling sessions [18]. The prosthetic fitting and training must begin within a month after the amputation for a higher chance of success. However, residual limb conditions such as the presence of edema or limb sensitivity and patient's psychological status may influence this time-frame [19, 39].

Besides prosthetic prescription and maintenance, upper limb rehabilitation also deals with phantom pain, skin problems in the stump area and vocational problems, by advising and identifying a possible employment. Phantom pain is only reported by people with acquired amputations and is usually worse in the first year, improving with time. When the amputation is planned, rehabilitation may prepare and help these people to understand what they will experience after the amputation [28].

Regarding psychological impact in amputees, upper limb loss may be more devastating in terms of body-image, social integration and post-traumatic stress disorder. Although this situation does not imply mobility difficulties, it is difficult to disguise with clothing. The absence of the dominant hand leads is even more crushing due to the necessity to relearn the simpler daily tasks. In this case, therapists should be careful with these issues and give the necessary support. Peer support with someone that experiences the same conditions may be helpful. Personal factors also influence the way amputees lead with their condition [28].

2.3.2 Prosthetic rehabilitation of congenital deficiencies

For children with congenital unilateral transverse radial limb deficiency, ACPOC recommends prosthetic fitting with a passive device at the age of six months, when the child is able to sit in a stable position [21]. The prosthetic introduction at early ages contributes to the psycho-motor development, promotes the use of both limbs in prehension activities and to crawl, ensures body symmetry during the child's growth, helps in the self-body perception and increases the chance of accepting more sophisticated prosthetic devices in the future. Therefore, it is important to introduce a prosthetic device before two years old, so these devices are accepted without the children's objection. Later prosthetic prescription may result in higher rejection rate as children may already developed compensatory methods [14, 15, 44].

An active terminal device should be introduced to the child between twelve and fifteen months. Three to five years is the common age to prescribe a body-powered prosthesis, followed by a myoelectric one during early adolescence. However, there are different opinions about the usage of these two types of prostheses by toddlers. Children with these types of lesions usually have a normal development and can be fully functional. The only differences are that they may never crawl, may start walking a little bit later due to the affected balance, or may need help in some specific activities. In short, these children can do almost everything, with or without prosthetic help [15, 21]. Moreover, there are also reports indicating that for many children it is easier to perform their daily tasks without their prostheses [45]. Thus, these tasks may be performed in a different way, by using their elbow, chin or knee to help them with bimanual activities [21].

Parents are crucial in the rehabilitation process along with a multidisciplinary team composed of pediatric orthopedics, occupational therapists and specialist technicians. Both should promote motion and strength exercises that ensure postural stability and a good relationship with the device, allowing the children to correctly develop their own methods to perform their daily activities [15, 39]. The proper use of the prosthesis and the family's support are essential for the functional independence of the children. However, it is important to be aware of the benefits and drawbacks of prescribing a prosthesis. Therefore, a proper rehabilitation program, adjusted to the child's age and motor and perceptual-sensory development is very important so the child could choose the best

prosthetic option as an adult in the future [14, 15].

When the congenital defects are detected before birth, the rehabilitation program may start before the child is born, in order to prepare the parents. Although several children refuse to wear a prosthesis, regular and planned assessments at least once a year, are important to anticipate additional demands as the children grow [15, 28]. Psychological support may be also provided to these children and their families. In addition, schools should be prepared to handle with these special conditions [21].

The quality of the prosthesis is determinant to the success of the rehabilitation, as it must withstand the resultant loads of the patients daily living tasks, be practical, comfortable and provide confidence at the same time [19]. Therefore, the therapist must provide all the necessary information to the patient and family so they can choose the best prosthesis for the patient. This choice must be made so the prosthesis reduces distress and optimize the patient's function. The therapist must be aware of the physiological and psychological needs of the patient in order to understand and fulfill the patients' expectations. Typically, the expectations of the patients and caregivers are higher than the reality [18]. In parallel, the patient must know the advantages and disadvantages of each prosthetic device which is being suggested to ensure that the advantages outweigh the disadvantages. Usually, the considered factors to prescribe a prosthesis are the level of lesion, age, family support, hobbies and daily activities, so that the prosthesis can be adjusted to the patient as much as possible [28, 37, 39].

2.3.3 User's needs

Many authors evaluate the prosthetic rehabilitation success according to how much time the patient uses the prosthesis throughout the day. Others defend that the prosthetic rehabilitation was successful if the prosthesis is used. Finally, it is also defended that the prosthetic success must consider function, prosthesis wear and patient satisfaction [18].

Despite the huge prosthetic offer, it is difficult to find a prosthesis that combines all the user's needs. People with upper limb disorders are not satisfied with the existent prostheses, leading to high rejection rates. Some of the reasons that contribute to the prostheses' rejection are their high weight, high repair costs and poor training. Discomfort and lack of functionality are the main factors that lead to prostheses abandonment [42, 46]. Table 2.1 displays the rejection rates of three types of upper limb prostheses in children and adults, obtained from a 25-year follow-up survey [47]. However, recent studies have shown that despite the prosthetic devices' evolution in the last decade, there was no significant change in the prostheses rejection rates [48].

Table 2.1: Mean rejection rates (%) of the three types of prostheses obtained from a 25-year follow-up survey [47]: the percentages of patients that did not use a prosthesis are also presented. The children’s rejection rate for this type of prosthesis is from R. Crandall and W. Tomhave’s study, since at the time of the survey only a single study reported on passive prosthesis use in the pediatric sector [49].

	Non-users	Passive	Body-powered	Electronic
Children	16	38	45	35
Adults	20	39	26	23

2.3.3.1 Comfort

Comfort is one of the most evident features that must be offered by the prosthetic device. Regarding comfort, the stump-prosthesis interface is the most significant part. People with acquired lesions usually complain about pain in the scar tissue that is often triggered when the patient wears a prosthetic device. Thus, the stump-prosthesis interface must be designed in order to minimize this effect [28]. Moreover, no child will probably use anything that provoke any kind of discomfort. Therefore, a prosthesis must have a good fitting.

Besides stump-prosthesis interface, prosthetic devices have to be as light as possible since excessive weight may lead to the rejection of the prosthesis [37]. Ultimately, if a prosthesis is highly sophisticated but it is not comfortable to wear or does not transmit safety to the user, it will be probably rejected [8].

2.3.3.2 Cosmetic

Cosmetic appearance is also a crucial aspect as is one of the main factors that lead to the rejection of prostheses. However, within the prosthetic area, this issue is still a problem to solve, because most models do not offer a completely natural look. Therefore, there is a need of a higher anthropomorphism level in the prosthetic industry. Anthropomorphism is the device’s capability to reproduce human features such as size, weight, shape or colour [10].

Another important factor is the cleanliness of the prosthesis. Thus, some users choose more sophisticated devices instead of weak skin reproductions. This choice is quite subjective and differs from person to person. It is expected that progress in this field will decrease prostheses rejection rates. Although cosmetic appearance is a universal need for all prosthetic users, it is a priority for those who wear cosmetic devices [5, 8].

2.3.3.3 Functionality

Functionality is also a very important parameter. Performing daily living activities such as eating and dressing is required by all the prosthetic users, no matter what their deficiencies or type of prostheses are. Although basic grasping operations are desired, upper

limb prostheses have some limitations regarding their control. Sensory feedback, stable grasps, fine motor skills, dexterity and flexibility are examples of attributes required by prosthetic users that improve these devices' functionality [5]. Yet, despite the improvements achieved up to the date, it is necessary to ensure that the prosthetic device can perform the most important types of grip: the power and precision grip. The sensory feedback should also be improved, ensuring a secure grip with force control. These requirements are needed not only to perform specific movements but especially to perform the activities of daily living [8, 10, 44].

2.3.3.4 Costs

Prostheses costs are also a significant aspect, as they are usually expensive devices. The higher the cost, the more technological the prosthesis is. However, only a few individuals can afford these devices. For children, costs are naturally higher as their growth will lead to frequent changes in the prosthetic device. Moreover, prostheses used by children are more likely to be damaged which also contributes to higher costs [10, 30].

2.3.3.5 Prostheses for children

Conventional prostheses are increasing their level of technology and complexity. Although these devices are suitable for adults, their weight and cost are not beneficial for children as they have special needs.

Prostheses designed for children must be small in size and weight. In addition, these prostheses need to have a higher resistance and to be easily fixed, as it may need to be frequently adapted due to repairs or adjustments. Unfortunately, a large number of prostheses do not adapt to children's growth. As children grow, their prostheses usually require socket and harness adjustments every 3 to 6 months. These adjustments are essential to maintain bilateral symmetry, support children's development and adapt their devices to their daily activities. Additionally, the entire replacement of the prosthesis is done every 1 to 2 years, which results in frequent medical consultations that may increase the rejection rate on children [21, 30, 37–39].

Therefore, it is necessary to develop prostheses that meet the basic user's needs in order to decrease their rejection. These prostheses must be practical and comfortable, functional, low-cost, easily fitted and aesthetically appealing. These demands are transversal to any age but are more significative in pediatric prostheses as they usually reject their prostheses due to their low functionality and comfort, high weight and unreal appearance [10, 12, 37].

ADDITIVE MANUFACTURING

Additive Manufacturing, more commonly known as 3D printing [50], is a group of automated technologies which use additive processes to create physical objects. These objects are built from a 3D [computer-aided design \(CAD\)](#) file by adding raw material layer-by-layer. This methodology is diametrically opposed to traditional subtractive methods that remove material to obtain the final product [51–53].

The CAD files, resultant from CAD software, contain a virtual solid model and describe its geometry and size. After the model is designed, the CAD file is exported to the [Standard Tessellation Language \(STL\)](#) format. These files are a triangulated representation of the object's surface, that contain a list of the spatial coordinates of the vertices of the triangles that together form the designed model. The *.stl* files are sent to a 3D printer slicing software that converts the model into multiple series of [two-dimensional \(2D\)](#) cross sections that correspond to the printing layers. Afterwards, the slicing program generates the G-code, a set of instructions for the 3D printer which indicates the coordinate values that the extruder needs to follow to print the designed model. The model may need support structures that can be generated by the slicing software or be defined by a CAD file [37, 53, 54]. The use of supports guarantee the dimensional accuracy of printed products [55].

AM is often used for rapid prototyping of new products, visualization, testing and mold making. However, due to the advances made in the capabilities, properties and materials for AM, these technologies have also been used to build final products in small series [50, 56–58]. The design freedom of AM enables new products with any shape, precise geometries and high dimensional accuracy by adjusting the process parameters. These designs would otherwise be impossible to produce so swiftly. The evolution of printing materials available in the market has contributed not only for a great range of AM applications but also for an easy customisation of products [10, 50–52, 56, 57]. Since these products are built by adding material layer-by-layer, the assembly phase might be eliminated. Therefore, the risks of localized stresses, which are common during this stage, are reduced. The main disadvantages of AM techniques are the possible formation of voids, anisotropic behaviour and laminated appearance. Nonetheless, it is important

to highlight that AM does not substitute the other existing production methods such as molding, forging, milling, injection, among others [51, 58].

Available printing materials are increasing progressively and range from poor quality stiff plastics to advanced multifunctional materials. These advanced materials include high-quality polymers, metals and metal alloys, wax, resins, ceramics and concrete to name a few. Materials for AM have different shapes and states as they can be liquid like inks or solid. When in solid state, AM materials can be filaments, powder, paste or sheets [53, 58, 59].

3.1 Additive Manufacturing Methods

There are seven distinct AM methods: powder bed fusion, vat photopolymerization, material jetting, material extrusion, sheet lamination, binder jetting and direct energy deposition [53]. The benefits and drawbacks of each technique are related with their accuracy, the possibility of using different types of materials and the associated costs [10]. Figure 3.1 compares the seven AM existing procedures, presenting their strengths, materials and alternative names. A more detailed description of each one of these methods can be consulted in Appendix A, except for material extrusion that is explored in Section 3.2.

Although “3D printing” is an alternative nomenclature for the binder jetting process, “3D printing” is more commonly used to describe all the AM methods. Therefore, for the purpose of this study “3D printing” will be used as a synonym of Additive Manufacturing, referring to Fused Deposition Modeling in particular.

3.2 Fused Deposition Modeling

Additive Manufacturing methods have been growing and so has material extrusion, of which one common name is **Fused Deposition Modeling (FDM)**. This technique has been growing in the past few years as a modeling, prototyping or manufacturing process [55] in areas like aerospace, automobile, construction and electronic industry and medicine [54, 56, 59, 61].

FDM has been widely applied in medicine since it can work with a wide range of materials. In tissue engineering, FDM has been used to create porous scaffolds for printing organs such as vessels, bones and soft tissue. Other examples of what can be done with 3D printing include tools for drug delivery with bioresorbable polymers, artificial bones, splints, dental repairs, hearing aids and micro batteries for smaller medical devices. Surgeries have also benefited from FDM as it helps the surgeons and medical students in the pre-surgical planning and training, increasing the success rate of the operation [54, 55, 59, 61].

Scanning technologies such as magnetic resonance imaging, **computed tomography (CT)**, X-ray and 3D scanning allows the gathering of accurate medical imaging data of anatomic structures of the patients with a high resolution. Thus, by combining these

3.2. FUSED DEPOSITION MODELING

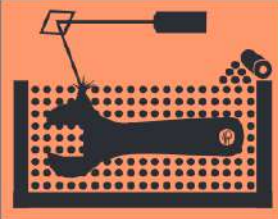
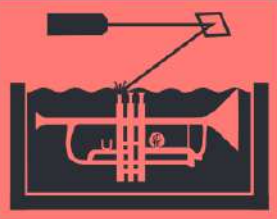

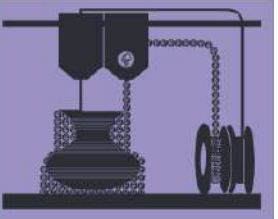
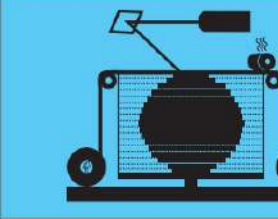
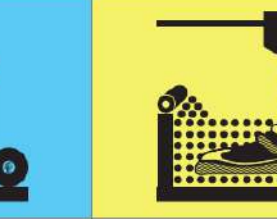
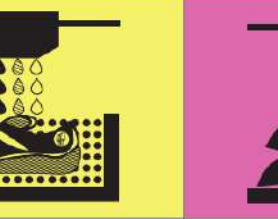
			
Powder Bed Fusion	Vat Photopolymerization	Material Jetting	Material Extrusion
Alternative Names			
SLS™ - Selective Laser Sintering DMLS™ - Direct Metal Laser Sintering SLM™ - Selective Laser Melting EBM™ - Electron Beam Melting SHS™ - Selective Heat Sintering MJF™ - Multi-Jet Fusion	SLA™ - Stereolithography Apparatus DLP™ - Digital Light Processing 3SP™ - Scan, Spin, and Selectively Photocure CLIP™ - Continuous Liquid Interface Production	Polyjet™ SCP™ - Smooth Curvatures Printing MJM - Multi-Jet Modeling Projet™	FFF - Fused Filament Fabrication FDM™ - Fused Deposition Modeling
Strengths			
- High level of complexity - Powder acts as support material - Wide range of material	- High level of accuracy and complexity - Smooth surface finish - Accommodates large build areas - Cheaper equipment	- High level of accuracy - Allows for full colour parts - Enables multiple materials in a single parts with discreet and gradual transitions - Smooth surface finish	- Inexpensive and economical - Allows for multiple colours - Can be used in an office environment - Parts have good structural properties
Materials			
Plastics, metal and ceramic powders, and sand	UV-curable photopolymer resins and rubber-like materials	Photopolymers, polymers and waxes (viscous thermosetting resins)	Thermoplastics such as ABS and PLA
			
Sheet Lamination	Binder Jetting	Direct Energy Deposition	
Alternative Names			
LOM - Laminated Object Manufacture SDL - Selective Deposition Lamination UAM - Ultrasonic Additive Manufacturing	3DP™ - 3D Printing ExOne Voxeljet	LMD - Laser Metal Deposition LENS™ - Laser Engineered Net Shaping DMD™ - Direct Metal Deposition (DM3D) LENS™ - Laser Engineered Net Shaping DMD™ - Direct Metal Deposition DM3D	
Strengths			
- High volumetric build rates - Relatively low cost (non-metals) - Allows for combinations of metal foils, including embedding components.	- Allows for full color printing - High productivity - Uses a wide range of materials	- Not limited by direction or axis - Effective for repairs and adding features - Multiple materials in a single part - Highest single-point deposition rates - No porosity - Allows printing onto existing objects	
Materials			
Paper, plastic sheets, metal foils and tapes	Powdered plastic, metal, ceramics, glass and sand	Metal wire and powder with ceramics	

Figure 3.1: Additive Manufacturing techniques: parallelism between their alternative names, strengths and materials. Adapted from H. M. Technologies [53, 60].

techniques with AM methods it is possible to customise medical devices for each patient [55, 61]. Product customization used to be a challenge due to its high costs. However, it is now simplified with the combination of 3D printing and scanning techniques [58].

3.2.1 Working principles of Fused Deposition Modeling

FDM is a layer-by-layer printing technique in which the nozzle moves through the printing plate in order to deposit the material in the desired position [53]. After the design is set and all the printing parameters are selected, the resulting G-code is uploaded to the 3D printer. The printing head is fed with the filament through the extrusion motor. The filament is heated up to its melting temperature and the printing head passes the melted material through the nozzle. Then, the material is deposited along the XY plane and solidifies. During the printing process, as the printed model increases its height layer-by-layer, either the printing head moves up or the printing bed moves down (along the Z direction). Each movement in the Z direction is performed with a delta correspondent to the layer thickness. This movement only occurs after each layer is finished. Supporting structures can also be printed and removed after the model is finished. Figure 3.2 shows the anatomy of the 3D printer used during this study, *The Original Prusa i3 MK3S+* by ©Prusa Research [54, 55, 62].

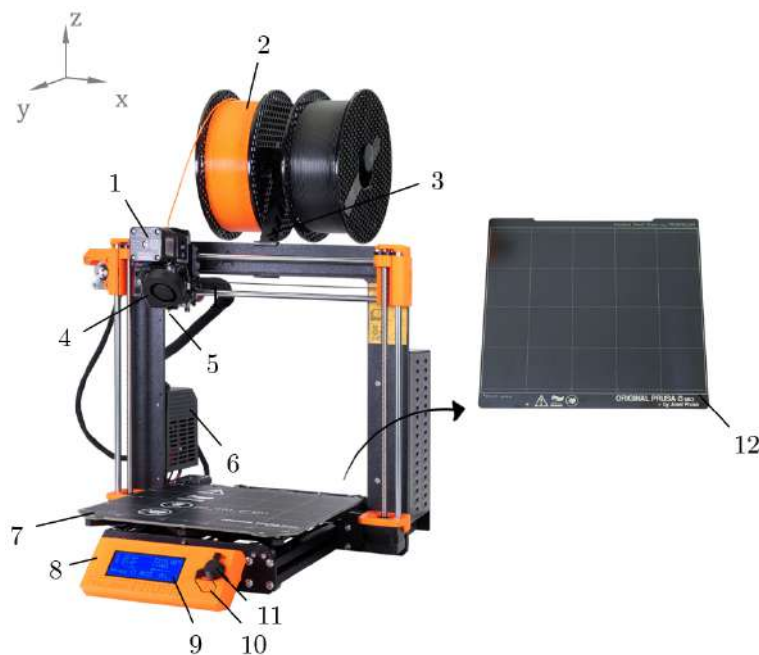


Figure 3.2: Anatomy of *The Original Prusa i3 MK3S+* by ©Prusa Research: 1. Extrusion motor; 2. Filament spool; 3. Filament spool support; 4. Fan; 5. Heating element and nozzle; 6. Motherboard; 7. Heating bed; 8. Control panel; 9. LCD panel; 10. Reset button; 11. Control knob; 12. Magnetic heating bed. Adapted from M. B. Burn *et al.* [37, 62].

Some printers have more than one extruder, which gives them the ability to print with more than one material. This technique has been growing in the past few years as a

modeling, prototyping or manufacturing process [55] in areas like aerospace, automobile, construction and electronic industry and medicine [54, 56, 59, 61].

FDM can use several materials including metals, ceramics and polymers. The filaments most commonly used in FDM include polymers such as PLA, [acrylonitrile butadiene styrene \(ABS\)](#), [polycarbonate \(PC\)](#), PC-ABS, polyamide, polycaprolactone and polyphenylsulfone. The thermoplastic character of these polymers is an essential property to ensure the layers fuse together during the printing process [55, 58, 63].

One of the most important aspects for a good printing quality is the first layer. Without it, the print will certainly fail since quality of the following layers depend on the first one [37]. Other factors like layer thickness, width, orientation and inter-layer distortion may lead to defects that compromise the properties of the printed object. The printing quality also depends on the time that the material takes to solidify. Between layers, the fibers of the melted material interact with the previous printed layers and bond. If the solidification occurs faster than it is desired, it may lead to void formation and other defects that influence the mechanical properties of the printed model [54, 58].

Therefore, disadvantages of FDM include weak mechanical properties and layer-by-layer appearance. These disadvantages are common in other AM techniques. Nonetheless, it is important to highlight that FDM's low-cost, short manufacturing time, good surface finish and high accuracy overweight these drawbacks. In addition, FDM requires small-size and easy-use equipment with an intuitive operating interface [55, 58, 63].

3.2.2 Prostheses made with Fused Deposition Modeling

The majority of the existent 3D-printed prostheses are built with FDM. There are also records of 3D-printed prostheses made with power bed fusion, vat polymerization and material jetting, but they are uncommon. The majority of the available designs does not require the printing of small details, which makes FDM the most suitable method for this purpose [10].

PLA and ABS are the main rigid materials used to print prostheses with FDM. The commonly used flexible materials include *Filaflex* patented by ©Recreus [64] and Ninjaflex® patented by NinjaTek® [65]. Ninjaflex® is a [thermoplastic polyurethane \(TPU\)](#) while *Filaflex* is a [thermoplastic elastomer \(TPE\)](#) with a polyurethane base and some additives [10, 65, 66].

PLA is the most used material in FDM due to its low-melting temperature that results in smaller temperature gradients and consequently, in less stress during the printing. PLA has a non-poisoning and non-irritating character as well as sound biocompatibility. The contact of PLA with water and carbon dioxide does not lead to contamination of the environment. In addition, its plasticity and stiffness does not decrease with time. Overall, these characteristics makes PLA a very good option for medical solutions [63].

Filaflex is available in the following hardnesses: 90A, 82A, 70A and more recently 60A. These values are related with the durometer hardness test that asses the mechanical

behaviour of elastomers. There are several types of scales defined by the American Society for Testing and Materials. The Shore A Hardness Scale is one of them and it measures the hardness of flexible materials in a scale from 0 to 100. Lower values correspond to more soft and flexible materials and higher values to harder materials [67, 68].

The *Filaflex 82A* is the most popular flexible material used in 3D printing. Its hardness means that the filament can be stretch up to 650% without breaking. After being stretched, the material returns to its original shape without suffering deformation or break. Furthermore, its flexibility is not altered by heat. *Filaflex* is odorless, resistant to solvents like acetone and fuel, it is non-toxic and can be in contact with skin. When extruding this material, some printing adjustments may be needed to make sure the printer does not clog [10, 66].

3.3 Design for Additive Manufacturing Principles

Additive Manufacturing is only beneficial (comparatively to the traditional manufacturing techniques) if used correctly. When poorly used, AM ends up being a replacement of the traditional methods. Instead, AM must be seen as new tool to improve the flaws of the existing manufacturing methods [69].

The **Design for Additive Manufacturing (DfAM)** is the process of adjust the model's design in order to optimize the AM methods and get the most out of each technique. The impact of DfAM is more important for final products than for prototypes, as this optimization could result in a waste of time and resources when developing pure prototypes. The application of DfAM differs according to each AM method but should follow the following principles [69–71]:

1. **Think additively:** the less material is used, the less are the costs and more is the saved time. Unlike the traditional methods that work by removing parts from a block material, AM methods work by adding material which leads to more ergonomic pieces.
2. **Design for orientation:** when the piece is being designed, the printing position must be considered, as different positions may result in different mechanical and aesthetical properties.
3. **Contour design:** the walls' thickness of the model to print must be a multiple of the extrusion width and height.
4. **Segment and bond parts:** bigger pieces may be segmented and bond together instead of use another method to print the model. Segmentation may also be a mean to simplify the final product.
5. **Add hardware:** the prototype or final product does not need to be entirely made by AM methods and additional components may be added.

6. **Minimize complications:** some designs may need support structures. However, they increase printing time, waste material and may result in poor printing quality. Therefore, supports should be avoided whenever possible.
7. **Critical Surface Treatment:** depending on the expected surface treatment, the number of bottom or top layers and the number of contours should be adjusted to guarantee that no post processing enters the infill of the component.

These principles offer different benefits for each application. Thus, depending on the final purpose of the model to build, they must be explored in order to achieve the best results.

PRESENT AND FUTURE TRENDS

This chapter describes the progresses on the the prosthetic field, particularly through Additive Manufacturing. In particular, a literature review on the present and future trends of the 3D-printed devices with flexible materials and aesthetical improvements is presented in the last section.

4.1 Overall technological progresses

There is evidence on the usage of prostheses since the times of ancient Egyptians. However, the first prostheses recognised as capable of performing rehabilitation aids were only built during the Rome and Greece civilizations. The most common alternatives to people with limb loss were peg legs and hook hands. Over time, the constant improvements in medicine have enabled several enhancements in the prosthetic field and, consequently, hooks are increasingly looking like human hands [27].

Medicine has been benefiting from several technological fields, including AM. AM was developed in the eighties and it has been used in several fields such as materials and mechanical engineering, computer technology, electronics and medicine. At the end of that decade, more than twenty AM techniques had been developed and have been used since, to produce prototypes and new products. In particular, FDM was patented in 1988 and has become a highlight in 3D printing since it enables the low-cost creation of complex geometries with a high accuracy [54, 55, 57, 63].

The expiration of the patents at the beginning of the last decade gave manufacturers the opportunity to develop new 3D printers. For this reason, 3D printers have become cheaper and more accessible. Thus, FDM is being used in schools, laboratories and by many home-users, leading to a constant improvement of this process. 3D printing online communities are a result of the growth of 3D printers into the household and of the advances in CAD software. *e-NABLE* community [9] has a wide variety of open-source objects, including prostheses [54, 58, 72]. The printing files, as well as the assembly instructions are available in these platforms. The prostheses' models can be modified according the individual's needs or to fit the children's growth [37].

4.2 3D-printed prostheses

Before 3D printing was widely available, upper limb prostheses were not designed considering the user's needs. As described in Chapter 2, clinicians and prosthetic manufacturers should be sensitive to user's needs. Hence, any progress made in the prosthetic field should be made considering answer these needs [3].

Thus, FDM appears to be a very good solution for the main problems of the most common prostheses. Table 4.1 shows the benefits and drawbacks of 3D-printed prostheses.

Table 4.1: Advantages and disadvantages of 3D-printed upper limb prostheses. Adapted from K. Tanaka and N. Lightdale-Miric [72] with extra sources where noted.

Advantages	Disadvantages
Lightweight and easy to use [73];	Limb function does not necessarily improve [44];
Low-cost when compared with other prostheses (5 to 500\$). This facilitates the prosthesis replacement as the child grows. The pricing is also very attractive for people from LMICs [19, 73];	The materials commonly used are thermoplastics that are sensitive to high temperatures (common in LMICs) [19];
Easy assembly that facilitates the replacement of the prosthesis' parts as the child grows or when some component is damaged [37, 72];	When extra parts or replacements are needed, it requires access to a 3D printer;
Their toy-like appearance makes these prostheses appealing to children [38];	The toy-like appearance makes these devices non-appealing for adults. Children reject them after a few hours of play;
These devices may promote social confidence in children;	These devices may not be applicable in all daily life activities as they might be fragile for some rough tasks;
Models can be customised to fit the user in terms of size, type of lesion, shape and colour, aiming to meet the user's needs [10, 73, 74];	Sizing modifications do not fit proportionally the child's body and the existent models do not accommodate all the types of hands deficiencies;
Open source and free models [73].	Lack of medical validation: these devices are not properly regulated or tested by any health entity [50, 73].

Most of these prostheses have very similar designs, consisting of VC devices with an anthropomorphic appearance. They use nylon tendon cables to create a composite grasp powered by the flexion of the wrist or elbow. Each one of the finger's cables is attached to the extremity of the correspondent finger. The other extremities are linked to a common structure, to ensure the fingers move at the same time. The fingers are connected to the metacarpal region structure through hinges, which is connected to the forearm gauntlet. Assembly starts from distal to proximal direction and additional components such as screws and velcro may be necessary [10, 37]. The *Raptor Reloaded*, the *Phoenix Hand v2* and the *Nazree's Prosthetic Hand* are three examples of this type of prostheses.

The *Raptor Reloaded* is a body-powered 3D-printed prosthesis developed by *e-NABLE's* designers. The *Raptor Reloaded* design is easy to print and assembly, and combines the best features of the existing prostheses until its creation. Therefore, it is a reference for the future 3D-printed prostheses. It is composed by 3D-printed snap pins, a modular tensioning system (composed by elastic bands and fishing line) and it can have Velcro or leather palm enclosures. The closure of the fingers is obtained through the flexion of the wrist. Therefore, it is necessary that the amputee still has wrist function. Figure 4.1 shows the *Raptor Reloaded* prosthesis. This device is cheap to produce, as its core materials only cost 35\$ [19, 75].



Figure 4.1: *Raptor Reloaded* prosthesis. Adapted from B. Phillips *et al.* [19].

Figure 4.2 presents the *Phoenix Hand v2* prosthesis, which is a voluntary closing wrist-powered device. This prosthesis is an improvement of the *e-NABLE Phoenix Hand* as it consists of a lighter and stronger version. The *Phoenix Hand v2* is composed by a whipletree mechanism that consists of a force transmission system which couples the fingers motion but also enables each finger to move independently from other fingers, allowing an adaptive grasp [76]. This prosthesis connects the index to the middle finger and the ring finger to the little finger [77].



Figure 4.2: *Phoenix Hand v2* prosthetic [77].

The *Nazree's Prosthetic Hand*, displayed in Figure 4.3, consists of a 3D-printed terminal device composed by three segments that somehow follow the shape of the hand's creases, allowing the simulation of the gripping motion. This terminal device has an inner whippletree mechanism that is pulled by a single cable. The *Nazree's Prosthetic Hand* connects the little finger to the index finger and the middle to the ring finger, unlike other prostheses such as the *Phoenix Hand v2*. All this cabling is hidden so that the prosthesis could resemble a human hand. Moreover, this terminal device can be covered by a silicon glove to appear even more like a human hand [78].



Figure 4.3: *Nazree's Prosthetic Hand* [78].

Although these prostheses are a practical and inexpensive solution, cosmetic and functional improvements are still needed. The majority of the existing 3D-printed prostheses are made of rigid materials. However, combining rigid and flexible materials could improve the performance of these devices. Although the stiff components lead to a stronger hand, these prostheses' surface does not adapt to the object that is being held. The usage of flexible filaments could simulate the compliance of the hand's skin, allowing to achieve

a stronger grip and avoiding the objects to slip [10]. Early studies have been focused on using AM to create more realistic 3D-printed prostheses with these materials, as detailed next.

In 2017, V. Lopes developed a cosmetic 3D-printed prosthesis customised for a two year old child, shown in Figure 4.4. A more real appearance of the prosthesis was obtained using scanning techniques. In particular, the stump's anatomy was obtained with 3D scanning and the anatomical features of the sound limb were assessed through CT scanning. The resulting files were explored with a set of CAD software in order to define the prosthesis design. Finally, two prototypes were printed, one with PLA and the other with *Ninjabflex* filament. Although these devices presented different characteristics, both were well accepted by the two-year-old child [17].



Figure 4.4: V. Lopes' cosmetic hand prosthesis [17]: (a) posterior view; (b) anterior view.

In 2018, F. Pinheiro developed a non-customized body-powered prosthesis, by combining flexible and stiff materials, such as *Filaflex* and PLA. The fingers were printed with *Filaflex* and the hand-body was printed using PLA. By using a flexible filament, F. Pinheiro tried to give the prosthesis a more natural appearance and avoided the exposure of the actuation cables and hinges. This level of anthropomorphism was tried to be achieved by using the *Loft* tool of Solidworks® software. Inner air chambers were added to the fingers' joints to allow the flexion of the fingers. The fingertips have an additional chamber, in which a rigid ring tied to the tendon cables rests. These rings are inserted through a small hole in the fingertips and are connected to the wire holes. Additionally, matching wire holes were also designed in the hand body, so that the tendon cables could reach the bottom of the hand-body. Figure 4.5 shows this study's prosthesis design in which the thumb is 70° from the hand body. Figure 4.6 presents the final prototype. Besides, the prosthesis' design, this study also included an analysis of the ideal printing parameters

for *Filaflex* [30].

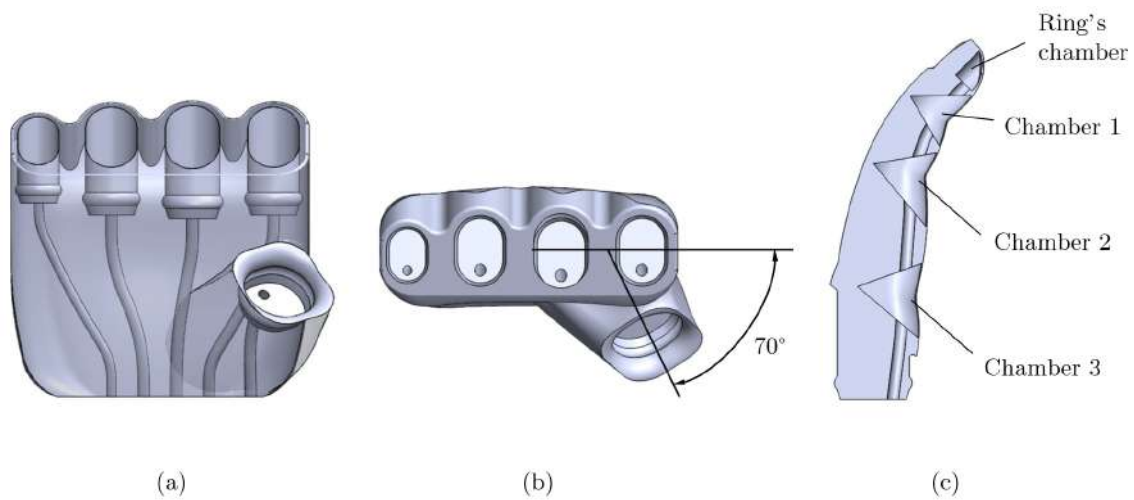


Figure 4.5: Design details of the components of the body-powered hand prosthesis developed by F. Pinheiro [30]: (a) anterior view of the hand body. The transparency of the surface allows to observe the inner components such as the fitting mechanism for the fingers and the wires' holes; (b) top view of the hand body in which can be seen the orientation of the thumb in relation to the hand-body; (c) inner design of the finger in which can be seen the chambers and the wire hole (cut along the sagittal plane).

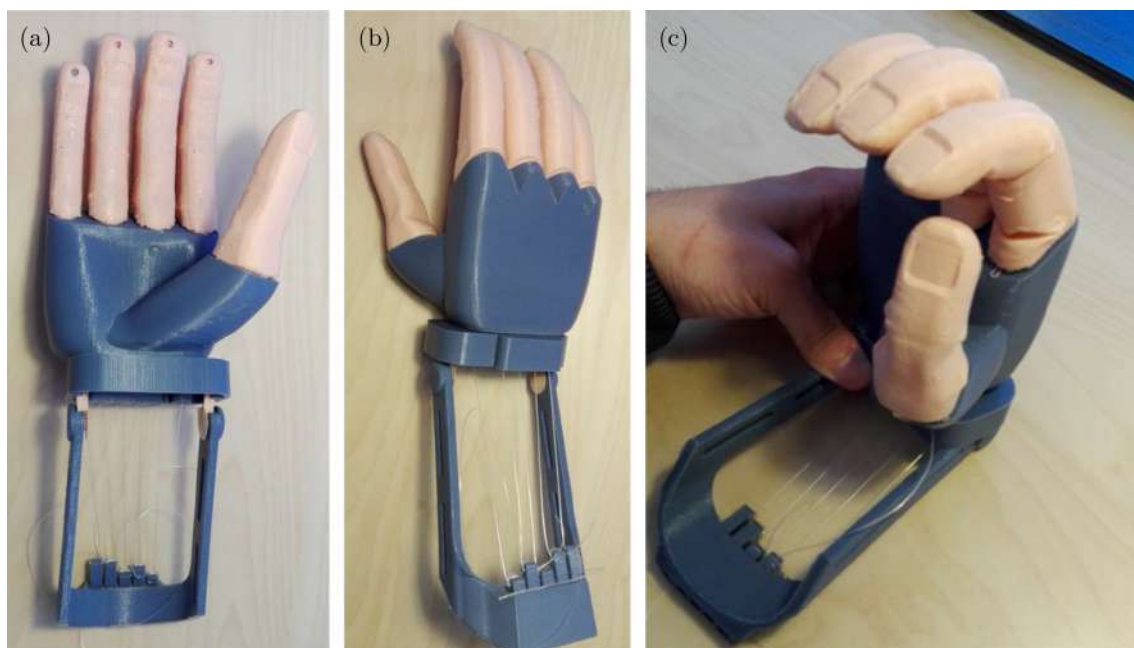


Figure 4.6: F. Pinheiro's body-powered prosthesis [30]: (a) latero-anterior view of the prosthesis not actuated; (b) latero-posterior view of the prosthesis not-actuated; (c) actuated prosthesis.

Despite the progress that has been made, there is currently no evidence of a 3D-printed body-powered prosthesis with a more realistic appearance. However, some recent studies have been exploring the use of flexible materials in certain components of their prostheses (rather than in the entire device) in order to increase the grasping performance or making the prostheses more comfortable.

J. Corveira developed a low-cost soft 3D-printed body-powered upper limb prosthesis, based on *e-NABLE's* prostheses. Soft silicone was added to the fingers and palm of the hand in order to increase the friction coefficient between the device and the objects. Therefore, the prosthesis could have a better grasping performance, adapted to various object shapes and sizes. Unlike *e-NABLE* prostheses, this prosthesis is not fully 3D-printed and is composed by a soft silicone that is molded around the endoskeleton [79].

R. Alturkistani *et al.* developed a 3D-printed passive prosthesis for patients with partial hand amputation in developing countries, using TPU and PLA. The contralateral hand is responsible for the grasping control of the device. The anatomical features of the patient's hands were assessed using 2D drawings and body casting, followed by 3D scanning. The developed prosthesis was inspired in *e-NABLE's Raptor Reloaded* hand, but the hand body and wrist parts were modified in subsequent prototypes with *Fusion 360* software by ©Autodesk [80] in order to better fulfil the needs of the patient. The fingers were printed using PLA and the palmar part of the device was printed using the flexible filament, increasing the fitting comfort [81].

Finally, X-Limb is a soft robotic with a human-hand-like morphology prosthesis made through FDM with 90A TPU and composed by inner actuation and control systems [82]. Figure 4.7 shows the prostheses developed by J. Corveira, R. Alturkistani *et al.* and the X-Limb.



Figure 4.7: Examples of other prostheses with components made of flexible materials (adapted): (a) body-powered prosthesis developed by J. Corveira [79]; (b) cosmetic prosthesis for finger replacement developed by R. Alturkistani *et al.*; (c) X-Limb, a robotic hand prosthesis [82].

Despite the success of these prototypes, even though they fulfil the basic user's needs, none addressed the need of improved cosmetic features. The passive prosthesis developed by V. Lopes is a good solution for younger children as these devices may be the first ones to be introduced to children. Nevertheless, the printing parameters and the used materials must be reviewed as the prosthesis present several printing defects. J. Corveira and R. Alturkistani *et al.* have good approaches to meet their studies' goals, but none of them consist of an aesthetically appealing option. X-limb is the solution which has the best aesthetical appearance. However, this device is an electronic solution. Furthermore, although it consists of a lighter and cheaper option, this device may not suitable for younger children.

The 3D-printed body-powered prosthesis developed by F. Pinheiro is the one that better meets the main goal of this study. However, there is still room for improvement. The fingers' design well as the thumb position need revision, aiming to give the prosthesis a more natural look. These adjustments must be done without compromising the prosthesis' functionality. Finally, the remaining design of the prosthesis must be also improved in terms of anthropomorphic shape.

Thus, there is a need to improve the cosmetic appearance of 3D-printed body-powered prostheses, without compromising the other user's needs such as comfort, lightweightness, low-cost and functionality. Flexible materials might be a key to solve some of the referred issues since they allow to achieve a more real appearance and establish some sensory feedback. However, it is still crucial to identify the needs of the patient receiving the prosthesis, aiming to design a highly customised prosthesis

CONCEPT DEVELOPMENT

This chapter describes the clinical case in which this study was based on, as well as the methodology used to develop a customised body-powered prosthesis with Additive Manufacturing. However, given that the prosthesis was developed through an iterative process (where the results of a given prototype influenced the methodology used in the following), most details are presented in Chapter 6.

5.1 Introduction to the Clinical Case

The prosthetic device developed during this study was based on a single clinical case. Since one of the main goals of this study consisted in customising the developed prosthesis, addressing more than one clinical case would be far too time consuming for the duration of this work.

The chosen clinical case was selected from the *Patient Innovation* program “*Dar a mão*” [83]. *Patient Innovation* is a Portuguese non-profit company that whose mission is to share medical solutions developed by patients, caregivers or collaborators. These solutions allow patients to cope better with problems imposed by their medical condition. Since 2018 and through this program, *Patient Innovation* has developed 3D-printed body-powered prostheses to offer to Portuguese children with upper limb deficiencies.

Within the available cases that integrated this program, the selected clinical case had to meet the following requirement:

1. The patient should have already used another 3D-printed prosthesis, so that this study’s prosthetic device is not the first that child has contact with;
2. The patient should have a functional wrist, capable of doing a 30° flexion and extension, so the developed prosthesis could be wrist-powered and the design could be simpler [37];
3. The patient should have a unilateral deficiency, so the sound hand could be used as a reference for the design of the prosthetic device;

4. The patient should not have a complex lesion, since in some cases, depending on the source of the lesion, it might exist excess of soft tissue in the stump area;
5. The patient should not live too far from the Lisbon area so possible measurements and testing sessions could be easier;
6. Both child and the family should have the capacity to deal with the expectations.

The selected clinical case was a four-year-old boy (at the time of the measuring session) with a left transverse metacarpal total deficiency caused by amniotic band syndrome¹. This child met all the aforementioned requirements. However, the main reasons for his selection were the nature of his lesion, his residence area and the fact that he had already had contact with a 3D-printed prosthesis.

5.2 Methodology

The methodology applied in this study was inspired in the Product Design and Development methodology [11]. The first step was defining the goals of this study through the identification of the main gaps in most upper limb prosthetic devices, as described in Chapters 2 and 4. Afterwards, the user's needs were identified in order to determine the specifications of the present prosthesis. Finally, the main concepts used to develop the prosthesis were generated based on these specifications.

The concept selection phase was performed aiming for a high level of customisation and functionality. During this phase, several prototypes were designed and tested.

Finally, the whole prosthesis was evaluated in order to identify possible improvement points for the future. Figure 5.1 presents the short version of the flowchart that illustrates the development process of the prosthesis. Appendix B presents a more detailed and thorough description of the used methodology.

5.2.1 Anatomical and functional features assessment

One of the main goals of this study was to design a highly customised prosthesis. In order to achieve a high level of customisation it was necessary to measure and assess the anatomical features of both limbs' extremities. Therefore, a protocol composed by two different methods was established to assess the anthropometric measurements and physical features of both limbs' extremities. The used methods consisted of simple measurements and body casting of both limbs' extremities, providing different types of information, from single to three-dimensional data. Before starting any procedure, an informed consent was presented to the child's carer, aiming to clarify all the study's goals and all the associated procedures.

¹Amniotic band syndrome results from fibrous bands that appear during the gestation period and wrap around some parts of the foetus, leading to deformation, malformation and disruption [84].

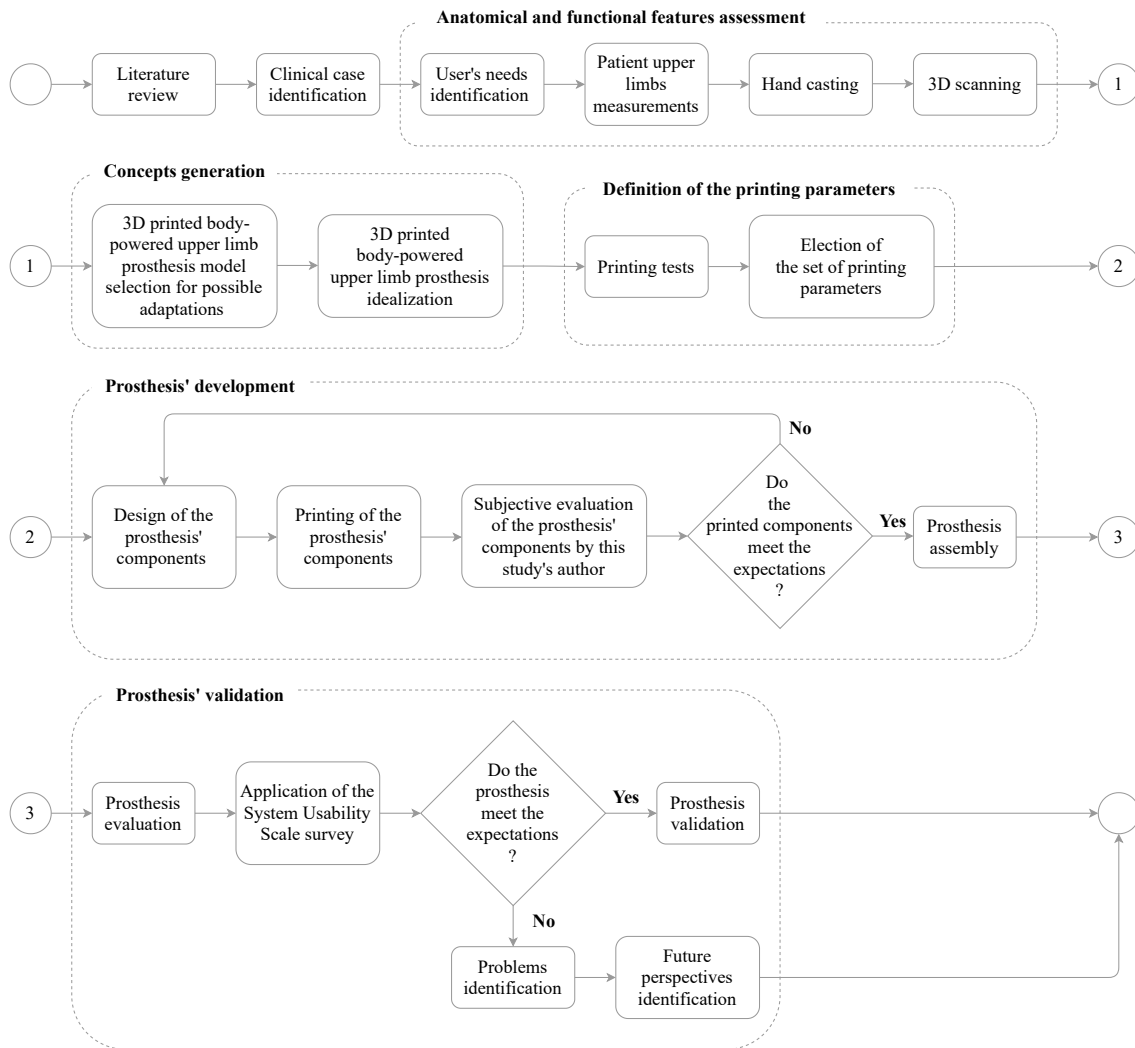


Figure 5.1: Methodology flowchart.

The first procedure consisted of measuring the child's upper limbs. It was composed by two parts. The first part consisted of a form aiming to collect personal data and the clinical background of the child. This form was inspired in the form used during the measurements sessions of *Patient Innovation*, within the scope of “*Dar a mão*” program [83]. Then, both limbs were measured according to the measurements guide from *e-NABLE* [9] where some photos were taken [85], with millimetre paper placed under the child's limbs for reference.

The second procedure was body casting. Before doing the extremities moulding, the child's limbs were greased with baby oil. Then, the limbs were immersed in a solution of alginate². The used alginate was *Orthoprint*, by ©Zhermack, which takes one and a half

²Alginate is a biopolymer obtained from brown seaweed. Alginate has unique thickening properties and is widely used in food, cosmetic and pharmaceutical industries [86]. Due to its gelling properties, alginate is perfect to make negative moulds and is commonly by dentists to make dental moulds.

minutes to solidify [87]. After this period, the limb was removed and cleaned, and the mould was filled with a plaster solution.

When the plaster was set and dry, the alginate was removed, and the resulting replicas were left to dry during a couple of days. After drying, the alginate remains were carefully removed with the help of a toothpick. Then, the replicas were sanded in order to smooth the surface and remove some plaster defects caused by air bubbles in the alginate. The existing holes caused by alginate lumps were filled with a brush soaked in plaster solution and the replicas were sanded once more to remove the plaster excess. Finally, some details of the sound hand such as nails and hand's creases were highlighted with a toothpick so the anatomical features could be preserved.

More detailed information could be consulted in Appendix C, where the established protocol is presented as well as the measurements' form and parental consent. It is important to refer that the presented documents were translated to Portuguese, so the child's parents could understand all the procedures and study goals.

5.2.2 3D scanning

A computer readable representation of the anatomical features of the child's limbs was obtained by 3D scanning the plaster replicas. Figure 5.2 shows the scanner that was used in this study, the *Ein Scan-SE* by SHINNING 3D®, which has a single shot accuracy of ≤ 0.1 mm [88].



Figure 5.2: The *EinScan-SE* by SHINNING 3D®.

The sound hand was scanned in six different positions and the undeveloped hand was scanned in three different positions. Each position was scanned using 30 turntable steps. For some positions, a support was necessary, in order to scan all the replicas details.

5.2.3 Design and printing

The design of the prosthetic device was made considering the DfAM principles, aiming to achieve the best results when printing the different components that compose the prosthesis.

The prosthesis' design is composed by different components that can be segmented in three parts: the fingers, the metacarpal region and the wrist. The entire design was made considering the extrusion width and height, so the designed walls could be a multiple of these values. The printing position was also a considered factor as well as the existence of support structures, that were avoided whenever possible. Supports were needed for designs with overhang angles less than 45° from horizontal [57].

The whole prosthesis was designed using *Fusion 360 CAD* software by ©Autodesk (version 2.0.10940) [80]. The resulting *.stl* files from the scanning were imported to this software and then modified in order to preserve the anatomical features of the child and to customise the prosthesis as much as possible. The sound hand replica was the first to be addressed.

After importing the *.stl* file, it was necessary to change its representation, from mesh to body (*Brep*) so it could be modified. However, to reduce the computational burden of dealing with a huge number of faces, its number was reduced up to the maximum recommended of 10 000, before doing the conversion. The obtained body representation was then segmented in order to individualize each finger and detach them from the metacarpal region. Figure 5.3 shows the process from the resulting mesh from the scanning until the finger segmentation. Finally, all parts were scaled to 110%.

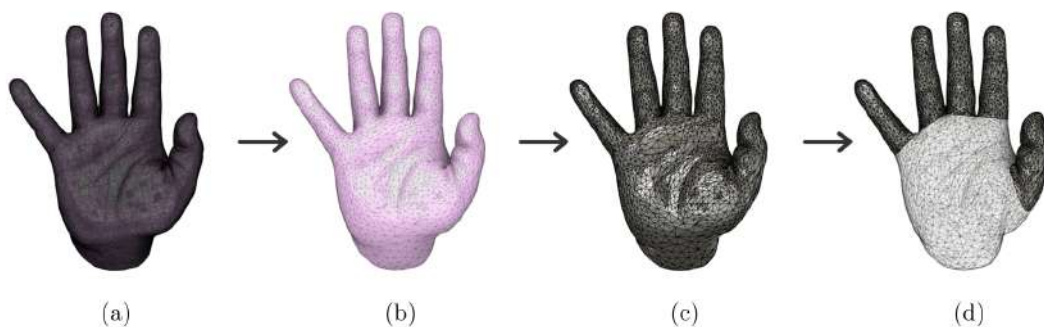


Figure 5.3: Modification process of the design file: (a) mesh representation with 104 797 faces; (b) mesh representation after reducing the number of faces to 10 000; (c) body representation; (d) finger segmentation.

5.2.3.1 Fingers design

The index design was the first to be addressed because its design was used as a reference for all the remaining fingers, except for the thumb. The developed design was inspired

in F. Pinheiro's study that used air chambers to ensure the finger could bend properly [30]. In addition to these features, inner cylindrical components were added to simulate the existence of phalanges.

The resulting fingers from the segmentation still presented some remaining parts of the metacarpal region. Therefore, it was necessary to remove them in order to obtain a planar surface at the bottom of the finger. Despite the post processing that was done before the 3D scanning, some defects were still present. Hence, the fingers' surface was computationally smoothed.

The replica of the child's hand had extended fingers. Therefore, it was necessary give them a natural curvature that would allow a proper bending. The flexion angles of distal and proximal interphalangeal joints of each finger were defined based on the K. Lee and M. Jung's study. Their study aimed to determine the extension and flexion angles of resting fingers in terms of forearm posture and shoulder flexion [89]. For the present work, the values defined were chosen considering the neutral posture of the forearm and a shoulder flexion of 0° . For **proximal interphalangeal (PIP)** joints, the considered value, represented as α , was the mean value (M) minus the **standard deviation (SD)** value ($M - SD$). For the **distal interphalangeal (DIP)** joints, the considered value, represented as β , was the mean value plus the standard deviation value ($M + SD$). Figure 5.4 represents the α and β angles. Table 5.1 displays the defined angle values used to curve the fingers.

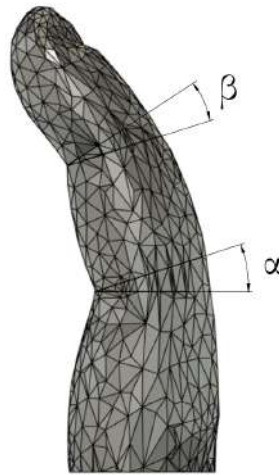


Figure 5.4: Representation of the extension and flexion angles of the interphalangeal joints: α is the angle of the PIP joint and β is the angle of the DIP joint.

Table 5.1: Interphalangeal joints' extension and flexion angles for each finger.

	Index	Middle	Ring	Little
α	$18^\circ (26 - 8)$	$16^\circ (27 - 11)$	$23^\circ (32 - 9)$	$23^\circ (34 - 11)$
β	$15^\circ (10 + 5)$	$15^\circ (10 + 5)$	$12^\circ (8 + 4)$	$19^\circ (12 + 7)$

The air chambers that enable the proper finger bending are a conical void structure. The cone's vertex has a 60° angle (θ) and its depth correspond to 90% of the transversal section length (L) where the vertex is inserted. These chambers simulate the interphalangeal joints and their vertex are located at $\frac{\alpha}{2}$ and $\frac{\beta}{2}$. Figure 5.5 illustrates the PIP joint design of the index finger.

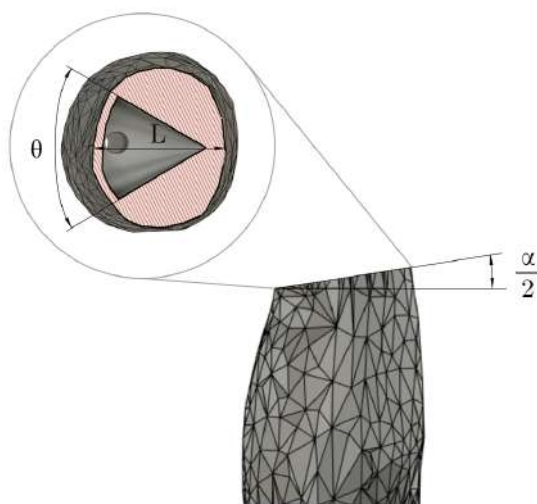


Figure 5.5: Design of the PIP joint of the index finger: θ corresponds to the chamber's opening angle, L is the length of the transversal section where the chamber's vertex is inserted and α is the extension and flexion angle of the PIP joint.

The fingertip also has a chamber where a rigid ring, tied to the tendon cable, rests. The ring is inserted in the chamber through an elliptic hole located in anterior region of the fingertip. This chamber is connected to a 2.1 mm diameter hole that goes lengthwise through the whole finger. The hole's centre is located at approximately $0.2L$ from the anterior region of the finger and follows the finger's curvature.

5.2.3.2 Phalanges design

The proximal and middle phalanges are slightly curved cylinders that follow the finger's flexion. The shape of the distal phalanx is similar to a curved cone. However, the vertex was replaced by a half of sphere with a radius of 0.25 mm. The extremities of the phalanges near the chamber are cut along the chambers shape. The distance between the top of the fingers and the top of the distal phalanges was defined according to the values from A. Buryanov and V. Kotiuk's study [90]. The considered value was the mean length of the soft tissues plus the standard deviation. The length of the soft tissues in the designed fingers corresponds to 63% of this value. Figure 5.6 illustrates the internal components that compose the fingers.

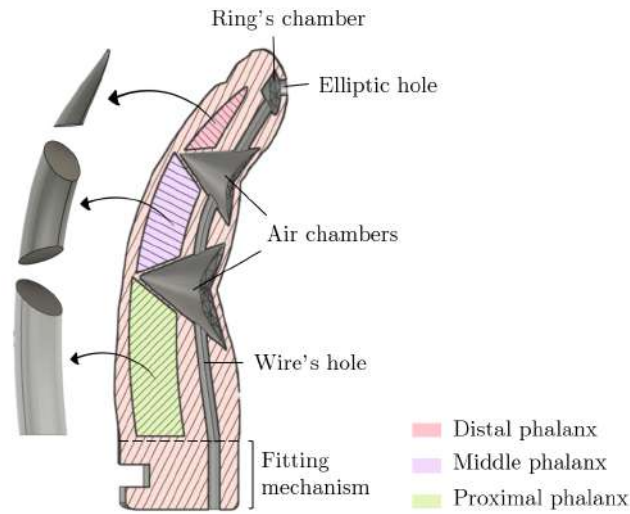


Figure 5.6: Inner mechanisms of the index finger: cut along the sagittal plane of the index finger and shape of the designed phalanges (left).

The phalanges' diameter was defined by crossing two studies: F. P. A. Buryanov and V. Kotiuk's study [90] as well as Schulter-Ellis and G. T. Lazar's study [91], which have performed analyses about the morphology of the human phalanges. By using *ImageJ* software [92], an open-source image processing software, it was possible to measure the projection of the midshaft width of each phalanx. These measures were made using an antero-posterior X-ray of a human hand from A. Buryanov and V. Kotiuk's study, displayed in Figure D.1. Each phalanx was measured ten times using *ImageJ*, and the considered value was the mean of these ten measurements (D). This value was compared with the mean (X) and standard deviation values from the F. P. Schulter-Ellis and G. T. Lazar's study. Then, it was verified if D was within the range of $[X \pm SD]$. The frontal plane was used to assess all the fingers, except for the thumb, in which the sagittal plane was used. Finally, the considered diameter for each phalanx design was equal to $0.63D$. Table 5.2 summarizes all the used values. The measurements made with *ImageJ* software are available in Appendix D.

5.2.3.3 Fitting mechanism design

The fitting mechanism is the structure that allows the fingers to fit in the metacarpal region. It is composed by three segments, each with 3 mm high. In distal-proximal order, the first segment is an extension of the fingers' base. The second and third segments have a diamond shape and the second one is smaller. The bottom edges of the third segment were rounded. Figure 5.7 shows the transversal sections of the three segments that compose the fitting mechanism.

Table 5.2: Phalanges' design values (mm): all the values were within the range of $[X \pm SD]$ [91].

Phalanges		Measured Diameter (D)	X [91]	SD [91]	$[X \pm SD]$ [91]	Considered Phalanx Diameter ($0.63D$)
Thumb	Distal	5.64	5.09	0.76	[4.33; 5.85]	3.55
	Proximal	7.31	6.97	0.92	[6.05; 7.89]	4.61
Index	Distal	6.22	5.64	0.77	[4.87; 6.41]	3.92
	Middle	8.99	9.35	0.45	[8.90; 9.80]	5.66
	Proximal	10.50	10.12	1.06	[9.06; 11.18]	6.62
Middle	Distal	5.91	6.06	0.66	[5.40; 6.72]	3.72
	Middle	9.30	9.47	0.70	[8.77; 10.17]	5.86
	Proximal	10.94	10.40	0.83	[9.57; 11.23]	6.89
Ring	Distal	5.25	5.57	0.92	[4.95; 6.19]	3.31
	Middle	9.20	9.01	0.70	[8.31; 9.71]	5.80
	Proximal	10.11	9.77	0.73	[9.04; 10.50]	6.37
Little	Distal	5.00	4.61	0.70	[3.91; 5.31]	3.15
	Middle	7.68	7.60	0.66	[6.94; 8.26]	4.84
	Proximal	8.61	8.93	0.88	[8.05; 9.81]	5.43

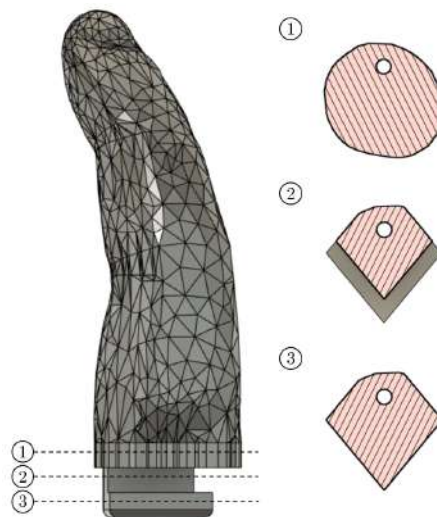


Figure 5.7: Fitting mechanism design with the different transversal sections of the segments that compose the fitting mechanism.

5.2.3.4 Metacarpal region design

The metacarpal region was designed using the *Loft* tool from the *Fusion 360* software. This tool connects different sketches located in different planes. This connection was oriented by rails, aiming to give the metacarpal region the desired anthropomorphic

shape. The majority of the rails were obtained by crossing the replica of the child's hand with different planes, and then redrawn according to the prosthesis' desired features.

The first step was to outline the hand shape by projecting it in the frontal plane. On the distal region, it was ensured that there was a spacing of at least 0.9 mm between each finger. The little finger was placed at a different level from the other fingers.

The proximal region was designed in order to better fit the child's stump. Therefore, the resulting file from the scanning of the stump was also modified and scaled to 110%. Then, the stump location was designed and customised in order to better accommodate the child's affected limb. Figure 5.8 shows the modifications made on the left limb extremity.

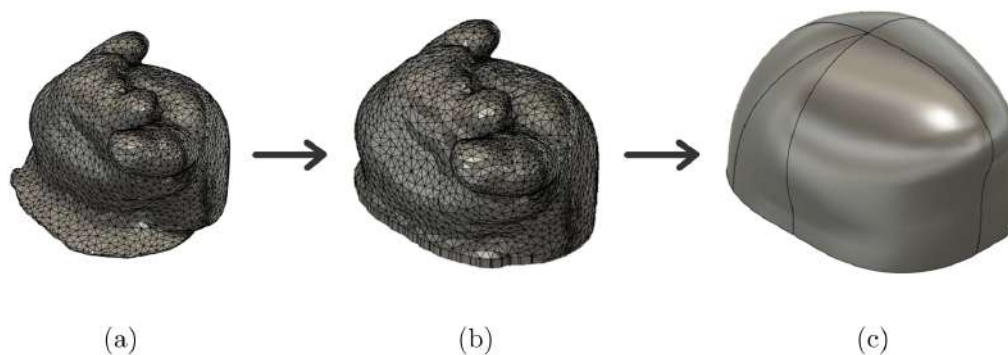


Figure 5.8: Left limb extremity modification process: (a) original replica of the mould of the child's left limb extremity; (b) removal of the excess of material and 110% scaling; (c) stump location design (positive mould).

After the metacarpal region was shaped, their inner mechanisms were designed. The stump-prosthesis interface and the fitting mechanism for the fingers were designed by removing material from the metacarpal region structure. In the palmar region, the diamond-shaped holes were added in order to ventilate the stump-prosthesis interface and to allow the child's skin to breathe.

Similarly to the fingers, the metacarpal region also contains an air chamber located in the metacarpophalangeal joints' zone to simulate their movement. This chamber has a 30° opening and is centred 20 mm above the top of metacarpal region component. Although the transversal section length varies along the metacarpal region, the chamber has a constant depth, which is equal to 75% of the length of little finger's transversal section where the chamber's vertex is centred.

The wires' holes start in the anterior region of the metacarpal structure and end at the posterior region of the wrist, outside the metacarpal region, forming a smooth curved path for the tendon cables go through. The holes have a diameter of 2.1 mm and are protected by a two-layer wall outside the metacarpal region. In the posterior region, their centres are 5.1 mm apart and follow the curvature of the bottom of metacarpal region.

In the wrist zone, two holes were added, one each side, in order to fit the thermo pins that connect the gauntlet to the terminal device, as in *Phoenix Hand v2* prosthesis [77]. Figure 5.9 illustrates the design of the metacarpal region.

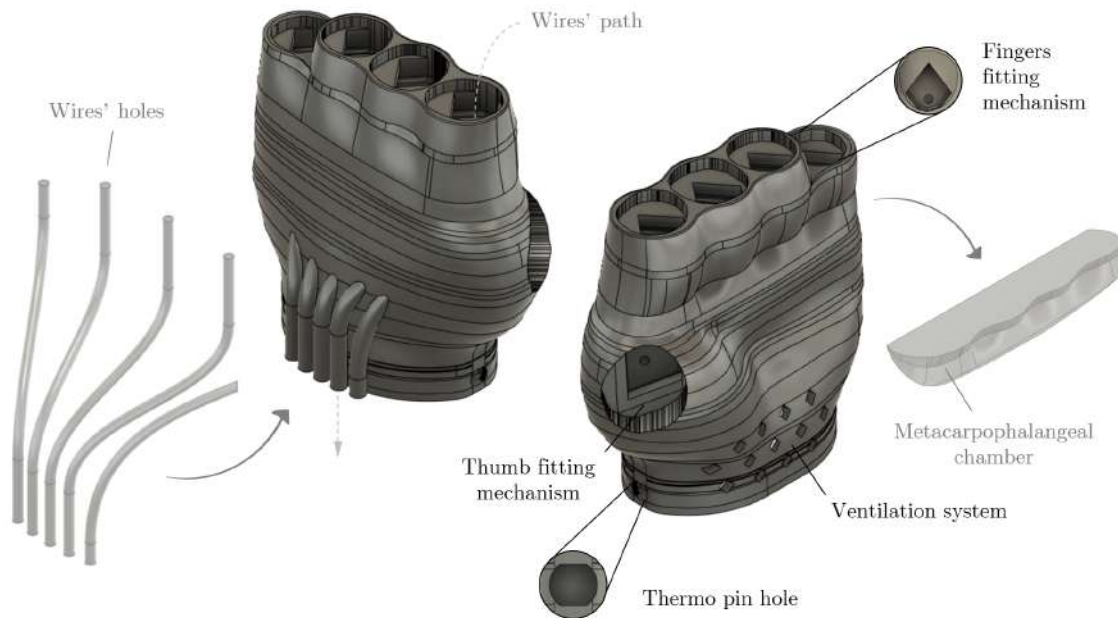


Figure 5.9: Metacarpal region design: lighter grey structures represent the inner mechanisms, in this case, the positive mould of the metacarpophalangeal chamber and the wire's holes.

Finally, an additional component was designed so it could be used as a printing modifier. Thus, the flexion of the metacarpophalangeal joint could be simulated since the modifier and the remaining metacarpal region were printed with different infill percentages. This component has the same shape as the designed metacarpal region and was also designed with the *Loft* tool. The used sketches were smaller and consisted of a -0.9 mm offset when compared to the previous sketches designed for the metacarpal region. The resulting body was then cut along a curve that simulates the thenar crease and along the shape of the stump location. This component is presented in Figure 5.10.

5.2.3.5 Thumb design

The thumb was designed differently from the other fingers due to its different location and anatomical features. Therefore, it was the last finger to be addressed and was designed in the last stages of the metacarpal region.

The first step was to choose the thumb location, which was defined by analysing the replica of the child's healthy hand. Then, the thumb's fitting mechanism was design similarly to the fitting mechanism from the remaining fingers (see Subsection 5.2.3.3).

Unlike the other fingers, no curvature was added to the thumb as it was already present in the scanned model. The thumb was designed with the same mechanisms as

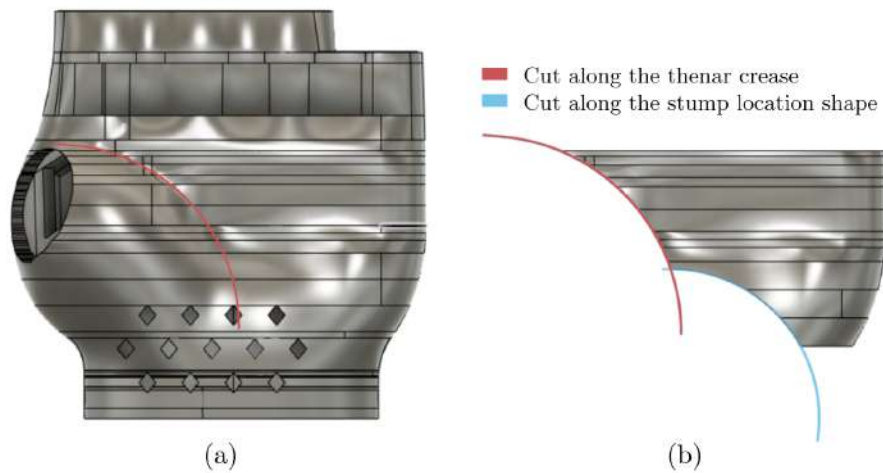


Figure 5.10: Design of the metacarpal region modifier: (a) anterior view of the metacarpal region; (b) anterior view of the metacarpal region modifier. The red curve corresponds to the design of the thenar crease and the blue curve to part of the shape of the stump location.

the remaining fingers: a conic chamber located in the interphalangeal joint's zone with 60° opening angle; an additional chamber in the fingertip with an elliptic hole and a 2.1 mm diameter hole that conducts the tendon cable. However, due to the thumb's location, this hole presents some differences regarding the remaining fingers. Figure 5.11 presents the design of the thumb.

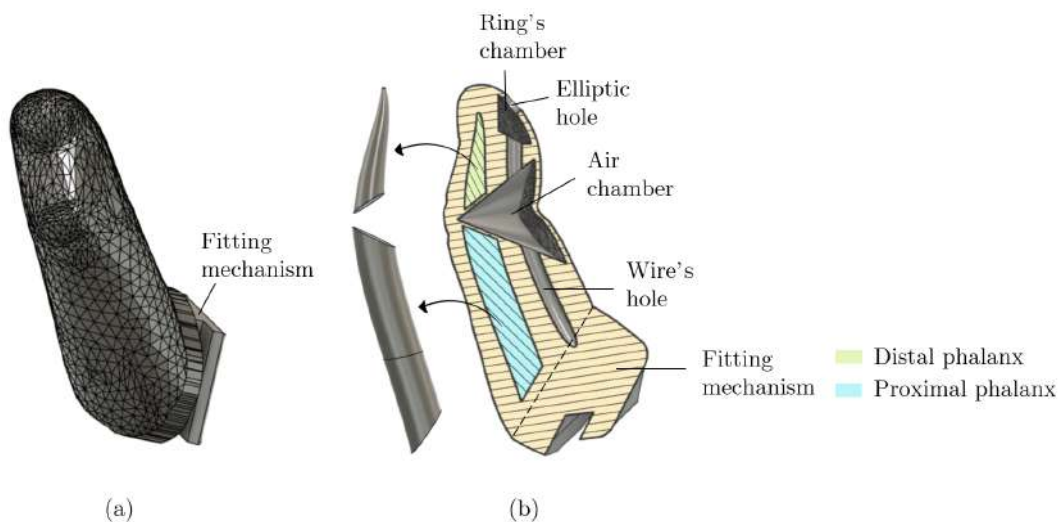


Figure 5.11: Thumb's design: (a) latero-posterior view of the thumb's design; (b) cut along the sagittal plane of the thumb and shape of the designed phalanges (left).

5.2.3.6 Wrist design

The design of the wrist was performed by adapting components from both the *Phoenix Hand v2* and the *Raptor Reloaded* [75] prostheses. These components were used to test the functionality of the developed prosthesis while using different tensioning systems. Figure 5.12 shows the components from the *Phoenix Hand v2* and *Raptor Reloaded* prostheses that were used. The thermo pins and the gauntlet were the only components which suffered modifications: the thermo pins were shortened according to the layer's width and height and the gauntlet had to be increased so it could fit the metacarpal region structure without damaging it. These modifications are displayed in Figure 5.13.

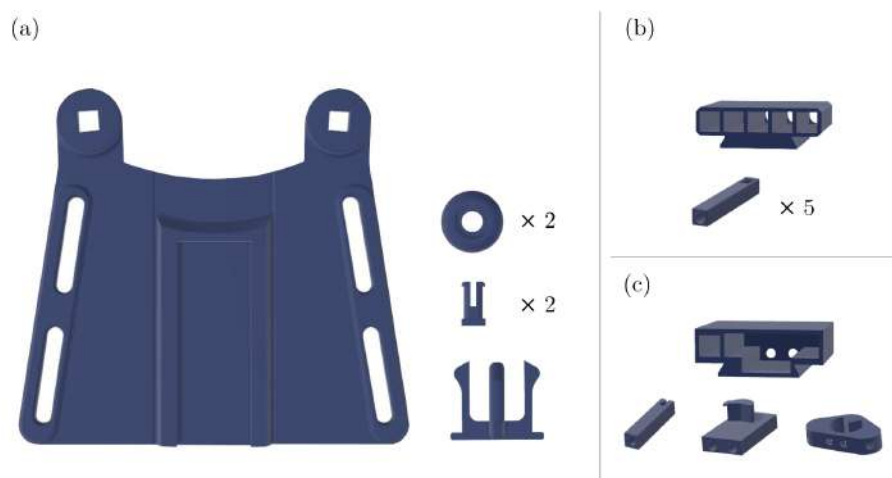


Figure 5.12: Components from *e-NABLE*'s prostheses used in the designed prosthesis: (a) components from the *Phoenix Hand v2* prosthesis. These components were used in all the functionality tests; (b) components of the tensioning system of the *Raptor Reloaded* prosthesis; (c) components of the tensioning system (whippletree) of the *Phoenix Hand v2* prosthesis.

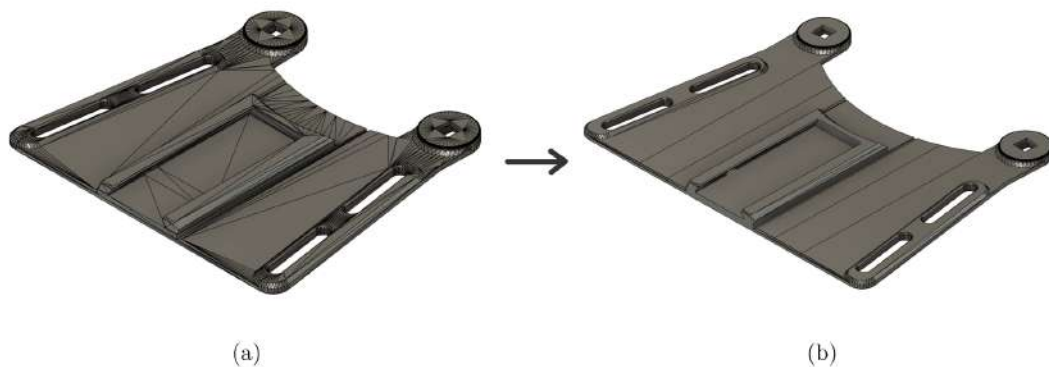


Figure 5.13: Gauntlet modification process: (a) original gauntlet from the *Phoenix Hand v2* prosthesis; (b) modified gauntlet. It had to be increased so it could fit the metacarpal region structure without damaging it.

Before any modification, it was necessary to identify the scaling percentage that better fitted the child. This value was identified according to the measurements performed on the child's healthy limb, namely the width and length of the sound hand (which correspond to the values B and C, respectively, presented in Appendix C). By using the *Multi-hand Sizing Guide*, available in *e-NABLE*'s platform, the scaling percentage was obtained [85].

5.2.4 Tuning of the printing parameters

The developed prosthesis is composed of a combination of flexible and rigid materials. The fingers and the metacarpal region were printed using *Filaflex 82A*, the wrist components were printed using PLA and the rigid rings as well as the testing pieces designed for pull tests were printed using [polyethylene terephthalate glycol \(PET-G\)](#).

Throughout the design of the fingers, several printing tests were made in order to determine the printing parameters of *Filaflex 82A* that would lead to the best printing quality and highest level of functionality. A good printing quality means that the models are printed with the fewest defects such as layers layer shifting, bad adhesion between layers, excess of extruded materials or void formation, among others. A high level of functionality means the printed models are easily flexed and have a similar behaviour to the human hand.

The 3D printer used during these tests was *The Original Prusa i3 MK3S+* by ©Prusa Research. The printing parameters were defined using the *PrusaSlicer* slicing software (version 2.2.0) [62].

During these tests, two main sets of parameters were defined: a first set (A) selected based on the technical data of the *Filaflex 82A* filament, and a second one (B) which consists of an improvement of the first set. However, besides the performed tests between these two sets of parameters, additional printing testings were performed, aiming to maximise the printing quality and the functionality of the fingers. The tests between set A and B were not significant for the present study as they led to several printing defects.

The main variables that were tested were: the number of printing walls, the infill, the printing speed, the amount of extruded material and the retraction. Figure 5.14, Figure 5.15 and Figure 5.16 present the printing parameters that were changed during these tests. Each branch of these figures correspond to the setting tabs of the *PrusaSlicer* software.

The printing position was also tested. Besides using nude *Filaflex 82A*, brown *Filaflex 82A* and white *Filaflex 70A* were also used during the tests. The search for the ideal parameters was obtained through an iterative process. Considering the visual features of the model resulting from a test with a certain set of printing parameters, the next test was performed by adjusting the printing parameters of the previous test. The tests were mainly performed over finger models. Appendix E presents the values of the printing parameters from the most relevant tests that were made.

The PLA and PET-G printing settings were the default values from *PrusaSlicer* software. PLA components were printed using the *Generic PLA* parameters as filament settings and *0.15mm QUALITY* parameters as print settings. The PET-G components were printed with *Generic PET* parameters as filament settings. However, the prosthesis' rings were printed using *0.05 ULTRADETAIL* and the testing pieces of the pull tests were printed with *0.15mm QUALITY* as print settings.

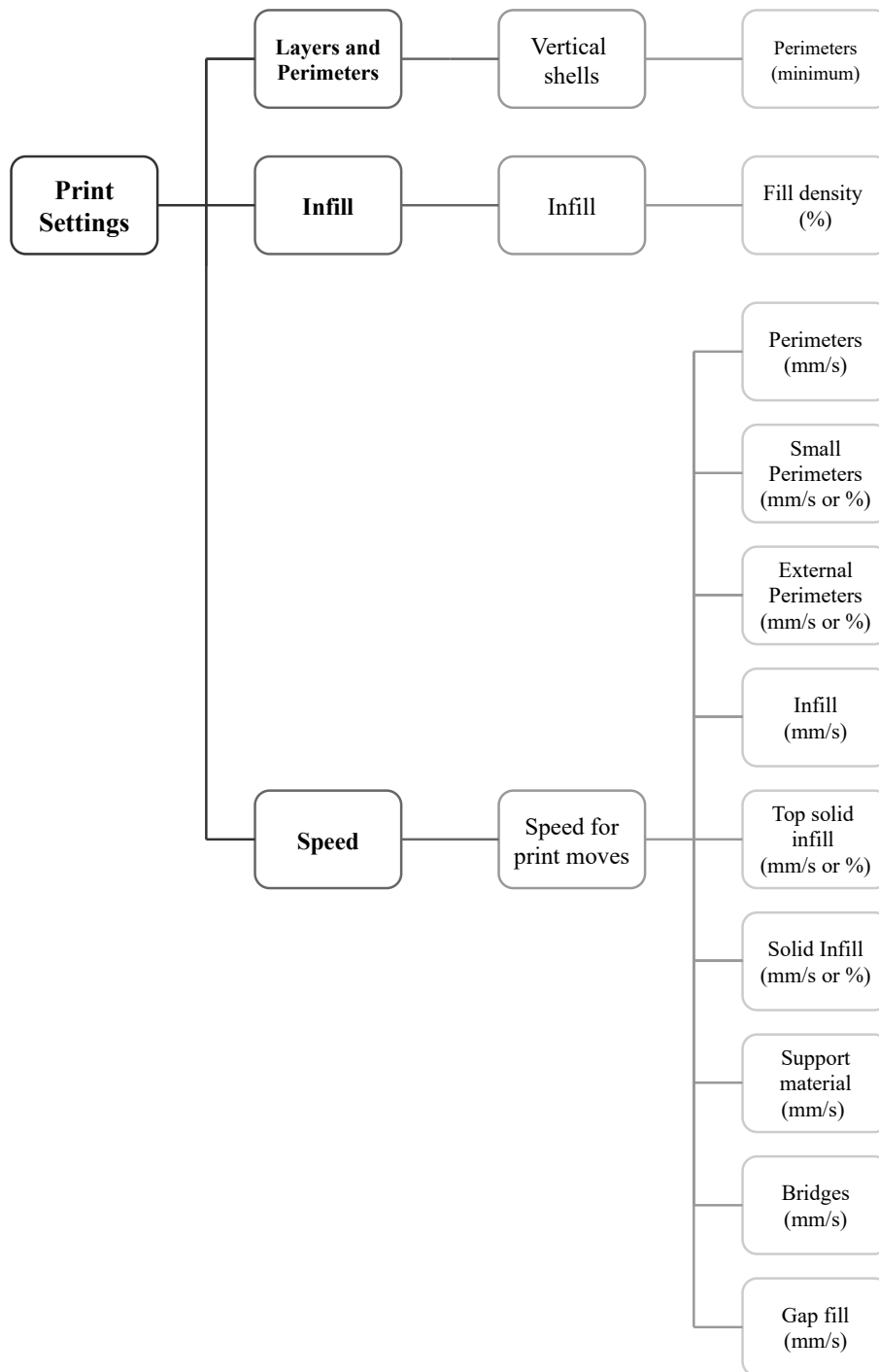


Figure 5.14: Tested printing settings of *PrusaSlicer* software.

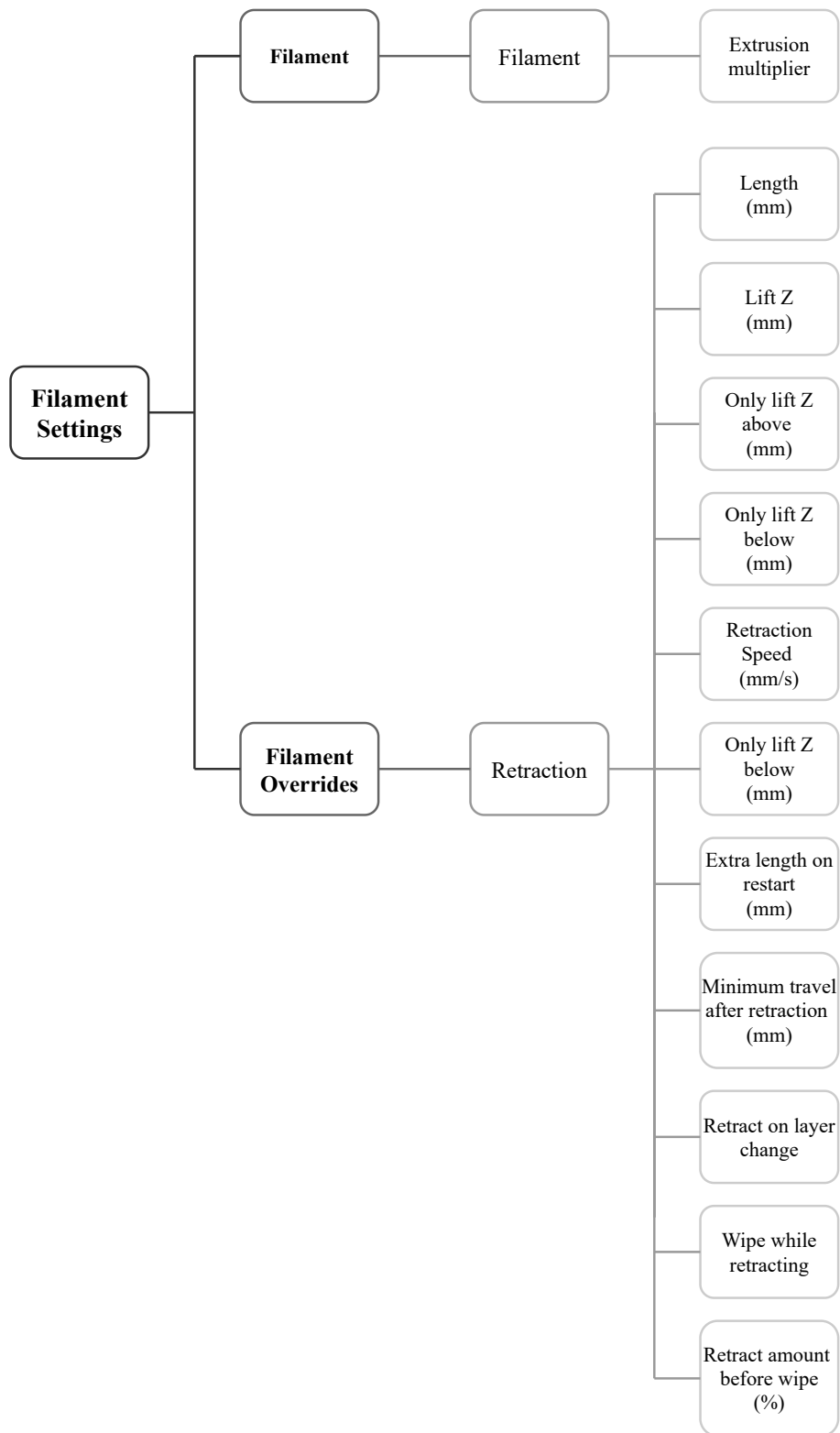


Figure 5.15: Tested filament settings of *PrusaSlicer* software.

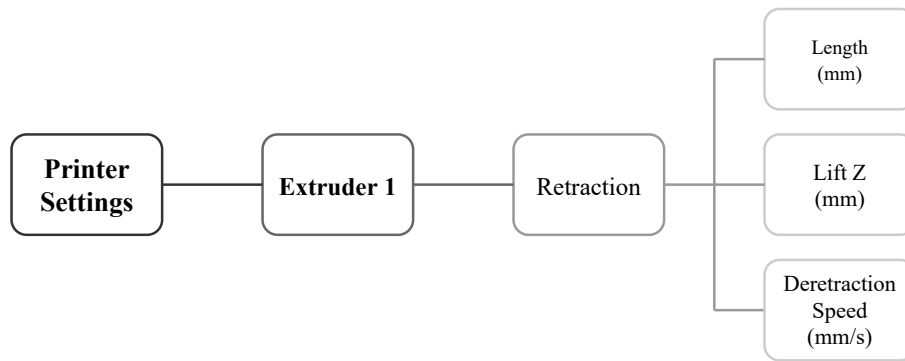


Figure 5.16: Tested printer settings of *PrusaSlicer* software.

5.2.4.1 Pull tests

During the design of the fingers, several models were developed and several printing tests were performed. These tests aimed for the best printing quality and the highest level of functionality, (i.e., the finger models that needed the smaller flexion forces). While the printing quality was assessed subjectively by looking at the obtained object, the flexural forces were measured using pull tests. Therefore, a protocol was developed in order to measure the force needed to bend each finger model. This protocol is made available in Appendix F.

The finger model under test was placed on a support fixed on an elevated structure with screws, where a guitar string passing through the finger could be pulled vertically. A dynamometer was used to measure the force applied on the fingers. This force was applied by using metallic cylinders which were placed inside a tissue bad tied to the bottom extremity of the dynamometer. Different forces were generated by combining different cylinders of different masses, causing the finger to bend. Consequently, the fingertip suffered an approximately vertical displacement that was measured with a dial gauge. The contact point of the dial gauge was in contact with a horizontal tab fitted to the top of the dynamometer. Hence, when the finger flexed, the dynamometer moved equally. Therefore, it was possible to measure the vertical displacement of the finger by measuring the vertical displacement of the dynamometer. The measurements stopped when the flexion of each finger reached a predetermined displacement of 10 mm. Figure 5.17 schematizes the setup of the described procedure. The design of the fingers' support and horizontal tab are displayed in Appendix F.

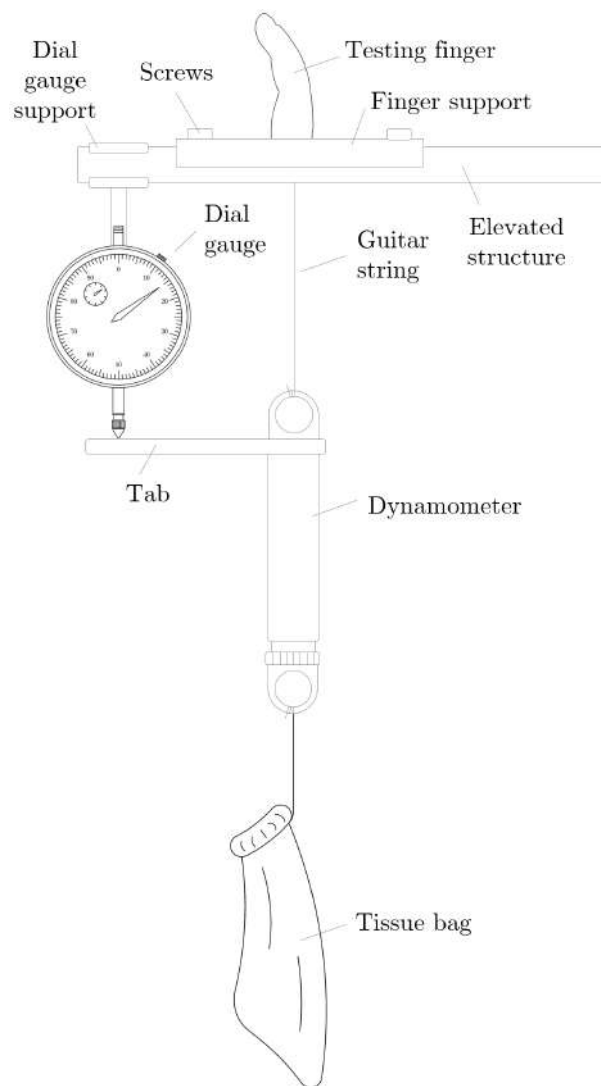


Figure 5.17: Pull tests setup.

5.2.5 Prosthesis assembly

The prosthesis was assembled after completing the component's design, printing and testing. Three similar prostheses were assembled:

1. The first prosthesis' fingers and metacarpal region components were printed with nude *Filaflex 82A* and the remaining components were printed with PLA with a similar colour. Its tensioning system is from the *Raptor Reloaded* prosthesis.
2. The second prosthesis is similar to the first one and the only difference is the brown colour of the filament. Its tensioning system is also from the *Raptor Reloaded* prosthesis.
3. The third prosthesis' fingers were printed with white *Filaflex 70A* and the remaining components with white PLA. The metacarpal region that composes this device has

none of the mechanisms that mimic the metacarpophalangeal joints, namely the air chamber and the modifier. The tensioning mechanism of this prosthesis is a whippetree system as the *Phoenix Hand v2*.

Despite the differences between the three prostheses, their assembly process is very similar.

5.2.5.1 First assembly mode

The first assembly mode corresponds to the assembly of the first and second prostheses, whose tensioning mechanism was inspired in the *Raptor Reloaded* prosthesis.

Figure 5.18 presents the main tools and components needed to assembly the first and second prostheses. The first step was the moulding of the gauntlet to the prosthesis' shape using hot water. Thereunto, the water was boiled in a pan. Then, the gauntlet was dipped in the hot water for ten seconds up to one of the marks that is shown in Figure 5.19. Afterwards, the gauntlet was moulded by pushing it against a flat surface like the sides of a box. When one of the sides of the gauntlet was moulded, the process was repeated for the other side. During this process it was important to take into account the opening of the bottom of the metacarpal region so the gauntlet could fit.



Figure 5.18: Prosthesis' components and needed tools for its assembly: 1. Matchsticks; 2. Measuring tape; 3. Thread; 4. Needle; 5. Scissors; 6. Phillips head screwdriver; 7. Fine tip tweezers; 8. Round nose plier; 9. Cutting plier; 10. Rings; 11. Fingers; 12. Metacarpal region; 13. Thermo pins and caps; 14. Gauntlet; 15. Tensioner pins; 16. Tensioner block; 17. M3 screws; 18. Retention clip; 19. Guitar strings; 20. Adhesive foam; 21. Paper moulds; 22. Grosgrain ribbons; 23. Velcro tape.

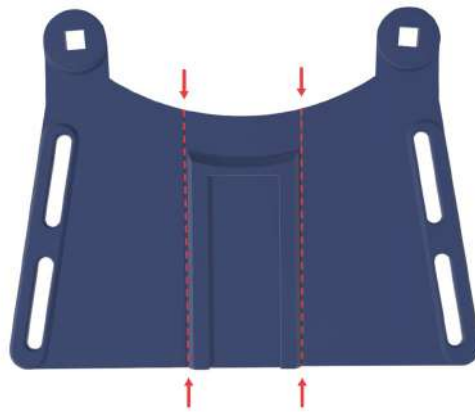


Figure 5.19: Marks for moulding the gauntlet in hot water.

After moulding the gauntlet, the stump-prosthesis interface was covered with self-adhesive foam. The foam was placed in three different main spots of the stump: on the distal region, posterior region and laterally. The shape of the foam was first outlined with a paper sheet. If the paper mould fitted the stump-prosthesis interface, then the self-adhesive foam would be cut in that same shape and placed on the prosthesis. Figure 5.20 shows the stages of this process.

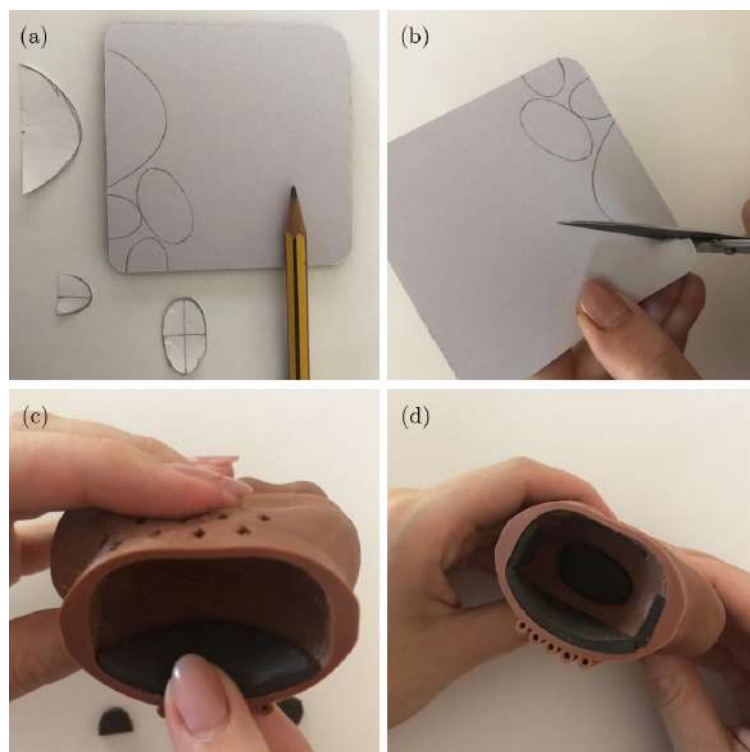


Figure 5.20: Stages of the placement of the self-adhesive foam: (a) transference of the paper moulds to the adhesive foam; (b) cut of the adhesive foam; (c) placement of the adhesive foam in the stump-prosthesis interface; (d) result of the placement of the different pieces of adhesive foam.

The next step was the assembly of the gauntlet to the metacarpal region. The two thermo pins were inserted into the metacarpal region structure and then the gauntlet was fitted in the outer side of these two pins. Finally, the two thermo pins caps were introduced to fix the gauntlet. This process is shown in Figure 5.21.



Figure 5.21: Connection between the gauntlet and the metacarpal region structure: (a) fitting of the thermo pins in the metacarpal region structure; (b) fitting of the gauntlet in the thermo pins; (c) introduction of the wrist pin caps.

The tensioner system was the next component to be assembled, as it is exemplified in Figure 5.22. Initially, the first tensioner pin was inserted in the tensioner block with its hole facing up. Afterwards, it was screwed with M3 screws about half-way, using a Phillips head screwdriver. The process was repeated for the remaining tensioner pins. After all the tensioner pins were inserted and screwed to the tensioner block, the block was slid into the gauntlet and fixed with the retention clip.

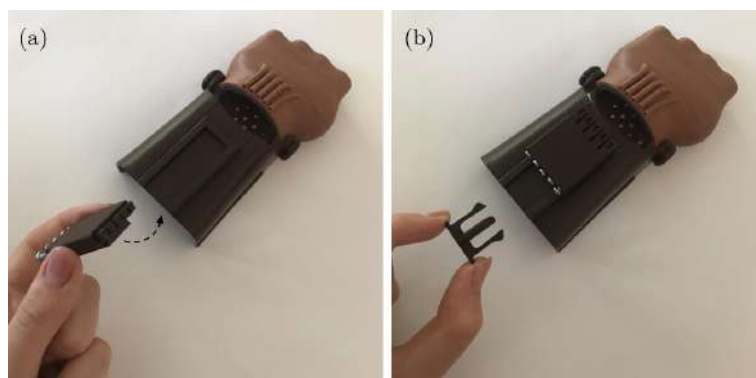


Figure 5.22: Assembly of the tensioner system: (a) insertion of the tensioner block in the gauntlet after screwing the tensioner pins; (b) blocking of the tensioner block with the retention clip.

The following stage was the assembly of the fingers. Before fitting them in the metacarpal region structure, a 0.032 in (≈ 0.81 mm) nylon guitar string (corresponding to a guitar's second string) was passed through the wire's holes of the fingers and

then through the metacarpal region in distal-proximal direction. The string used for the thumb had a quarter of the length (≈ 290 mm) of the original string. The string used for the remaining fingers had a third of the length (≈ 380 mm) of the original string. When the strings were inside the two structures, the fingers were fitted in the metacarpal region, and the proximal extremities of the wires were tied to the tensioner pins. This process is illustrated in Figure 5.23. During this process, a round nose plier was used to help to pull the strings while tying the knots. When all the fingers were fitted and the strings were tied to the tensioner pins, the PET-G rings were inserted into the distal extremity of the strings and tied as close as possible to the finger. After tying the knots around the rings, the rings were inserted in the chambers located in fingertips with the help of fine tip tweezers. Finally, all the excess of string on both sides was cut off, as it can be seen in Figure 5.24.

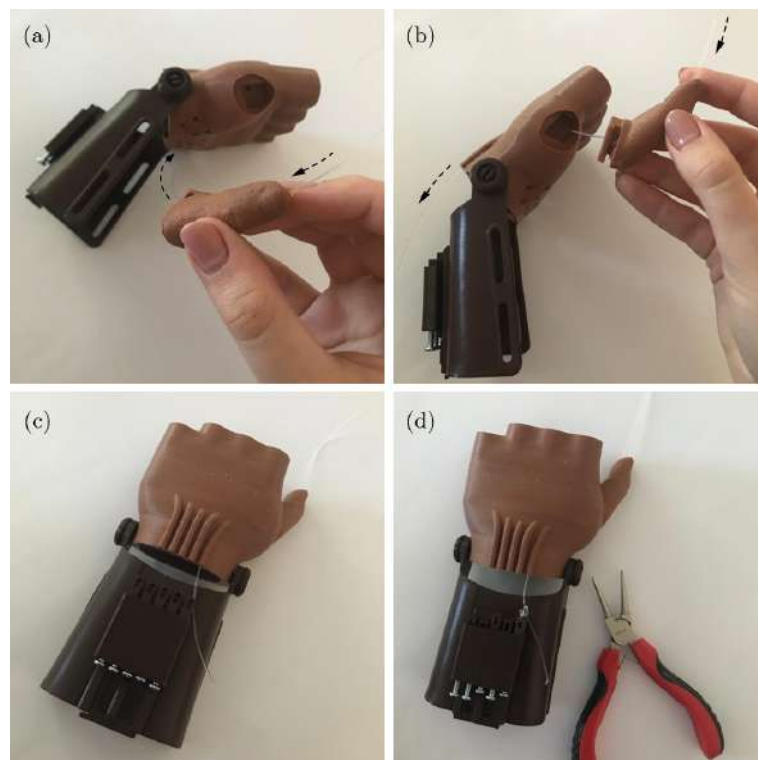


Figure 5.23: Assembly of the fingers: (a) insertion of the guitar string in the wire's holes of the fingers in distal-proximal direction; (b) insertion of the guitar string from the finger into the metacarpal region; (c) fitting of the finger (thumb) in the metacarpal region; (d) proximal extremity of the wire tied to the tensioner pin.

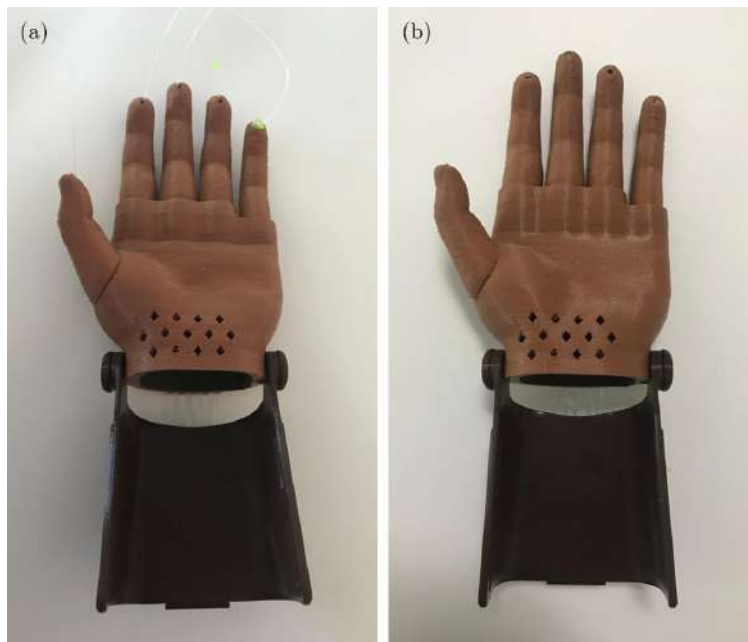


Figure 5.24: Insertion of the PET-G rings: (a) rings tied to the strings near the finger; (b) cut of the strings excess after tying and inserting all the rings into the fingertips chambers.

The last stage of the prosthesis' assembly was the straps. The straps consist of two Grosgrain ribbons and two pieces of adhesive Velcro tape. The dimensions of the ribbons and tape are shown in Figure 5.25. After cutting the straps, their extremities were burned with a matchstick, so that the straps did not shred. Before sewing the straps to the gauntlet, the Velcro tape was fixed, and the straps were ironed in order to increase adhesion. During the ironing, the straps were protected by a towel, so the Velcro tape would not melt. Figure 5.26 presents the process of burning the straps' extremities and sewing.

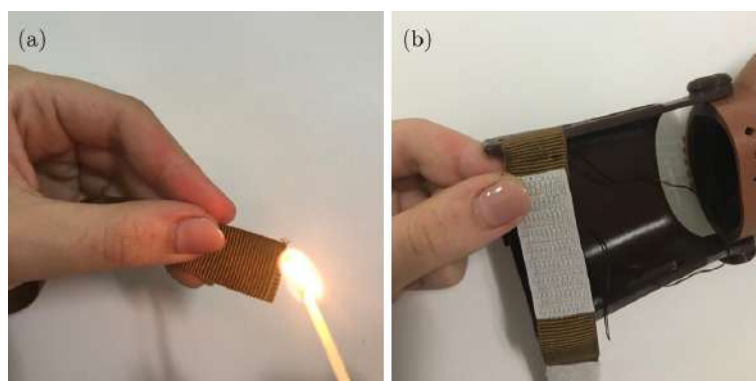


Figure 5.25: Dimensions of the Grosgrain ribbons and Velcro tape.

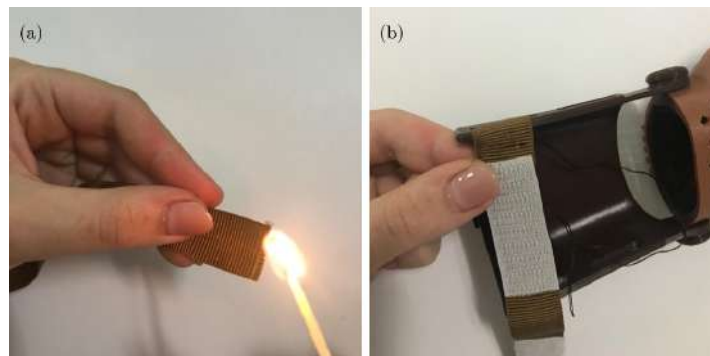


Figure 5.26: Assembly of the straps: (a) burning of the Grosgrain ribbons' extremities; (b) sewing of the straps to the gauntlet.

5.2.5.2 Second assembly mode

The second assembly mode was inspired in the *Phoenix Hand v2* prosthesis, which uses a whippetree system as tensioning mechanism. This mode of assembly was used on the third prosthesis, which was designed with the aim of testing some of the concepts that were developed in the course of this study, but did not work in the original developed prosthesis. Despite the differences regarding the tensioning mechanism, some assembly steps are equal for both modes. Figure 5.27 presents the needed materials and tools to assembly this prosthesis.

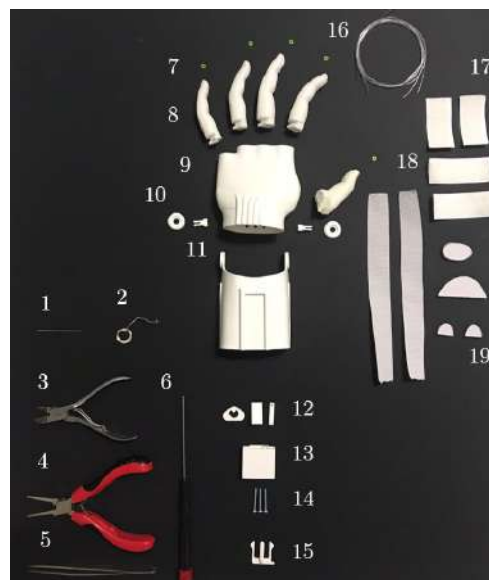


Figure 5.27: Third prosthesis' components and needed tools for its assembly: 1. Needle; 2. Thread; 3. Cutting plier; 4. Round nose plier; 5. Fine tip tweezers; 6. Phillips head screwdriver; 7. Rings; 8. Fingers; 9. Metacarpal region; 10. Thermo pins and caps; 11. Gauntlet; 12. Whippetree, swivel pin and thumb tensioner pin; 13. Gripper box; 14. M2.5 screws; 15. Retention clip; 16. Guitar strings; 17. Velcro tape; 18. Grosgrain ribbons; 19. Adhesive foam.

The first step was the insertion of the wrist pins. The thermo pins of this prosthesis present some differences when compared with the ones of the original prosthesis. These pins had to be inserted from the inside of the stump-prosthesis interface and were designed differently, since the metacarpal region structure was not flexible and their fitting system had to be modified. Figure 5.28 presents the design of the metacarpal region of this prosthesis as well as its pins and Figure 5.29 presents their assembly. After assembling the thermo pins, the adhesive foam was placed and the gauntlet was connected to metacarpal region structure.

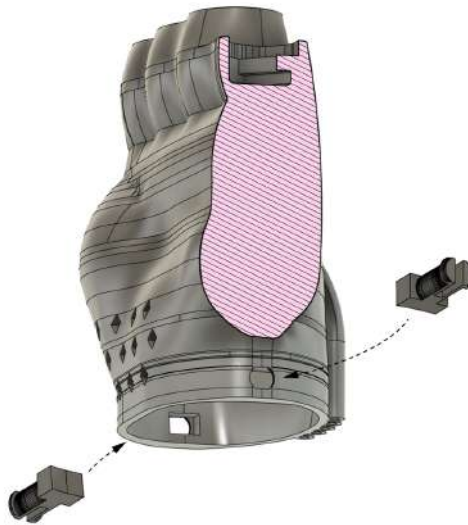


Figure 5.28: Design of the metacarpal region and thermo pins of the third prosthesis: the sectional cut shows the absence of the chamber that mimics metacarpophalangeal joints.

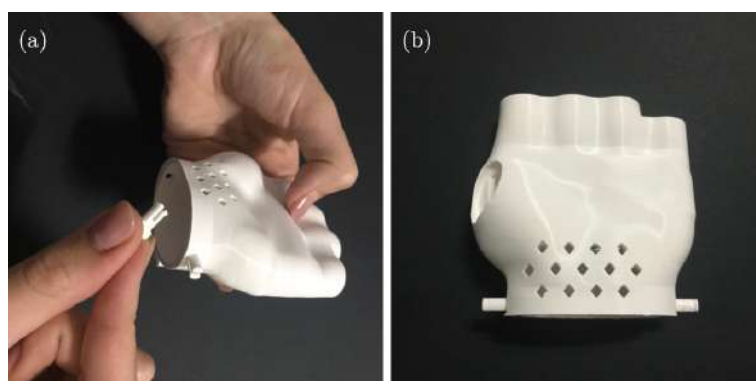


Figure 5.29: Fitting of the pins in the metacarpal region of the third prosthesis: (a) the pins are fitted from the inside of the stump-prosthesis interface in the counterbored holes; (b) thermo pins after being fitted in the metacarpal region.

The fingers' assembly was also different, as they are connected with each other through the whipltree system. The index is connected to the little finger and the middle finger is connected to ring finger by the same guitar strings. The used strings had a half of the

length (≈ 580 mm) of the original string. The thumb was not connected to any finger. Therefore, the length of the string used to operate the thumb remained the same (≈ 290 mm) as well as their assembly process. For the remaining ones, the strings were inserted in one of the fingers in distal-proximal order, passed through the metacarpal region and through the whippetree. Then, the inverse path was made and the connection to the other finger was made in proximal-distal order and then inserted in the other finger. The string of the pair index-little fingers was passed through the external holes of the whippetree component and the string of the pair middle-ring was passed through the internal holes. After connecting each pair of fingers, the fingers were fitted in the metacarpal region structure. Figure 5.30 illustrates the stages of the process of connecting the metacarpal region to the fingers.

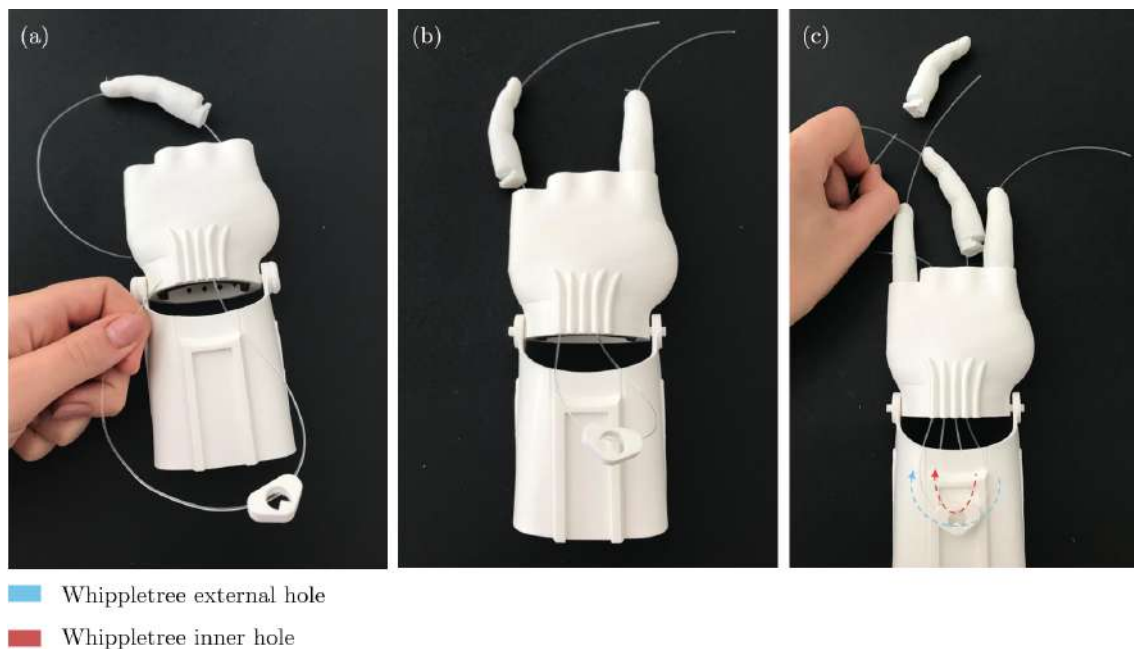


Figure 5.30: Connection of the fingers to the metacarpal region: (a) the strings connect the fingers (except for the thumb) and are inserted in distal-proximal order, then pass through the whippetree holes and are then inserted by doing the inverse path; (b) the fingers are fitted in the metacarpal region after being connected; (c) the index connects to the little finger and the string passes through the whippetree external hole, while the middle connects to the ring finger and the string passes through the inner hole.

When all the fingers were fitted, the gripper box was slipped into the gauntlet and the whippetree component was placed inside the gripper box along with the swivel pin, as indicated in Figure 5.31. Then, the gripper box was slid as forward as it could go and the swivel pin was fixed with two M2.5 screws. After fixing the swivel pin, the retention clip was placed. Once it moves independently, the thumb was tied to tensioner pin and the pin was fixed with other M2.5 screw. Then, the rings were inserted in the distal extremities of the strings and tied to them. The rings were introduced in the fingertips'

chambers and the excess of wire was cut off. Finally, the straps were assembled.

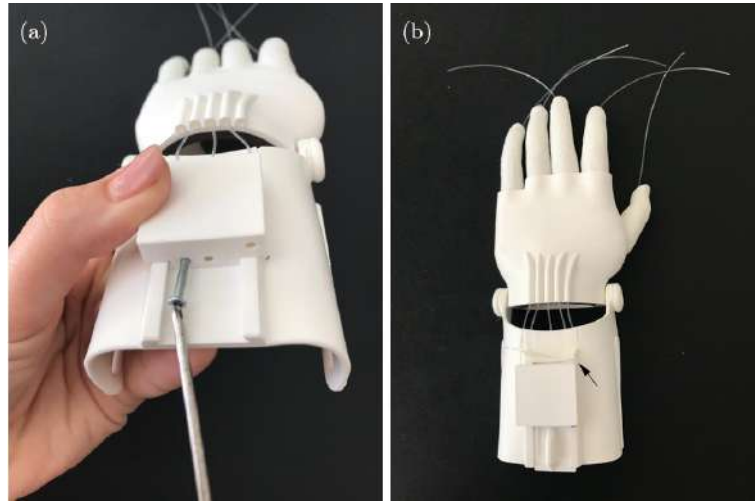


Figure 5.31: Assembly of the tensioning system of the third prosthesis: (a) fixing the swivel pin with screws to the gripper box after placing the whippletree and the swivel pin inside the gripper box; (b) tying of the thumb to the tensioner pin.

5.2.6 Prosthesis evaluation

The evaluation of the prostheses was made after the assembly of the three devices. The three devices were evaluated in terms of functionality and cosmetic appearance. The development costs, the total of printing time and their weights were also assessed.

In addition, the resulting prostheses were presented to the child and his family. In order to measure their level of satisfaction, a survey with the [System Usability Scale \(SUS\)](#) was used. This tool allows to measure the usability of a wide variety of products or services. It is composed by ten questions with five response options that goes from “Strongly agree” to “Strongly disagree”, which correspond to 5 and 1 scores, respectively. These responses were then converted to a score calculated according to the equations 5.1, 5.2 and 5.1, in which x_y is the score of the question y . The score’s scale ranges from 0 to 100 and a score above 68 is considered to be above average [93, 94].

$$a = \sum_{i=1}^5 x_{2i-1} - 5 \quad (5.1)$$

$$b = 25 - \sum_{i=1}^5 x_{2i} \quad (5.2)$$

$$SUS_{score} = (a + b) \times 2.5 \quad (5.3)$$

Besides the standard questions that compose the SUS, ten additional questions were also developed. These questions follow the logic of the SUS questions and are specific to

the developed prostheses in this study. Since this second questionnaire is similar in terms of positive and negative connotation to the SUS questions, this questionnaire was evaluated using the same formulas. Appendix [H](#) presents the survey that was presented to child's family.

RESULTS AND DISCUSSION

Developing prosthetic devices that meet the basic user's needs has been challenging. AM have emerged as the solution of some of the main problems of the prosthetic field since it leads to more affordable, lighter and customisable devices. This study aims to present the development of a 3D-printed body powered for a four-year-old child that meets his essential needs while being aesthetically pleasing. During this study, several attempts were made to achieve a high level of functionality and anthropomorphism. This chapter presents and discusses the results of the development process of this prosthesis, in which the several prototypes and created concepts are analysed. Some suggestions for further improvements are also presented.

6.1 Anatomical and Functional Features Assessment

The procedures used to assess the anatomical features of both the child's limbs were chosen in order to meet one of the main goals of this study: a high level of customisation. Capturing the anatomical features is crucial to develop customised prosthetic devices and may be the key to reduce the rejection rate of these devices, especially in younger ages. However, there is a lack of procedures to customise these devices. Over time, Plaster of Paris has been used for socket customisation. However, more recent methods as 3D scanning allied to AM have been the key to develop customised prostheses with a reduction of production costs, time and intermediary steps [17]. Thus, assessing these features was essential for the course of this study. The chosen methods were simple measurements and body casting. The usage of more than one method, due to their redundancy, allowed to reduce to a minimum the need for additional data collection sessions during the prosthesis' development.

The family and the child were actively involved during the whole procedure. Somehow, the parents are users too and sometimes they want the prosthesis more than the child. The procedures took place at the child's home, which helped him to be more confident. Before performing any procedure, the first step was to give the child's confidence. Therefore, some finger's prototypes (already in study at the time) were presented to the

child so he could understand what was happening.

All the questions from the initial data collection form were answered by the child's mother. Both the wrist and elbow joints of the child were functional and able to do the flexion and rotation movements. Using scissors was the most difficult task for the child. However, the child was able to perform all his daily living activities without the help of a prosthesis, including using cutlery to eat. Regarding prosthesis use and prescription, the child had just had contact with the *Unlimbited Phoenix Hand* model from *e-NABLE* platform [95], provided by the *Patient Innovation's* program [83]. The prosthesis was delivered in February 2019, almost a year and half before this study's measurement session.

6.1.1 Measurements

Unlike the measurements and photos from the *e-NABLE* guide [9], which are used to size the prosthesis model before printing, the main procedure to assess both limbs' extremities anatomy was body casting. Thus, the measurements and photos taken within the scope of the defined protocol were performed solely as auxiliary data. Table 6.1 presents the measurements made to both limbs of the child. Figure 6.1 presents the photos that were taken during the first procedure.

Table 6.1: Results of the measures of both upper limbs of the child (cm).

Measurements Identification	1 st Measurement	2 nd Measurement	3 rd Measurement	Mean
A	16.0	15.8	15.9	15.9
B	9.3	9.2	9.3	9.3
C	6.0	6.2	6.0	6.1
D	7.8	8.1	8.1	8.0
E	19.2	19.0	19.2	19.1
F	18.1	18.2	18.3	18.2
G	13.2	13.3	13.2	13.2
H	18.9	18.8	19.0	18.9
I	17.0	17.2	17.1	17.1
J	11.1	11.2	11.2	11.2
K	17.1	17.1	16.9	17.0

Unfortunately, at the time of the procedure, the child was only capable of reproducing one of the three photos (Figure 6.1a). Thus, this episode ended up influencing the following procedures as the child got frustrated with the situation. However, this procedure was later performed by the child's mother so the child could reproduce the photos without any pressure from strangers. The results are displayed in Figure 6.1b-c.

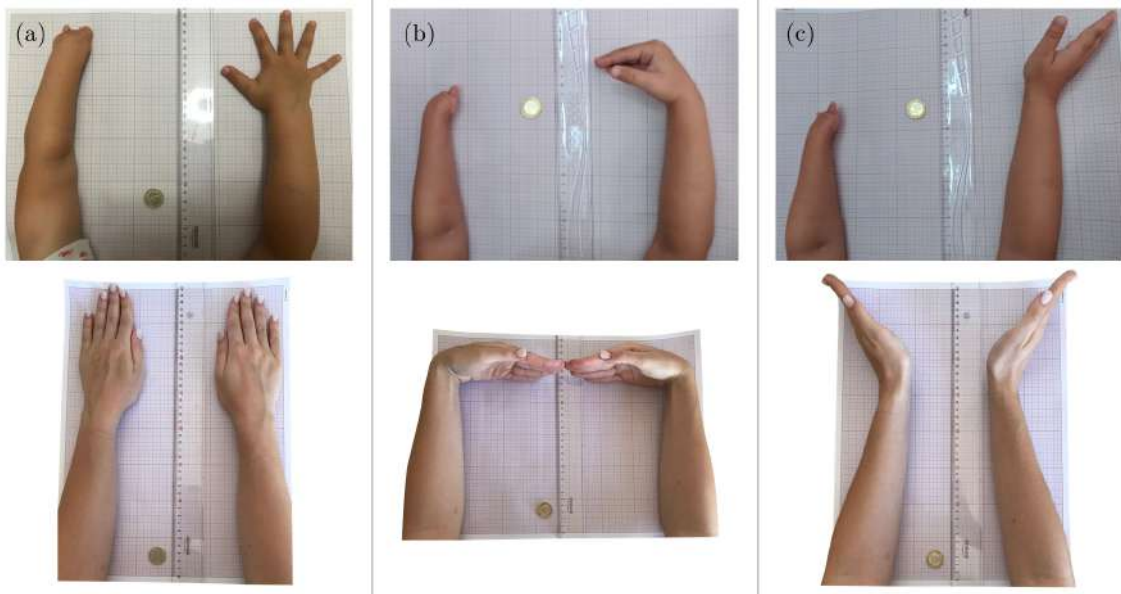


Figure 6.1: Results of the positions' reproduction: the pictures displayed above are the reproduction of the ones displayed below; (a) first position; (b) second position; (c) third position.

6.1.2 Body casting

The casting of the sound hand and stump were used in order to have replicas that could be scanned instead of exposing the child to a long-time consuming procedure that would probably result in damaged data due to involuntary movements of the child [17]. Moreover, having a replica of the child limbs avoided further meetings with the child, since additional measurements that were not taken in sequence of this protocol could have been done without the child being present. However, more than one attempt was necessary to obtain a replica of the sound hand.

The first alginate solution did not solidify. Hence, instead of having a vertical impression, the body casting had to be made with the sound hand placed horizontally. One day after, the plaster was removed from the alginate. However, the replica of the sound hand was broken. The high ambient temperatures at the time and the car trip were the likely reasons for the plaster to break as previous experiments had worked well.

A second attempt was made and cold water was used to retard the alginate solidification. Nevertheless, the child's emotional state and the water's temperature hindered the sound's hands impression as it was difficult to maintain the child quiet. This time, more than one replica was made to avoid repeating the procedure. Although the alginate and the plaster were kept in a fresh environment during the solidification process, the replicas broke once more. This revealed that the fragile character of the fingers was the reason for the replicas to break as they could not stand the alginate's weight.

Finally, a third and last attempt was made due to the persistence of the child's mother. The intention was to replicate the fingers only. Without pressure from strangers it was possible to replicate the whole hand. However, during the sanding process, some fingers broke. Nonetheless, it was possible to join them by using nail polish to seal up the surface and then glue them together. After drying, the defects in the broken area were filled with more plaster and sanded once more. Figure 6.2 presents the results from the three attempts of the body casting procedure that were not successful, and Figure 6.3 presents the replicas that were scanned. As can be appreciated from Figure 6.3, the final results were very good despite the tumultuous process.



Figure 6.2: Body casting failures: (a) first body casting attempt with two broken fingers and presence of air bubbles; (b) second body casting attempt where it was made more than one replica. Both present air bubbles, broken fingers and poor quality; (c) third body casting attempt made by the child's mother with broken fingers.

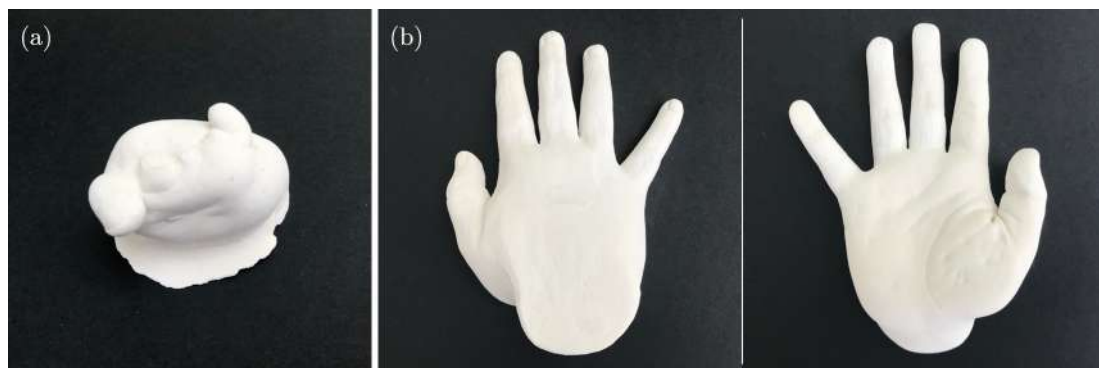


Figure 6.3: Upper limb's extremities of the child replicas made with plaster: (a) left extremity. The left limb has a transverse metacarpal total deficiency resulting from amniotic band syndrome; (b) posterior (left) and anterior (right) views of the right sound hand.

During the development of the protocol to assess the child's anatomical features, photogrammetry was also studied as a potential procedure to assess the anatomical features of the child's upper limbs. Photogrammetry is a technique used to reconstruct 3D objects from bidimensional images based on different perspectives [96]. However, in order to have a full reconstruction of the child's limbs, it would be necessary that the child did not move his limbs while the photos were being taken. This is impossible, even for an adult. The solution was to use a transparent platform where the child could rest his upper limbs, such as a glass or an acrylic board. Therefore, it would be possible to take pictures around the limbs from different perspectives. Nevertheless, when testing this possibility with an adult, the solution ended up failing as the photogrammetry software, *3DF Zephyr* [97], could not reconstruct the photographed object due to the reflex of the glass.

Furthermore, this procedure would have been too much for the child if it had been added to the protocol. Although the chosen procedures were not harmful to the child, it is extremely complicated to predict what will be a child's behaviour during any procedure. At first, the body casting was expected to be appealing for the child due to the colour and consistence of the alginate's solution, but it was still a stressful activity.

Despite the setbacks during the protocol, this protocol can be reproduced with other patients with similar disorders for future work. For this study, the body casting and the measurements would have been enough and there was no need to photograph the child's limbs. Nevertheless, a solution to perform all the procedures would be to perform different procedures in different days. However, this solution may be dependent on the child and family's will.

6.2 3D Scanning

3D scanning was the chosen method to obtain a computer readable representation of the plaster replicas of the child's upper limbs extremities. Figure 6.4 shows the accuracy of the representations resulting from the 3D scanning. This accuracy would not be probably obtained if the scan was performed over the upper limbs of the child rather than on the plaster replicas.

Although three attempts were needed until a replica of the whole sound hand was obtained, the body casting is more advantageous than directly scanning the child's limbs. While the quality of the 3D scanning a body part can be compromised with the patients' movement, the 3D scanning of an object does not have this problem.

In addition, the usage of alginate and plaster is suitable, given their biocompatibility and biodegradability. Alginate is biocompatible and biodegradable and has several biomedical applications such as wound healing, drug delivery and tissue engineering [98]. Plaster of Paris, also known as calcium sulphate, has been used for bone grafting due to its properties, including biocompatibility and biodegradability [99]. Thus, body casting followed by 3D scanning is a safer procedure that leads to better results than the ones resulting from 3D scanning applied directly to the patient.

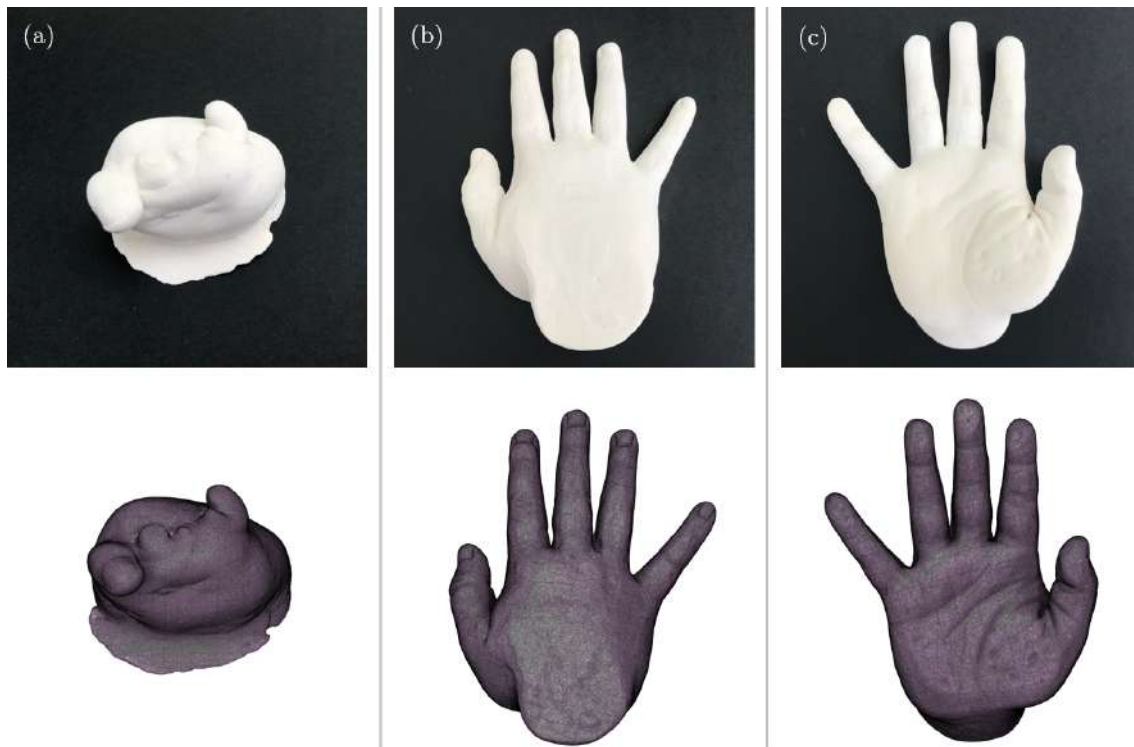


Figure 6.4: Comparison between the plaster replicas (above) and *.stl* files resulting from the 3D scanning procedure (below): (a) left upper limb's extremity; (b) posterior view of the right sound hand; (c) anterior view of the right sound hand.

6.3 Prosthesis Design

The prosthesis' design was made considering the DfAM principles, aiming to achieve the best printing results.

The “Design for orientation” principle was a major concern as the printing position was always considered during the design process. Before designing any component, the printing positions were defined beforehand, since different printing positions result in different mechanical and aesthetical properties. Once defined the printing position, it was possible to consider the other DfAM principles. The “Minimize complications” principle was followed whenever possible and support structures were avoided by using overhang angles higher than 45° from the horizontal.

The entire device has a contour design in which the thickness of the walls of the components that compose the prosthesis are a multiple of the extrusion width and height.

The prosthesis' design was divided in three stages: the fingers, the metacarpal region and the wrist. Therefore, the prosthesis is composed by different components that connect with each other. By being composed by different components, the prosthesis and the printing process are simplified, following the “Segment and bond parts” principle. This segmentation also allows to satisfy one of the user's needs that are required for children:

the easy replacement if anything breaks or if new components are needed due to child's growth. Moreover, the segmentation allows the simplification of the assembly process since the prosthesis' design follows the fifth DfAM principle by being composed by other components that are not 3D printed.

In order to divide the prosthesis's design in stages, the replica of the sound hand had to be segmented in two parts: the fingers and the metacarpal region, so each part could be modified individually. Before this segmentation, the *.stl* file had to be changed, from mesh to body representation. However, *Fusion 360* [80] cannot follow this command for mesh files with a high number of faces. Thus, the number of faces was reduced from 419 190 to 10 000 faces. Figure 6.5 shows the mesh representations before (Figure 6.5a) and after (Figure 6.5b) the reduction operation, in which no significant differences in terms of anatomical features can be seen.

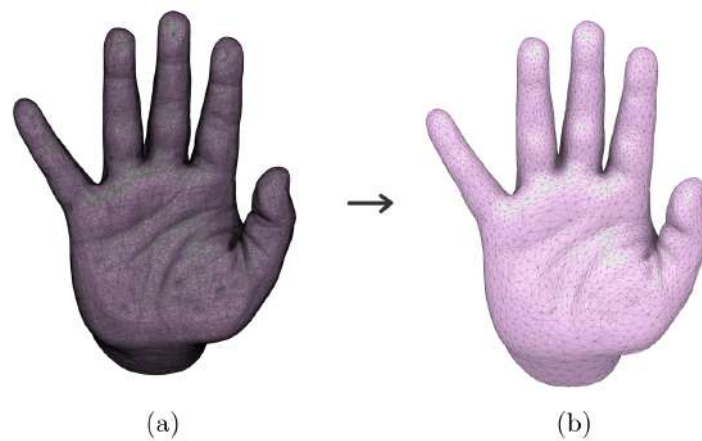


Figure 6.5: Number of faces reduction process: (a) before reduction operation; (b) after reduction operation.

6.3.1 Fingers design

The fingers were the first components to be addressed since there were previous studies about 3D-printed body powered prostheses with fingers made of *Filaflex* [30]. The design of the index was the first to be studied as it would be used as a reference for the remaining fingers, except for the thumb. Therefore, several prototypes were made in order to achieve the best functionality possible.

6.3.1.1 First prototypes

Before assessing the anatomical features of the child, the design of the index finger was already being studied. A 23-year-old female finger was casted and 3D scanned. Therefore, the finger mechanisms could be studied even though there was no anatomical information about the child. Moreover, besides allowing the development of several prototypes for

the fingers, the casting and the 3D scanning of the plaster replica of the female finger were used as a test for the methodology used in the anatomical features' assessment.

The fingers designed by F. Pinheiro had air chambers that ensure that they bend properly [30]. This mechanism was implemented in the designed fingers of this study but underwent some modifications. F. Pinheiro suggested an opening angle for the chambers of 60° for the index finger. However, F. Pinheiro's prosthesis was not conceived for a child. Furthermore, the depth of the chamber was a concrete value that was not suitable for this study. Therefore, the first prototype was designed with air chambers with a 60° opening angle and a depth of 90% of the transversal section length where the chamber's vertex is inserted. Besides the air chambers, these prototypes also have three cylinders that simulate the phalanges. Figure 6.6 shows the female finger plaster replica, as well as its 3D scanning resulting presentation and the last prototype made from the replica of the female's finger. Although these first prototypes were far from the final design, they end up being very useful as a mean to gain the child's trust during the assessment of his anatomical features and to explain the purpose of the whole session.

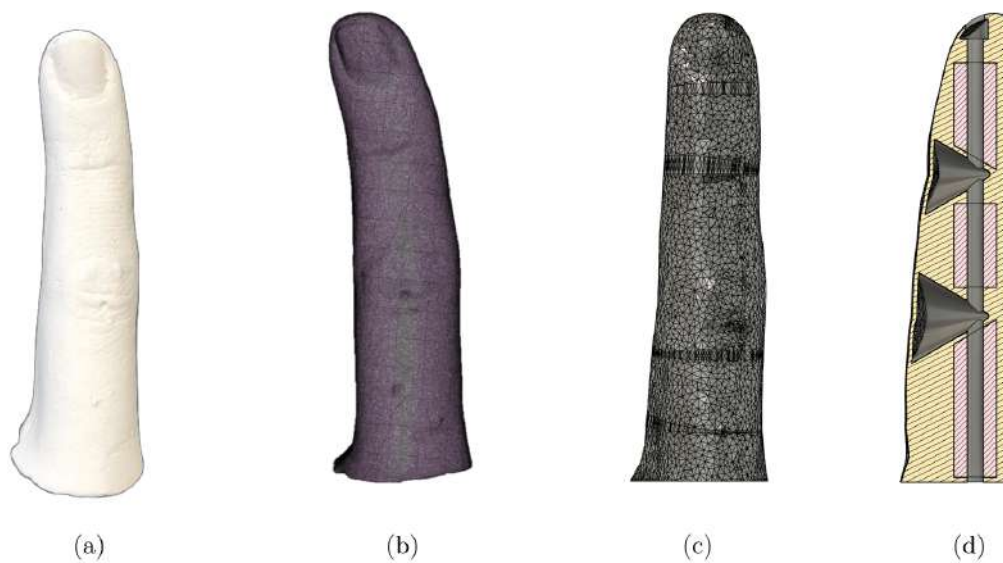


Figure 6.6: First prototypes of the index finger designed based on an adult female finger: (a) plaster replica of the index finger; (b) 3D scanning of the plaster replica result; (c) exterior design of the last prototype; (d) inner mechanism of the last prototype (cut along the sagittal plane, chambers with 90% depth and a opening angle of 60°).

6.3.1.2 Second prototypes

The aim of this study was to develop a 3D printed body-powered prosthesis for a four-year-old child, unlike the prosthesis from the study of F. Pinheiro [30], which designed a prosthesis for an adult. Consequently, his suggested values for the air chambers were not

suitable for the present study.

Therefore, it was necessary to investigate which were the values that would give the fingers the best functionality. The reference value for the opening angle of the chambers was 60° , which was suggested by F. Pinheiro [30]. The remaining tested values were a variation of $\pm 5^\circ$. The reference value for the chambers' depth was 90% of the transversal section length where the chamber's vertex was inserted, which was previously used in the first prototype. However, this value was the highest depth value that was tested. The other two tested depth values were 80% and 85%. Altogether nine models were designed, which consisted of the resulting combinations of these values (55° , 60° , 65° and 80%, 85%, 90%). Figure 6.7 presents the external design of these models.



Figure 6.7: External design of the second prototypes: these prototypes all present the same external appearance and differ only internally.

Figure 6.8 presents the inner mechanisms of the nine designed models, that only differ internally in the chambers' design.

Regarding the design of these prototypes, there are only a few differences when compared with the previous one. Besides the original fingers being replicas from different people, the design of the distal and proximal cylinders that mimic the phalanges and the ring chamber are different as it is illustrated in Figure 6.9.

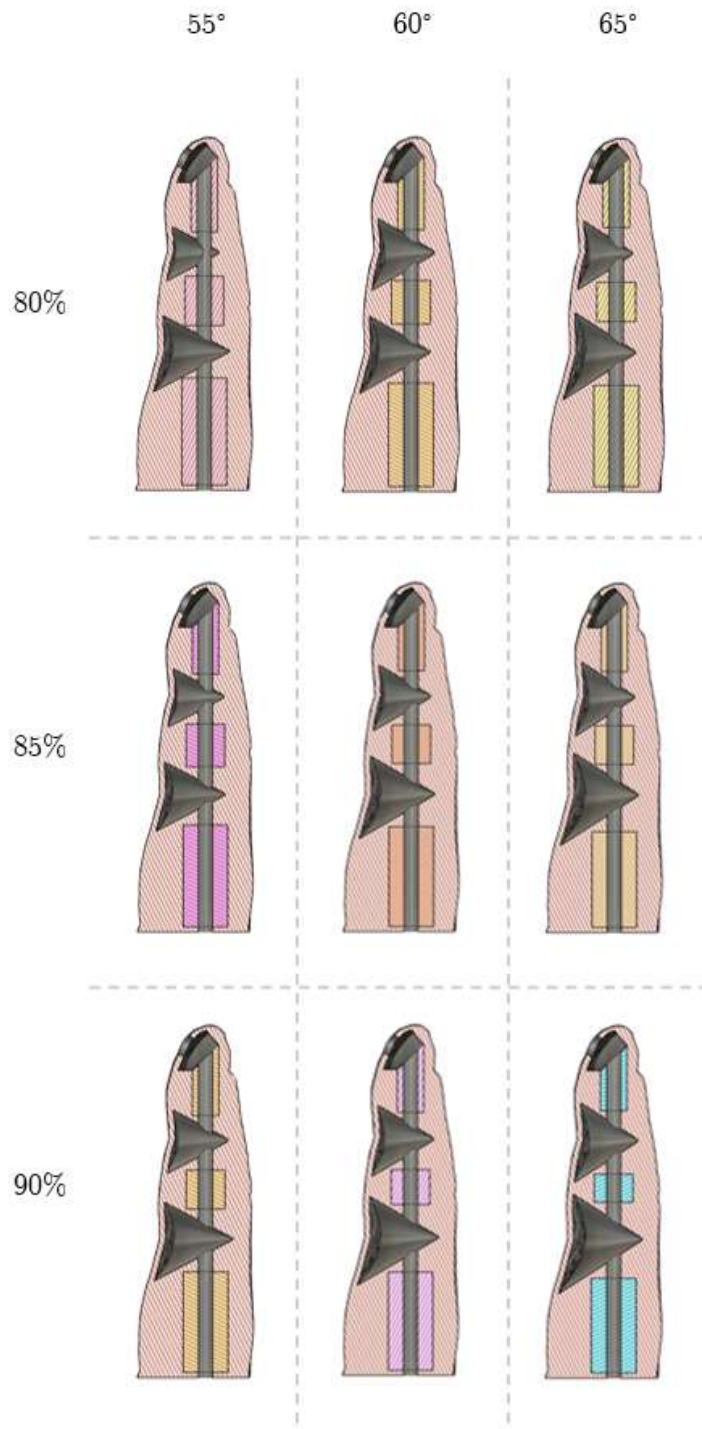


Figure 6.8: Inner design of the second prototypes (cut along the sagittal plane): these models are externally equal but the chambers that mimic the interphalangeal joints have different opening angles and depth. These models were designed in order to evaluate which were the values of opening angles and depth that would lead to a better performance when flexed.

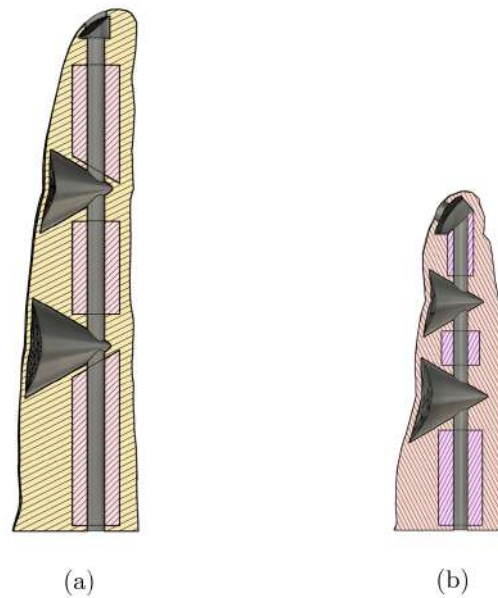


Figure 6.9: Comparison between the inner mechanisms of the first (a) and second (b) prototypes (cut along the sagittal plane, chambers with 90% depth and a opening angle of 60°).

The second prototypes are composed by two cylinders, simulating the middle and proximal phalanges, and a third cylinder, which corresponds to the distal phalanx, with a diagonal cut at the top that is connected to the ring chamber. On the other hand, the first prototype has two cylinders (the distal and proximal phalanges) with diagonal cuts that follow the chambers design, and the distal cylinder is not connected to the ring chamber.

These differences are related with the printing methods. The first prototype was developed to be printed in a dual extruder printer, a *Li3Dei Dual* printer, a modified *Wanhao duplicator 4s* [100], in which the phalanges components would be printed with PLA and the remaining finger with *Filaflex*. However, there were several issues with this printer, most notably overlaps between PLA and *Filaflex*, and poor *Filaflex* quality. Thus, the printer was replaced by *The Original Prusa i3 MK3S+*, a single extruder printer by ©Prusa Research [62]. In order to work around the problem of printing the models composed by two different materials in a single extruder printer, a start-stop system was developed. The inner components printed with PLA were previously printed and during the printing with *Filaflex*, the printing was paused and the PLA components were inserted. Therefore, some of the PLA components could not be cut diagonally as it would not be possible to insert these components without compromising the printing. Nevertheless, the distal cylinder was the only component that could have a diagonal cut without compromising the printing due to the ring chamber's shape. This cut was added in order to help the flexion of the finger. By adding this cut, it is ensured that the force applied by the strings do not have only a vertical component that causes the fingers compression, but also a horizontal component that creates a moment and causes

the finger to bend. Figure 6.10 illustrates the location of the pausing layers of the start-stop method used to print the second prototypes. However, this method had its own set of issues. Thus, the fingers ended up being printed using only *Filaflex* with different infill percentages to mimic different soft and hard components.

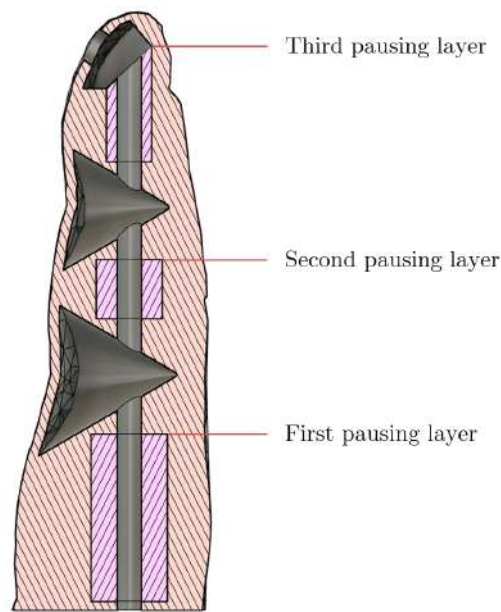


Figure 6.10: Location of the pausing layers of the start-stop method (cut along the sagittal plane, chambers with 90% depth and a opening angle of 60°).

In order to assess the best combination of values, these fingers were submitted to pull tests. However, even though air chambers were implemented in these fingers, due to their straight form, it was necessary to apply very high forces to bend the finger. When these forces, higher than 25 N, were applied by pulling the guitar string manually, none of the fingers bended. Moreover, for the purpose of this study, the forces applied correspond to the force necessary to bend only one finger, which would be unfeasible for a child. Hence, these fingers could not be tested by using pull tests and would not work only with the child's wrist flexion. Further improvements needed to be made in the design so the fingers could bend properly.

However, although it was not possible to evaluate these fingers through pull tests, it was noticed that fingers with bigger chambers were easier to bend. These chambers would correspond to higher values of the opening angles and depth. This difference is illustrated in Figure 6.11 where the fingers with the smaller (55°, 80%) and bigger chambers (65°, 90%) are compared. These results were expected, as the fingers with bigger chambers contain less material that opposes the bending motion, in opposition to the fingers with smaller chambers.

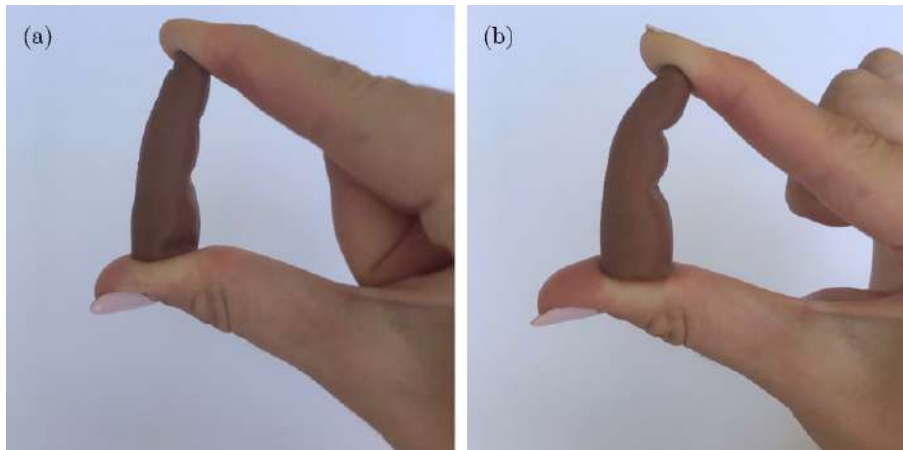


Figure 6.11: Parallelism between flexing an index model with smaller chambers and bigger chambers: (a) smaller chambers (55°, 80%); (b) bigger chambers (65°, 90%).

6.3.1.3 Third prototype

In view of the results that were previously obtained with the second set of prototypes, one of the possible culprits for the high forces that were needed to bend the fingers was their small size. Although bigger chambers had revealed better results, the size of the fingers could be the reason why such high forces were needed to bend them. Therefore, the previously designed model with an opening angle of 60° and 90% depth was scaled to 140%. However, the size increasing revealed worse results when bending the finger as it can be seen in Figure 6.12. Since the width of the walls is the same for the different models, as the size of the model increases, the ratio between the amount of printing walls and infill decreases. Thus, it is easier to bend a bigger model as the walls are denser than the infill. Unfortunately, the bending of the finger is not done correctly. Figure 6.13 presents the slicing of the bigger model and the original one, in which it can be seen the differences in area between the walls and infill for both models.

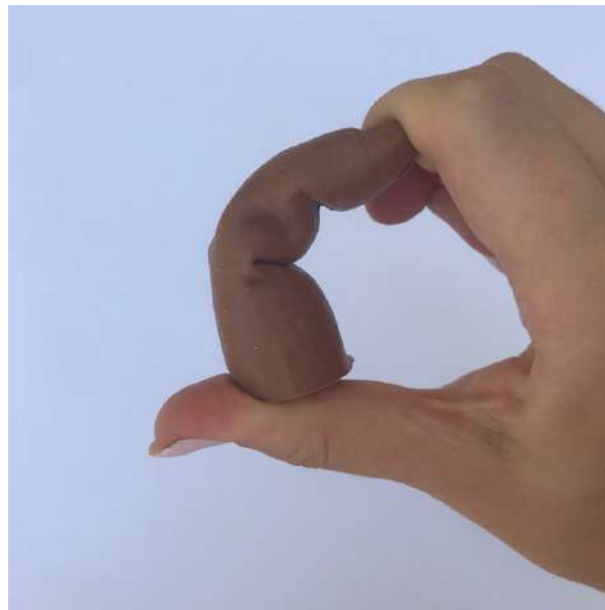


Figure 6.12: Flexion of the third prototype: this index model was scaled to 140% in order to evaluate if the size of the models had some influence in their performance. However, it revealed worse results, especially in the middle phalanx area.

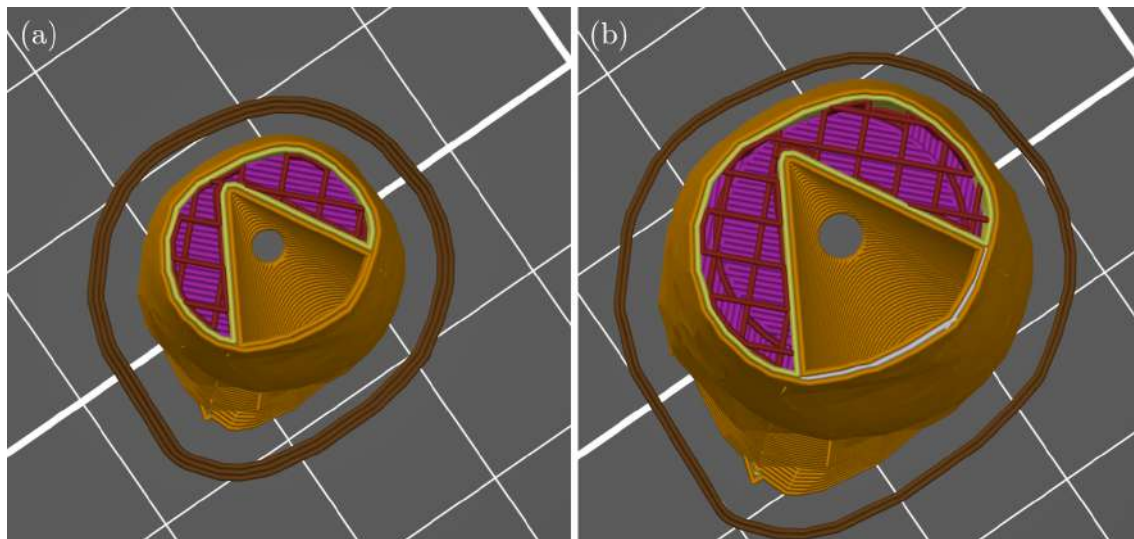


Figure 6.13: Slicing of the of the original second prototype and its replica scaled to 140%: (a) original model; (b) scaled model. The amount of infill is higher in the scaled model, which facilitates its flexion.

6.3.1.4 Fourth prototype

Considering the results of the second and third prototypes, it was verified that bigger chambers led to better results and that increasing the size of the fingers would not improve the functionality of the fingers. Therefore, no sizing change was made, and the nine combinations of testing values were reduced to three as only the higher depth (90% of the transversal section length) was evaluated.

The three designed models had a similar structure and the only difference between each other was their chambers with different opening angles (55°, 60°, 65°). Regarding the previous prototypes, the main difference is the position of the wire hole and the changes that were performed in the cylinders that mimic the phalanges. The wire hole was moved to a more anterior location and the phalanges were not mimicked by only one cylinder but by two cylinders connected with each other, so the wire hole could pass through them. The new location of the wire's hole favoured the flexion of the finger since there is less material opposing the movement. Figure 6.14 compares the design of the second and fourth prototypes.

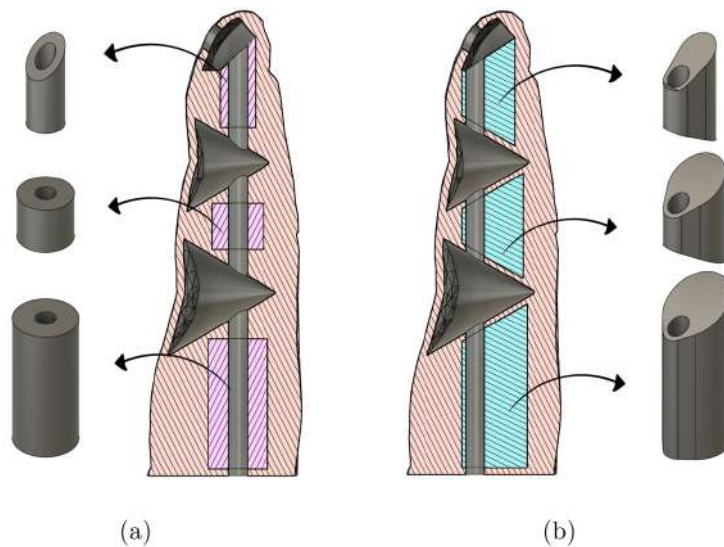


Figure 6.14: Comparison between the second (a) and fourth (b) prototypes (chambers with 90% depth and a opening angle of 60°): cut along the sagittal plane of the index finger and shape of the designed phalanges. The structures that mimic the phalanges were modified due to the displacement of the wire's hole to a more anterior location.

Moreover, in the design of these three models, the components that simulate the phalanges have diagonal cuts that follow the chambers' shape as the fingers were printed with *Filaflex* only. However, these modifications did not present significant changes in the fingers' functionality when flexed manually.

6.3.1.5 Fifth prototype

One of the main goals of this study was to develop a highly customised prosthesis. Hence, it was important to preserve as much as possible the anatomical features of the child's sound hand. However, when analysing the fingers designed by F. Pinheiro [30], the main difference between them and the first prototypes developed in this study was the curvature of the fingers. Besides giving a more natural look, this curvature helps in the flexion of the finger as the part of the movement is already done, and gives the prosthetic hand a functional position. Therefore, in order to improve the functionality of the fingers, a soft curvature was added to the designed fingers.

The flexion angles of the distal and proximal interphalangeal joints of each finger were defined according to a study that determined the extension and flexion angles of resting fingers in terms of forearm posture and shoulder flexion [89]. During the development of this prototype, it was considered the minimum value possible for the considered posture, i.e., the mean value minus the standard deviation value ($M - SD$) for both interphalangeal joints. For the index finger, these values correspond to 18° ($26 - 8$) for the proximal interphalangeal joint and 5° ($10 - 5$) for the distal interphalangeal joint.

In this case, only one prototype was designed in order to avoid more waste of material. The designed prototype had chambers with an opening angle of 60° and is presented in Figure 6.15. The structures that simulate the phalanges are similar to the previously designed in the fourth design. However, due to the finger's curvature, only the proximal structure is composed by one cylinder, as the string could not pass through the other two cylinders without an extra structure.

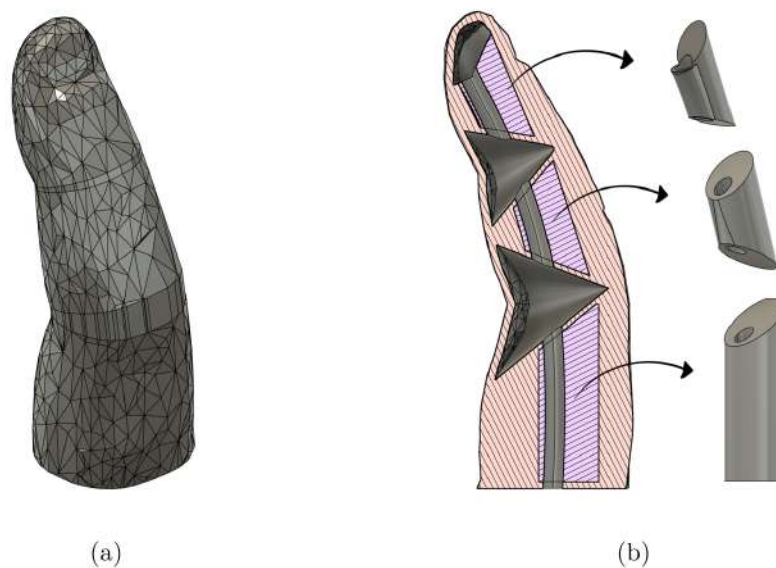


Figure 6.15: Design of the fifth prototype (chambers with 90% depth and a opening angle of 60°): (a) external design; (b) inner design, cut along the sagittal plane of the index finger and shape of the designed phalanges (right).

This design revealed to have a better functionality. However, the performance of the distal interphalangeal joint was not the desired one since the flexion of the finger was mainly focused in the proximal interphalangeal joint.

6.3.1.6 Sixth prototype

Notwithstanding the upgrades of the fifth prototype, it was necessary to make some improvements. Despite the finger's curvature, the flexion angle of the distal interphalangeal joint was not significative. Therefore, the curvature of the finger was intensified by increasing the flexion angle of the distal interphalangeal joint.

The first choice would be increasing the angle to the mean value suggested by K. Lee and M. Jung's study [89]. However, the difference would probably not be significant as the difference would be only 5° , the equivalent of the standard deviation. Hence, the chosen angle was the mean value plus the standard deviation ($M + SD$), which leads to a greater difference. For the index finger, this angle corresponds to 15° .

Figure 6.16 shows the difference between the fifth and sixth prototypes. Besides the flexion angle of the distal interphalangeal joint, there are no relevant design differences, except for the phalanges structures which were adapted to the present design.

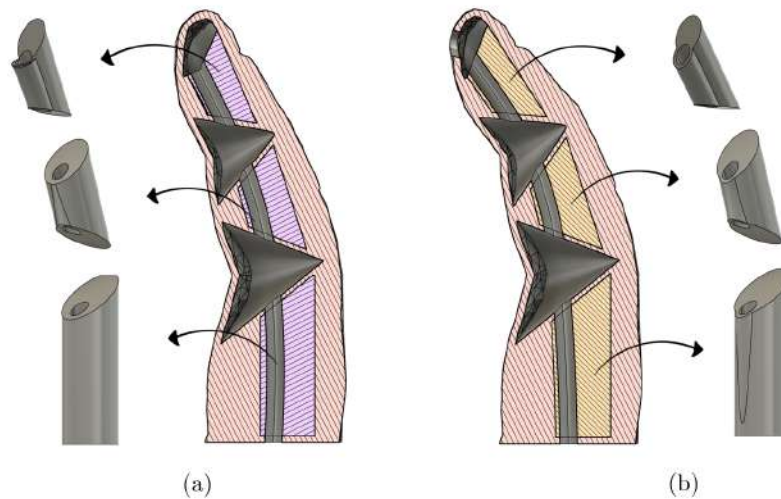


Figure 6.16: Comparison between the fifth (a) and sixth (b) prototypes (chambers with 90% depth and a opening angle of 60°): cut along the sagittal plane of the index finger and shape of the designed phalanges.

The increasing of the flexion angle of the distal interphalangeal joint revealed satisfactory results as flexing the finger became easier. However, there was still some resistance while bending the finger. Once more, three similar fingers were designed with different chambers' opening angles, but the flexing resistance was similar for the three models. This resistance could be related with the location of the wire's hole.

6.3.1.7 Seventh prototype

Considering the previous prototype, the main goal of this prototype was to relocate the wire's hole, especially the proximal extremity.

The proximal extremity of the wire's hole was moved from $0.5L$ of the bottom surface of the index finger from the anterior region of the finger to $0.2L$. Therefore, there is less material opposing the movement. By moving the wire's hole to a more anterior location, the components that simulate the phalanges became independent of the wire's hole.

One of the possible causes for the high difficulty in bending the finger could be the greater amount of walls resulting from the phalanges components. When these components are connected to the wire's hole as in the previous prototype, the ratio between the amount of walls and infill increases and it is harder to flex the finger. Thus, this segregation promotes the flexion of the finger.

Besides the wire's hole relocation and the segregation between this hole and the phalanges components, the shape of the phalanges was also curved in order to help the finger bending.

The combination of these features resulted in a high level of functionality. Given these results, this prototype was selected as the final model. Figure 6.17 shows the design of the seventh prototype, which was used as model for the remaining fingers. Thus, three similar models with different opening angles were designed and were submitted to pull tests in order to assess which values should be applied. The results of these tests are displayed in Figure 6.18. The opening angle of the final model was 60° since this value led to lower tensioning forces that resulted in a greater displacement, revealing that is easier to bend this model.

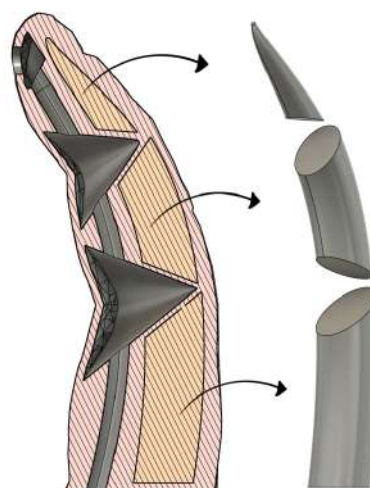


Figure 6.17: Inner design of the seventh prototype (chambers with 90% depth and a opening angle of 60°): cut along the sagittal plane of the index finger and shape of the designed phalanges (right).

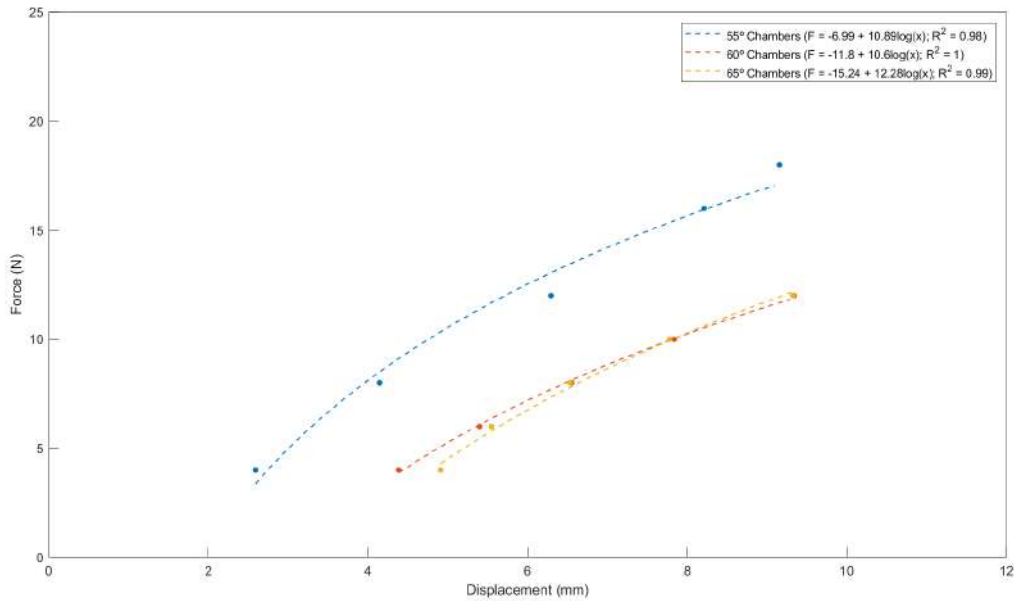


Figure 6.18: Results of the pull tests used to select the opening angles of the chambers.

6.3.1.8 Other prototypes

Despite the good results of the seventh prototype, two more tests were run in order to assess if additional modifications had a positive outcome in the functionality of the fingers. All modifications were made over the seventh prototype.

The first test was the elimination of the phalanges' components. Eliminating these structures decreases the number of printing walls, which are harder to flex. However, this modification did not improve the functionality as the finger did not bend correctly. Figure 6.19 shows the design of this prototype and Figure 6.20 illustrates the incorrect flexing of this prototype.

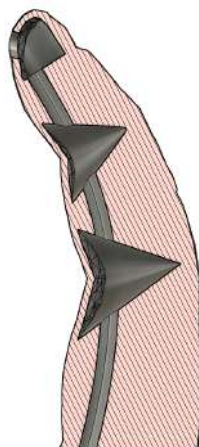


Figure 6.19: Design resulting from removing the phalanges structures (cut along the sagittal plane, chambers with 90% depth and a opening angle of 60°).



Figure 6.20: Flexing of the finger prototype with no phalanges: this index model was designed without phalanges to evaluate if the reduction of printing walls would influence their performance. However, it revealed worse results, especially in the middle phalanx area.

The second modification was the thickening of the chambers' external wall in order to have no more than one layer separating the interior of the chamber from the exterior. Two tests were made, one with a wall thickness of 0.6 mm and other with 0.3 mm. The original thickness of the seventh prototype was 0.9 mm, which equals to the width of two printing layers. Figure 6.21 compares the seventh prototype with these prototypes. However, these modifications did not improve the fingers as they compromised the printing quality as it can be seen in Figure 6.22.

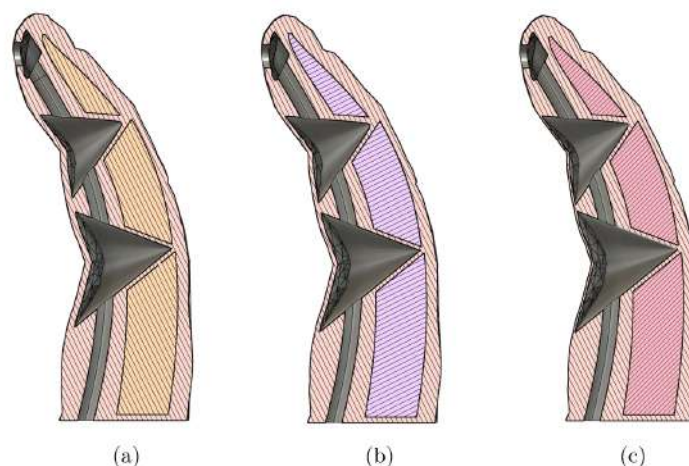


Figure 6.21: Comparison of the inner design of the seventh prototypes and the models with thicker chambers' walls (cut along the sagittal plane of the index finger, chambers with 60° and 90° depth): (a) seventh prototype with 0.9 mm wall thickness; (b) seventh prototype with 0.6 mm wall thickness; (c) seventh prototype with 0.3 mm wall thickness.



Figure 6.22: Printing results of the finger prototypes with thinner chambers' external walls: seventh prototypes with 0.6 mm (left) and with 0.3 mm wall thickness (right).

6.3.1.9 Phalanges design

In the first three prototypes that were designed, the diameter of the components that simulate the phalanges had random values of diameter, that were chosen considering the printing layers width. The proximal phalanx was the bigger one and the distal phalanx the smaller one.

However, in order to apply the same method for all the different fingers, the phalanges' diameter was defined by crossing the information of two different studies: F. P. A. Buryanov and V. Kotiuk study [90] as well as Schulter-Ellis and G. T. Lazar study [91]. Both studies present similar samples, composed by individuals of both genders from 19 to 78 years old [90, 91].

Ten measurements to the projection of the midshaft width of each phalanx were made in order to decrease the measurement error. The considered value was the mean of these ten measurements. Then, this value was crossed with the values from the F. P. Schulter-Ellis and G. T. Lazar's study [91].

After these values were validated, the diameter of each phalanx was scaled to 63%. This value results from the ratio between the length of the child and a 23 year-old female's index fingers. This method was considered valid as the female could fit in the studies' samples and both genders are included. Moreover, since children grow at different rates, there are no studies performed in children. Therefore, for the present purpose, which is to define the size of the structures that mimic the child's phalanges this could be a good method, as the main goal is to provide a sense of touch similar to a human hand.

6.3.1.10 Fitting mechanism

The aim of the fitting mechanism is to fix the fingers to the metacarpal region. The assembly must be simple, so the fingers could be easily fixed or removed in case anything broke or need replacement. However, the fingers must have a system that prevents the separation of the fingers from the metacarpal region when the prosthesis is being actuated. This mechanism was only designed after the distal region of the metacarpal region was finished.

The first attempt consisted of an extension of the finger's bottom extremity that was inspired in the mechanism from F. Pinheiro study [30], in which a small protrusion enables the fingers to be fixed, but prevents the finger to be easily removed during the prosthesis' actuation. Moreover, a square blind hole was added to the finger's bottom extremity in order to block the rotation movement of the finger. However, this mechanism did not work since the dimensions of the protrusions would lead to a high distance between the fingers. Thus, the hand's anthropomorphism of the prosthesis would be compromised. Figure 6.23 displays the first prototype of the finger's fitting mechanism.

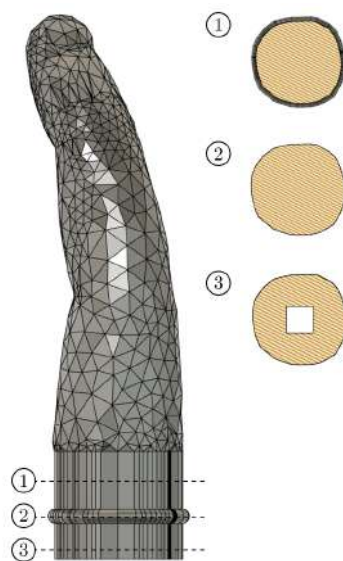


Figure 6.23: First prototype of the fitting mechanism with the different transversal sections of the segments that compose this fitting mechanism.

The second attempt was very similar to the final design, which is composed by three different parts. In distal-proximal order, the first segment is an extension of the fingers' base. The second segment have a diamond shape and the third segment is a cylindrical body. The second segment is smaller and the bottom edges of the third segment were rounded. Nevertheless, after testing this mechanism with a small cube simulating the fitting hole of the metacarpal region, the finger did not fit due to the shape of the third segment that was too big to pass through the second segment of the hole. Figure 6.24 shows the second prototype of the fitting mechanism and Figure 6.25 shows the cube that

simulated the fitting hole of the metacarpal region.

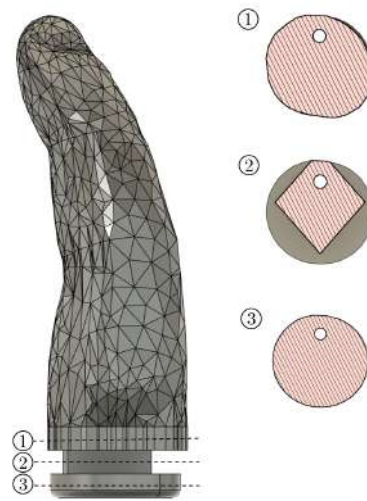


Figure 6.24: Second prototype of the fitting mechanism with the different transversal sections of the segments that compose this fitting mechanism.

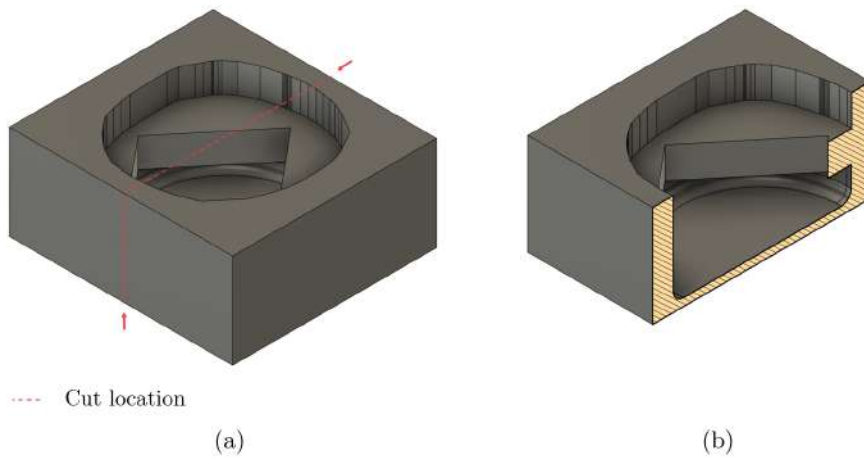


Figure 6.25: Test cube to simulate the second prototype of the fitting hole of the metacarpal region: (a) test cube; (b) test cube with a cut along the sagittal plane of the finger.

The third and last attempt (displayed in Figure 5.7) was an improvement of the second. The only difference is the shape of the third segment. In this model, the third segment has also a diamond shape, but with the bottom edges rounded. The same cube test was ran and the finger was easily fixed. As desired, the removal offered some resistance, which is needed during the actuation of the prosthesis but sufficiently simple if for any reason the fingers need to be removed.

6.3.1.11 Fingers design overview

The design of index finger suffered several modifications until it achieved the final design, which was used as model for the remaining fingers. The thumb presents some differences, and its design process was different from the others fingers due to its different morphology. During the thumb's design, some difficulties were felt due to its different location and anatomical features. However, the chosen methodology and the respective values have shown great results for all the five fingers.

Despite all the operations that were made, the fingers have shown a high level of anthropomorphism and the anatomical features of the child's fingers were preserved and not compromised. Thus, notwithstanding all the prototypes that were made, the final methodology could be easily applied to other children's fingers in order to design highly customised prostheses, increasing their long-term adhesion.

6.3.2 Metacarpal region design

In addition to the cosmetic appearance, one of the main goals of this study was to improve the functionality of the existing 3D-printing body-powered upper limb prostheses. The majority of these prostheses only perform power grasping [10] without adapting to the shape of the object. Nevertheless, some 3D-printed prostheses have mechanisms that enable the prosthetic hands to adapt to the object shape while grabbing it.

The *Nazree's Prosthetic Hand* is one of these examples, whereby it was the main inspiration to design the metacarpal region of the present prosthesis. Figure 6.26 shows the first draft of the metacarpal region, which was also composed by three segments and would be composed by an inner whiplike mechanism. The main goal was to have different components made with different materials, PLA and *Filaflex*. Thus, this structure could be printed using the start-stop method or segmented in different components that would be assembled later. However, due to the high level of customisation that was desired, especially regarding to the size of printed hand, including all these mechanisms as well as creating space so the child could place the stump would be difficult. Therefore, in order to simplify the metacarpal region design, the first approach was to design a **minimum viable product (MVP)**, in which the whiplike would be external as in the *Phoenix Hand v2*.

During the development of the metacarpal region, different prototypes were designed. Moreover, in order to avoid material waste since it was a bigger component, some of the tests were made by only printing a portion of the metacarpal region structure. Unlike the fingers, this structure was built from scratch.

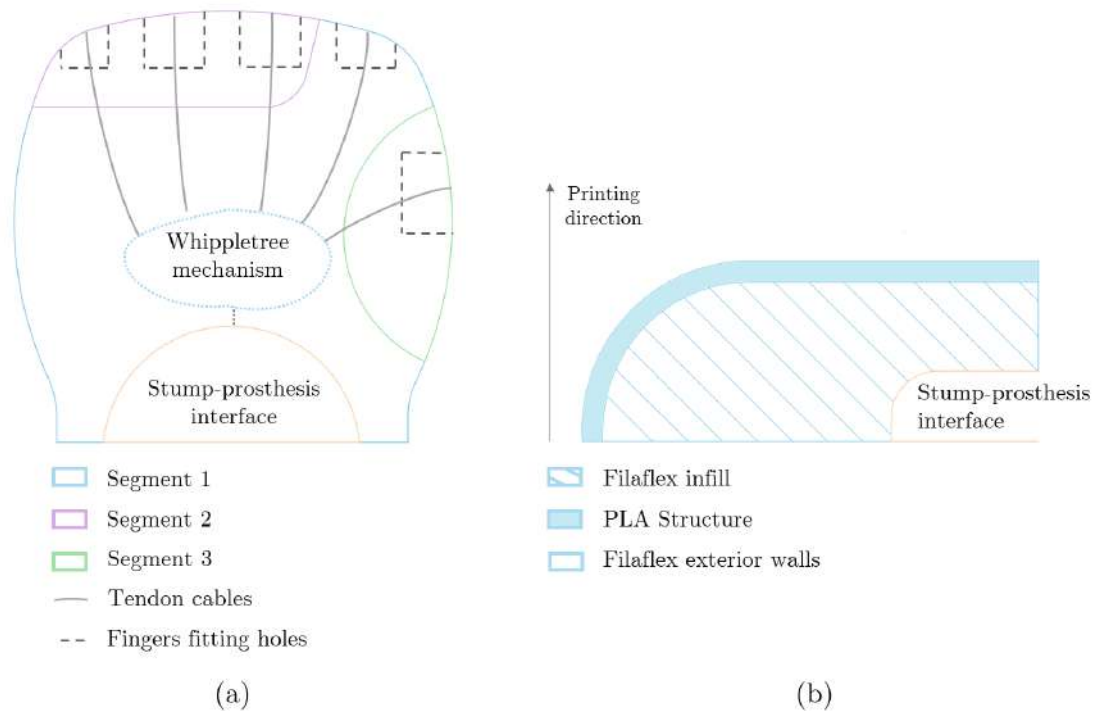


Figure 6.26: First draft of the metacarpal region structure, inspired in the *Nazree's Prosthetic Hand*: (a) inner mechanisms. Segments 1 to 3 would be articulated to simulate the motion of the metacarpal region while gripping; (b) printing scheme. This structure would be printed by using the start-stop method. The PLA parts, namely the segments 1 to 3, would be printed previously and then inserted in a *Filaflex* shell during its printing.

6.3.2.1 First prototype

The first prototype was the simplest and presented a poor level of anthropomorphism, with some sharp edges. From the frontal plane perspective, there are some similarities with the child's hand shape. However, from a sagittal perspective, the volume of the metacarpal region is higher than desired. This higher volume was caused by the stump-prosthesis interface. The distal surface of the metacarpal region has an unevenness for placing the little finger, so its distal phalanx could be at the level of the middle phalanx of the ring finger as in a human hand. The fingers are separated from each other by 0.9 mm, the equivalent to the width of two printing layers. Moreover, this prototype also contains a single 30° chamber that simulates the metacarpophalangeal joints. Designing a single chamber allowed to simplify the prototype without compromising its motion as during the performance of a power grasp, even if adapted to the object, in general, these joints move equally. Additionally, a more rigid structure was designed with the aim to help the flexion of the metacarpal region. This structure was used as an infill modifier. Figure 6.27 presents the external and internal design of this prototype.

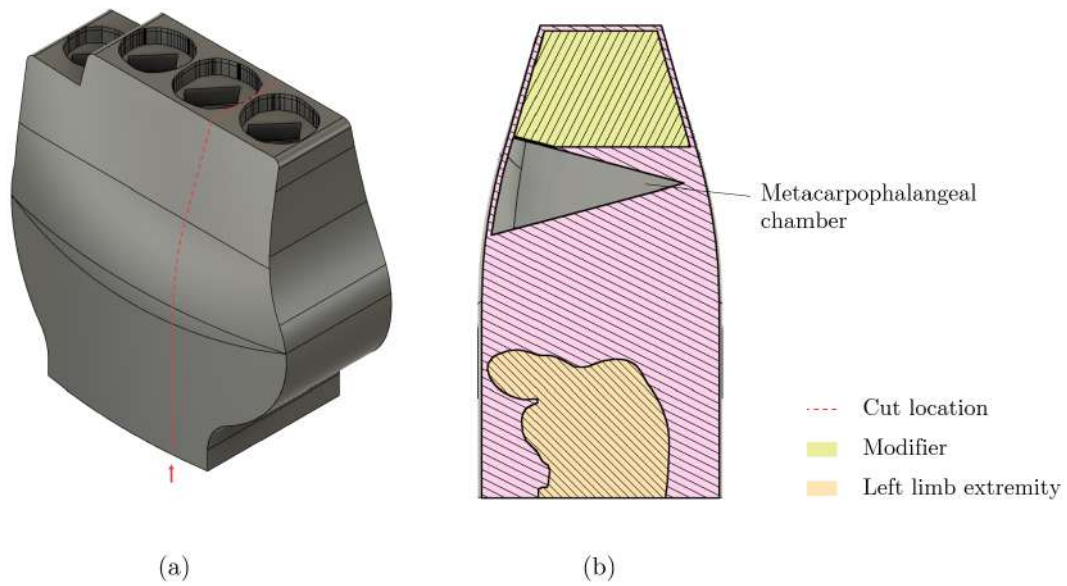


Figure 6.27: Design of the first prototype of the metacarpal region: (a) external design; (b) inner design, cut along the sagittal plane of the metacarpal region.

Although this prototype had been entirely designed, only a portion was printed in order to test the chamber. However, the results were not good due to the shape of the hand. When the printed model was flexed, the excess of material went outside instead of going inside, as it can be seen in Figure 6.28. This happened because the most proximal volume is higher than distally. Since it consists of a testing model, no supports were removed, and the printing quality had no special relevance.

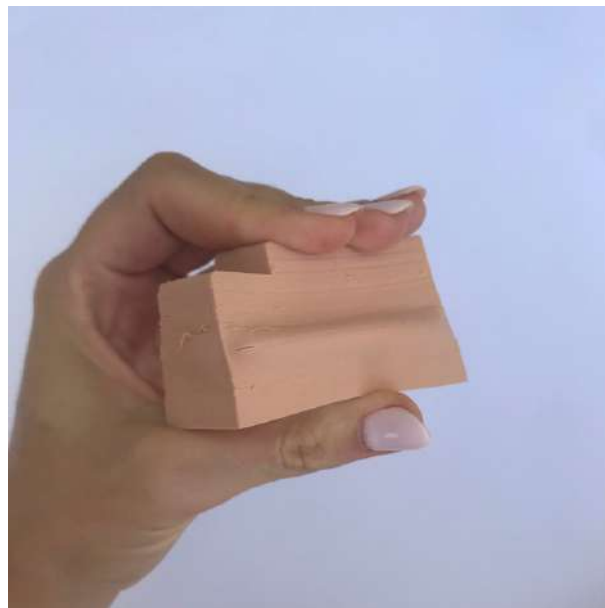


Figure 6.28: Flexion of the first prototype of the metacarpal region: in order to avoid more material waste, only part of the prototype was printed.

6.3.2.2 Second and third prototype

The second and third prototypes are very similar to each other. However, they present large differences from the first prototype, especially regarding the anthropomorphism level.

Unlike the first prototype, these prototypes were designed with the aim to be a better replica of the human hands, even though they were still MVPs. In order to avoid the behaviour of the first prototype during the metacarpal region flexion, the distal palmar crease was one of the features that was more important to reproduce. Figure 6.29 shows the external design of the second and third prototypes, in which is possible to see the reproduction of this crease as well as the knuckles. These features were obtained by using the *Loft* tool from *Fusion 360*, which allows to easily customise the designed bodies' shape, through the use of rails. Like the first prototype, these models also have an unevenness for placing the little finger, and the fingers are separated by 0.9 mm. This time, only a portion of the metacarpal region was designed and no rigid structure to help the flexion of the metacarpal region was added.

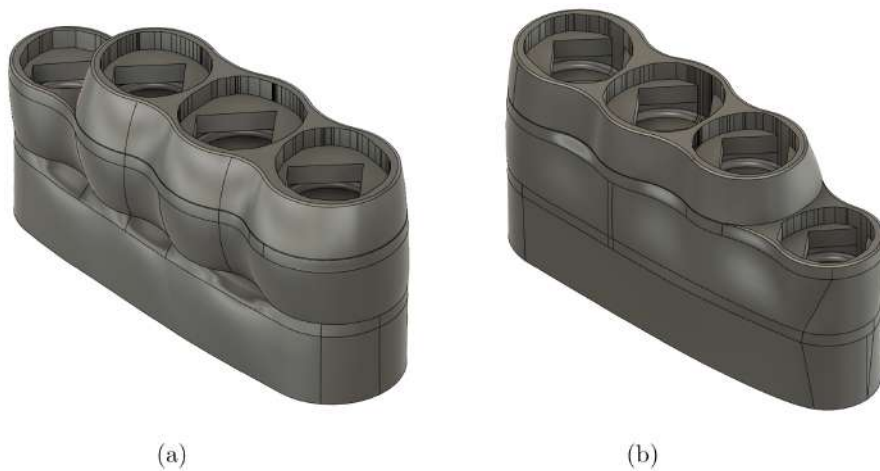


Figure 6.29: External design of the second and third prototypes: (a) latero-anterior view; (b) latero-posterior view.

The second and third prototypes have different chamber angles, as indicated in Figure 6.30. After printing the second prototype, the flexion of the metacarpophalangeal revealed the desired behaviour, which can be seen in Figure 6.31. However, the flexion of the model needed a high level of strength. Therefore, the third prototype was designed with 35° chamber and was printed with the set B of printing parameters, while the first one was printed with the set A. These modifications led to better results as it was easier to flex the metacarpal region. Figure 6.32 presents the results of the third prototype.

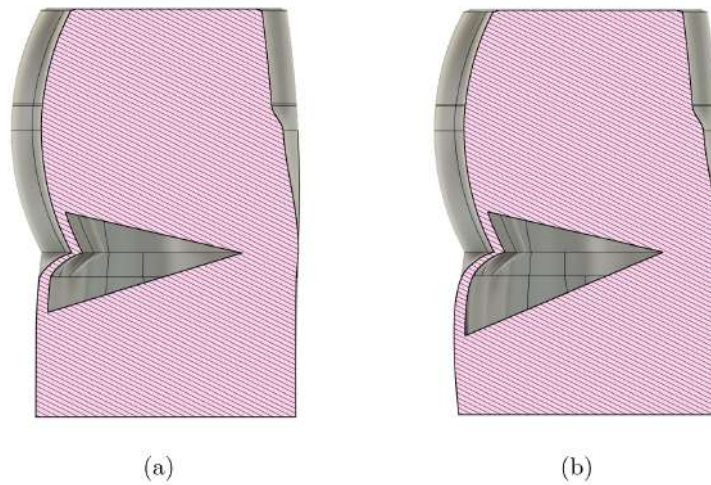


Figure 6.30: Inner design of the second and third prototypes (cut along the sagittal plane): (a) second prototype with a 30° chamber ; (b) third prototype 35° chamber.

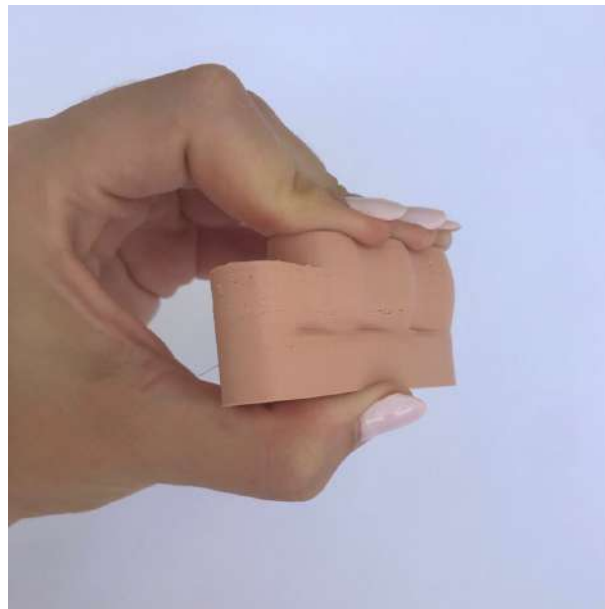


Figure 6.31: Flexion of the second prototype of the metacarpal region: in order to avoid more material waste, only part of the prototype was printed.



Figure 6.32: Flexion of the third prototype of the metacarpal region: in order to avoid more material waste, only part of the prototype was printed.

6.3.2.3 Fourth prototype

The fourth prototype consisted of an improvement of the second and third prototypes. Unlike these ones, the fourth and the following prototypes were entirely printed.

This prototype was designed using the *Loft* tool. The rails of the previous prototypes were improved in order to achieve a good level of anthropomorphism, with smooth curves and creases. One of the main difficulties while using the *Loft* tool was to make sure that the rails were connected to the sketches, which does not always happen. Besides the child's hand shape, the stump shape had also influence in the rails design as the stump was also scaled to 110% and should fit into the metacarpal region's volume. Although this prosthesis aims to be highly customised, the stump location is not the exact replica of the child's left limb extremity as the child possesses some moving digital buds. Therefore, in order to give the child more movement freedom, the stump location was designed following the shape of the main curves of the child's stump.

Twenty-two diamond-shaped holes were designed on the anterior region of the metacarpal region structure in order to ventilate the stump. Sweating while wearing a prosthesis is practically inevitable and may lead to the creation of microenvironments which are prone to skin problems. Moreover, sweating can affect the prosthesis fitting and increase the chances for rejecting this device [28]. Although these holes may compromise the aesthetical appearance of the prosthesis, the ventilation of the stump allows to minimise the discomfort. These holes have a diamond shape in order to avoid the necessity of printing supports, which would be necessary for other shapes such as squares or circles.

The wires' holes start in the anterior region of the metacarpal region structure and end at the posterior region, near the wrist, outside the metacarpal region, forming a curved path for the tendon cables go through. This path was smoothed as much as possible to prevent the formation of breaking points that would damage the wires and the prosthesis while operating it. The holes have a diameter of 2.1 mm and are protected by a two-layer wall outside the metacarpal region. Their centres in the posterior region are 5.1 mm apart and follow the curvature of the bottom of metacarpal region.

One of the main difficulties of this prototype was to choose the thumb location and design its fitting mechanism due to its location and position.

As the previous ones, this prototype has a 30° chamber to mimic the metacarpophalangeal joints. Besides the better results of the third prototype with a 35° chamber, this prototype was designed with a smaller chamber to take less space. However, while the previous prototypes were printed using the set A of printing parameters, this prototype was printed with the set B with 5% infill and the results were very satisfactory. Additionally, a second chamber was added to simulate the thumb's metacarpophalangeal joint, which follows the shape of the thenar crease. However, this chamber did not work as expected due to the small infill percentage and the shape of the chamber, which was smaller than desired due to the small amount of free space. Figure 6.33 presents the design of the internal and external design of the fourth prototype. Its printing results are displayed in Figure 6.34, in which some printing defects are visible. Some of these defects resulted from the absence of printing supports and others are simply printing errors.

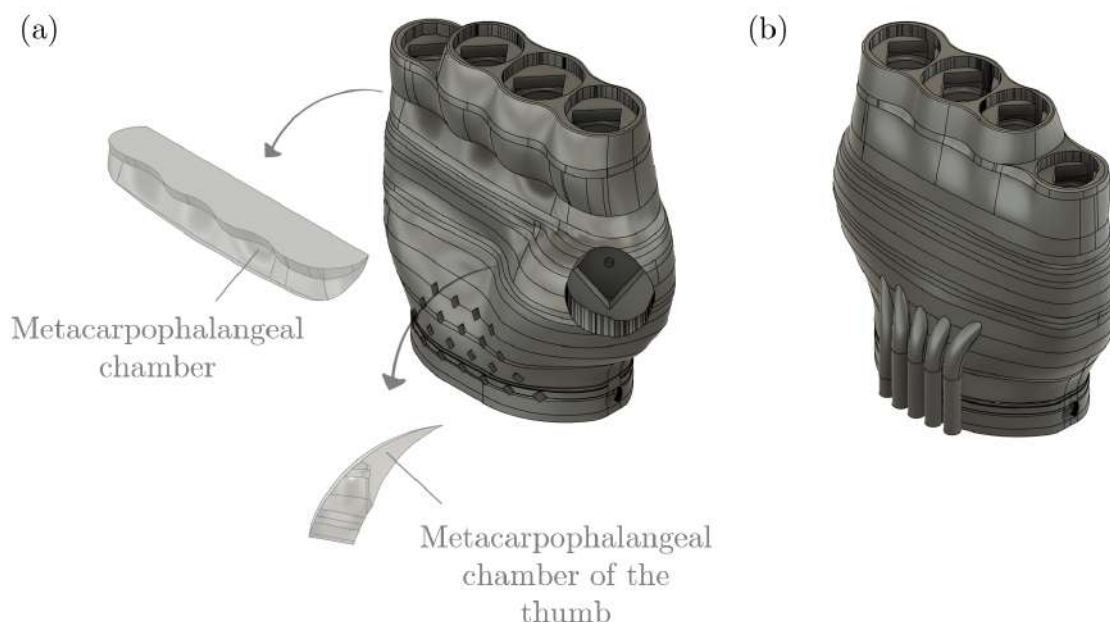


Figure 6.33: Design of the fourth prototype of the metacarpal region: lighter grey structures represent some of the inner mechanisms, namely the positive mould of the metacarpophalangeal chambers; (a) latero-anterior view; (b) latero-posterior view.

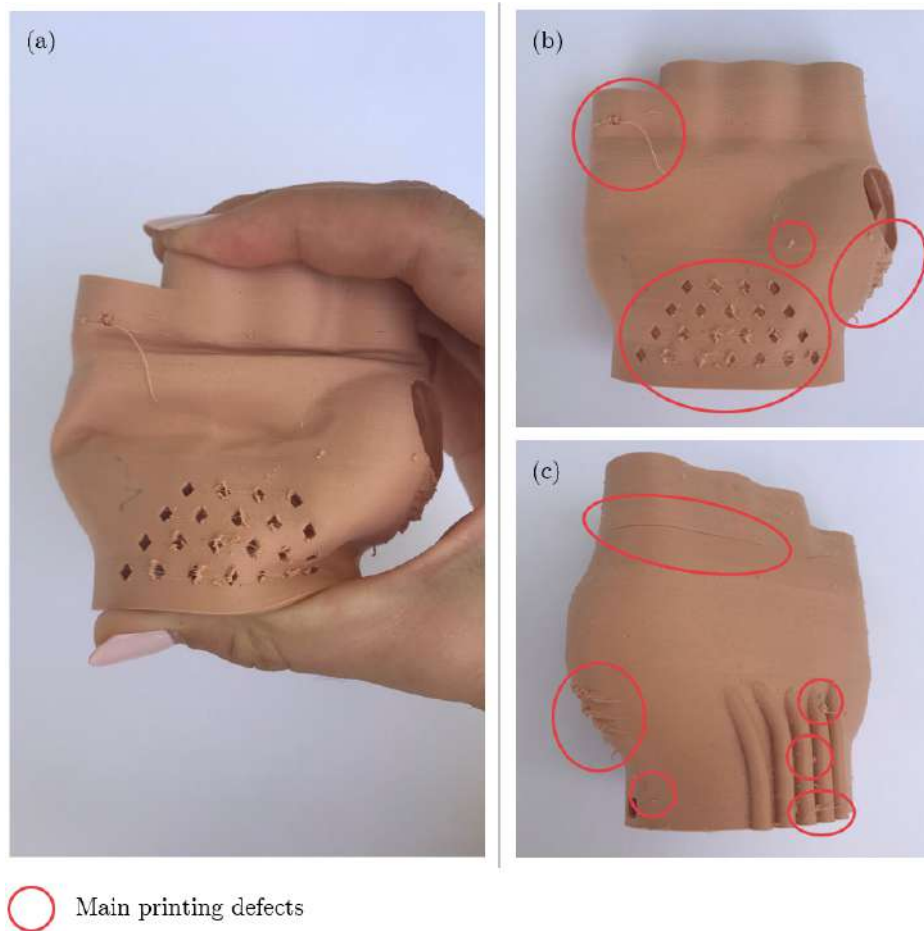


Figure 6.34: Printing results of the fourth prototype of the metacarpal region: (a) flexion of the prototype (anterior view); (b) printing defects present in the anterior region of the prototype; (c) printing defects present in the latero-posterior region.

6.3.2.4 Fifth prototype

The fifth prototype only differs from the previous one in two aspects. The first difference is the size of the diamond-shape holes, which was increased. When printed, the diamond-shaped holes of the fourth prototype had several printing defects, caused by the size and proximity of these holes. Therefore, the distance between the holes as well as their size were increased. Figure 6.35 compares the external design of the fourth and fifth prototype.

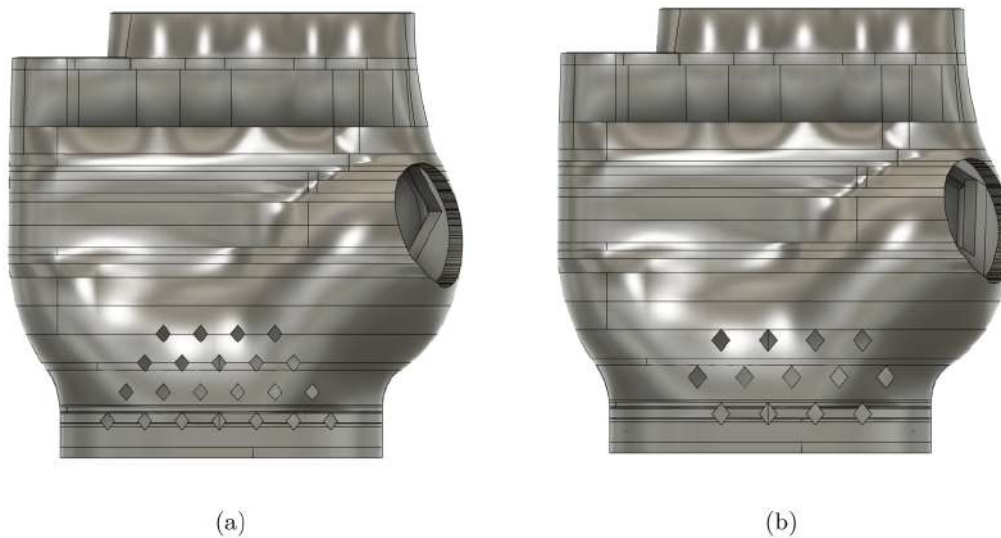


Figure 6.35: Comparison between the external design of the fourth (a) and fifth (b) prototypes of the metacarpal region (anterior view).

The second difference is the absence of the chamber that mimics the metacarpophalangeal joint of the thumb. In view of the results of the fourth prototype, this chamber was removed. Thus, an additional component was designed to mimic this joint, so it could be used as a printing modifier. This component has the same shape of the designed metacarpal region and was also designed with the *Loft* tool. The sketches are smaller and consist of an -0.9 mm offset in comparison with the previously designed sketches for the construction of the metacarpal region. The resulting body was then cut along a curve that simulates the thenar crease and along the shape of the stump location. By using a different infill percentage, the volume with less material density bends towards the denser volume simulating the flexion of the thumb's metacarpophalangeal joint. Therefore, the whole metacarpal region was printed with 5% grid infill and the modifier with 10% rectilinear. The printed prototype is displayed in Figure 6.36 in which can be seen the results of the flexion of the metacarpal region when bended. Although there was a great improvement in the thumb's functionality, by handling the printing model, it was noticed that the volume occupied by the modifier was still too flexible. Besides these results, several printing defects are still present. Moreover, it is possible to observe the influence of the diamond-shaped holes in the printing quality.

In view of the printing results of the fourth prototype, the amount of supports, especially below the thumb's location, was reinforced. However, some printing defects are still visible in this area.

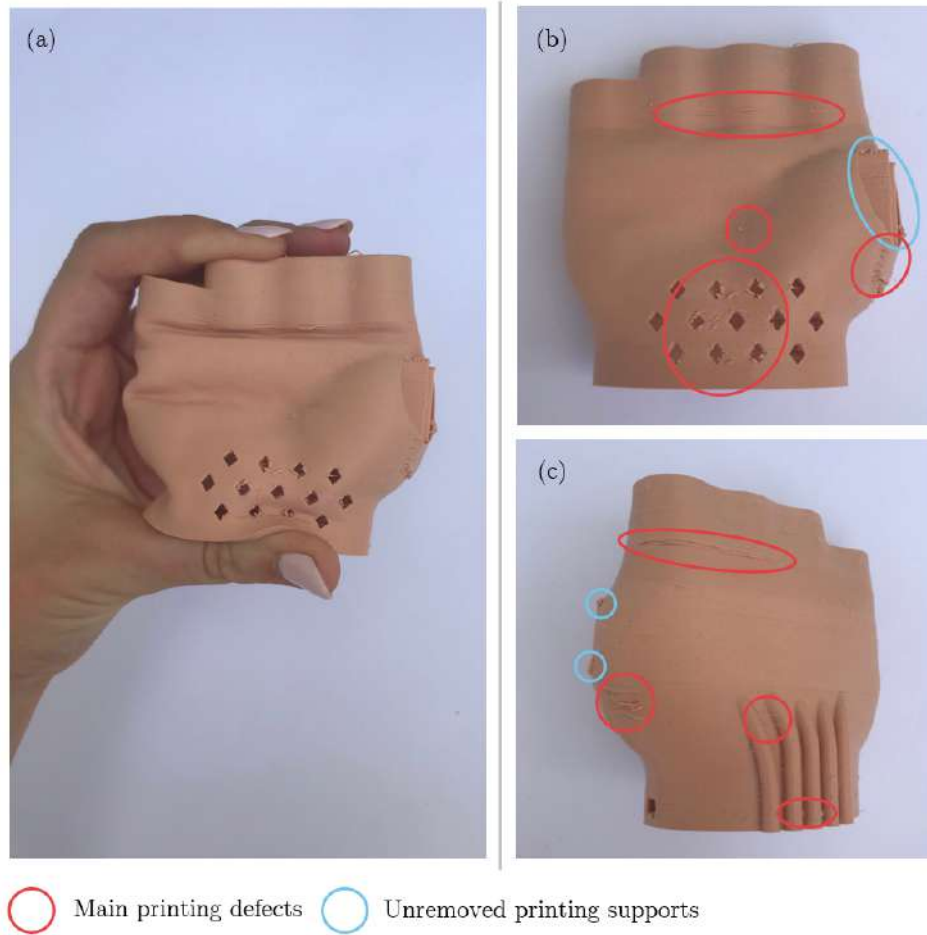


Figure 6.36: Printing results of the fifth prototype of the metacarpal region: (a) flexion of the prototype (anterior view); (b) printing defects present in the anterior region of the prototype; (c) printing defects present in the latero-posterior region.

6.3.2.5 Sixth prototype

The sixth prototype is the mirrored version of the fifth prototype and the remaining differences are only printing settings and the printing position. Given that the supports added to the previous prototype were not enough to prevent printing defects below the thumb's fitting position, this prototype was printed upside down. By printing the model in this position, the amount of needed supports is reduced and so the odds of having printing defects. However, as it can be appreciated in Figure 6.37, the printing was stopped due to layer shifting. This might be explained by the fact that by printing the model upside down, the volume of the first layers is smaller. Therefore, with the material elasticity, the model becomes more vulnerable to the printer movements causing layer shifting.

Finally, the modifier infill percentage was increased to 15% to make this volume a little more rigid, but flexible enough to mimic the soft tissues of the hands. Although this

model was not totally printed, by handling this volume, the results are very satisfactory.

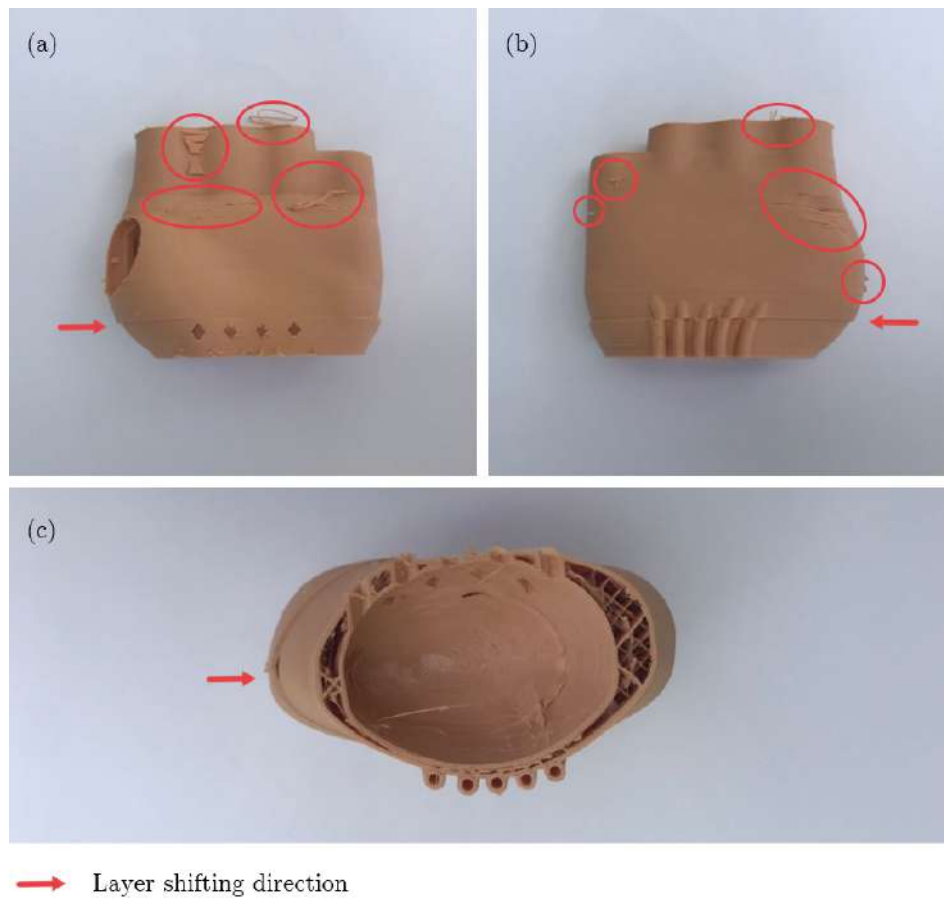


Figure 6.37: Printing results of the sixth prototype of the metacarpal region: unfinished printing due to layer shifting; (a) printing defects present in the anterior region of the prototype; (b) printing defects present in the posterior region of the prototype; (c) bottom view of the prototype.

6.3.2.6 Seventh prototype

The seventh prototype was the final prototype. The only difference from the sixth prototype was the printing position. Since printing the model upside down also led to printing defects, which were considered to be worse than the defects caused by the supports in terms of aesthetics and functionality, it was decided to print this model right way up. The supports were changed once more and the results are displayed in Figure 6.47. Although there are still some defects, these results were considered minor, especially for an MVP.

6.3.2.7 Metacarpal region design overview

Unlike the fingers, the metacarpal region was designed from scratch, inspired in the features of the child's sound hand. Although this structure was not entirely customised, it was possible to achieve a high level of anthropomorphism using the *Loft* tool, even

though it consists of an MVP. There are several aspects that need to be improved and solved. However, there is a great belief that the final model might be equally attractive to children and their families due to its human features that are clearly visible, such as the knuckles or the palm creases. Therefore, after further improvements, such as increasing its functionality and enhancing some aesthetical features such as the wires conduction, this model could be applied to any child as a standard model. Some specific creases and the size of each child's hand should be enough to customise this structure, which simplifies the process of building a prosthesis since these features are not difficult to replicate. Moreover, having a standard structure is also beneficial for children with bilateral absence of the upper limb's extremities.

Besides of the inherent difficulties of using the *Loft* tool, one of the main difficulties was to design the thumb fitting mechanism due to its different location and anatomical features. Additionally, although it was not a major concern as the model consists of an MVP, inserting the whippetree inside the metacarpal region would have been impossible. The size of the hand and the presence of other important mechanisms, such as the chamber that mimics the metacarpophalangeal joints, would make this impracticable. Thus, this model ended up being a fusion of ideas from both *Nazree's Prosthetic Hand* and the *Phoenix Hand v2* since it is not segmented but its mechanisms follow the nature of the hand's creases and the whippetree is located externally.

Regarding the printing of this model, the achieved results are very satisfactory even though there are some printing defects. One of these defects is common to the three last prototypes and is localized near the metacarpophalangeal joints area. This defect is caused by the angle of the chamber, which corresponds to less than 45° from the horizontal plane. Therefore, this structure needed supports. However, these supports would not be possible to remove as they would have been internal. Thus, no supports were used, even though this choice would lead to printing defects. Although this printing defect did not compromise the functionality of this chamber, in the future, a new solution to solve this problem must be studied. Nevertheless, the settings that were chosen are a very faithful replication of the different tissues that compose the human hands.

6.3.3 Wrist design

The wrist design was the simpler stage in the whole process of developing this prosthesis as all the components that were used are from other prostheses. Since the initial idea was to use a whippetree mechanism, all the used components are from *Phoenix Hand v2*, even though the tensioning system of the main prosthesis is from the *Raptor Reloaded* prosthesis [75]. However, this fact had no further influence as the gauntlet, the thermo pins, their caps and the retention clip are the same for both prostheses.

Before any modification, it was necessary to identify the scaling percentage that better fitted the child. This value was identified according to the measurements performed on

the child's healthy limb. For this study, the obtained percentage was 100%, with a confidence of 77% for the *Phoenix Hand v2* and 82% for the *Raptor Reloaded*. Tables 6.2 and 6.3 show the confidence percentage for each scaling percentage of both prostheses. Although lower scaling percentages have presented higher confidence values, these percentages were discarded as they present negative and null values. For both prostheses, the first positive value was 95%. However, since the prosthesis components were scaled to 110% to follow the child's growth, the components from the the *Phoenix Hand v2* and *Raptor Reloaded* were scaled to 100% (rather than 95%).

Table 6.2: *Phoenix Hand v2* Sizing Guide: below 94%, the sizing percentages are disposable values with no physical meaning.

Size (%)	93	94	95	100	105	110	115	120	125
Width of Hand	-1	0	1	4	7	11	14	17	20
Length of Hand	33	34	35	42	49	56	62	69	76
Confidence (%)	84.0	83.0	82.0	77.0	72.0	67.0	62.0	57.0	52.0

Table 6.3: *Raptor Reloaded* Sizing Guide: below 94%, the sizing percentages are disposable values with no physical meaning.

Size (%)	93	94	95	100	105	110	115	120	125
Width of Hand	-1	0	1	4	7	11	14	17	20
Length of Hand	23	25	26	32	38	45	51	57	63
Confidence (%)	88.7	87.7	86.8	82.0	77.3	72.5	67.8	63.0	58.3

Finally, the thermo pins and the gauntlet were the only components that were modified. The dimensions of the thermo pins were reduced to a multiple of the layer's width and the gauntlet was increased to match the dimensions of the metacarpal region structure.

6.4 Tuning of the Printing Parameters

The developed prosthesis is composed of a combination of flexible and rigid materials, *Filaflex 82A* and PLA, respectively. However, some components developed throughout this study were printed using PET-G, namely the rigid rings and the testing pieces made for the pull tests. The reason why these components were made of PET-G instead of *Filaflex* is because PET-G has higher tensile strength than PLA [101].

During the development of the prosthesis, especially throughout the fingers' design, several printing tests were made with the aim of determining the best printing parameters for *Filaflex*. The definition of these parameters was made considering the printing quality as well as the functionality of the fingers. Moreover, it is important to highlight that some of these tests were performed using mainly nude *Filaflex 82A*. However, due to

the unavailability of this material, some of the tests were performed using brown *Filaflex* 82A.

Regarding PLA and PET printing, the used parameters were the default ones from *PrusaSlicer* software as the settings of these two filaments have been widely explored. Moreover, it is important to highlight that the rigid rings and the testing pieces have different print settings since the rings were very small and needed to be printed with higher accuracy.

6.4.1 First printing approaches

The first intention of this study was to use a dual extruder printer. By using this type of 3D printer, it would have been possible to print a single piece composed by two different materials. The *Filaflex* would have been used to mimic the soft tissues, and the PLA to mimic bone tissue and for some inner mechanisms. For example, the first prototypes of the fingers were designed to be printed with *Filaflex* and PLA. Indeed, several printing tests were made using a *Li3Dei Dual* printer, a modified *Wanhao duplicator 4s* printer. However, most of these tests revealed a bad printing quality, as it can be appreciated in Figure 6.38. The main pointed reasons for these results were the room temperature and the extruder clogging. Nevertheless, it was not possible to solve these problems despite all efforts to identify their cause. Moreover, given it was a modified printer, it was more difficult to find the possible sources of the printing problems. Thus, it was decided to substitute this printer.

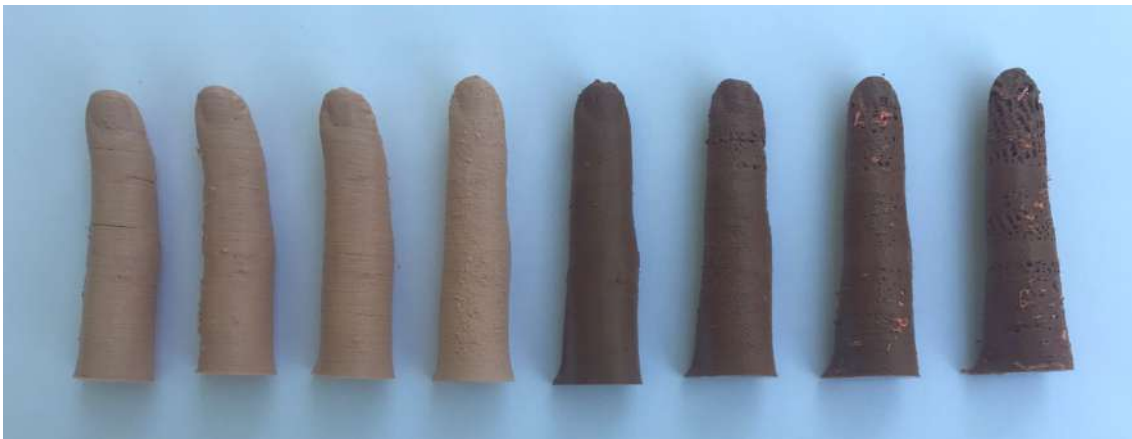


Figure 6.38: Results of the first printing approaches: several printing tests were made using a *Li3Dei Dual* printer, a modified *Wanhao duplicator 4s* printer. Due to a series of printing problems and resulting defects, this printer had to be replaced.

The second printer that was used was *The Original Prusa i3 MK3S+*. Several tests were made in order to find the best printing quality while printing *Filaflex*. These tests were only performed while printing this material, as printing with flexible material presents some additional challenges when compared, for example, with PLA, which has been widely used in the AM field. These tests consisted of consecutive iterations upon a previously determined set of parameters, which was defined within the scope of other studies that were undertaken at the Department of Mechanical and Industrial Engineering of NOVA School of Science and Technology. The printing models used in these experiments were the fingertip of the child's index, with different types of holes to insert the ring, since this part of the fingers is the one who usually presented more defects in previous printings. The last set was then used for further tests that were performed throughout this study.

The Original Prusa i3 MK3S+ is not a dual extruder printer. Hence, it would be impossible to print models composed of two different materials with this printer. Nonetheless, a methodology named "start-stop" was developed to allow to print a model with two different materials. This method consisted of printing part of the prosthesis' components with *Filaflex*, leaving a void space for inserting previously printed PLA components. When printing with *Filaflex*, the printing was stopped at specific layers and the PLA components were inserted. After inserting these components, the printing with *Filaflex* could continue. Figure 6.39 shows the results of the first test that was made to verify the feasibility of this method. Despite the success of this test, when applying this methodology to the fingers, the results were not the expected. Figure 6.40 presents the results of using the start-stop method for printing the fingers, in which can be seen several defects. Most of the printed fingers using this method broke when bended at the stopping layer or the next layer did not adhere to the previous one. In those who did not break, it is possible to see the marks of the stopping layers, which compromise the printing quality. The fingers' functionality would also be compromised as they would probably break after some bending cycles.

As alternative, in order to obtain different volumes with different hardness, it was decided to print the models only with *Filaflex* and use different infill percentages in different structures. Thus, this alternative was tested with an index model in which the phalanges were printed with 90% infill and the remaining finger model with 15%. The results were very satisfactory as this difference of infill percentage was a very faithful replica of the human fingers in terms of sense of touch.

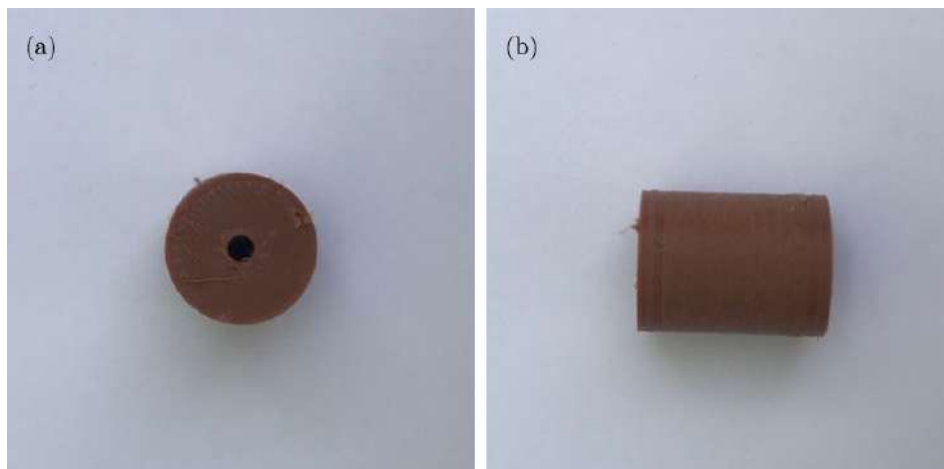
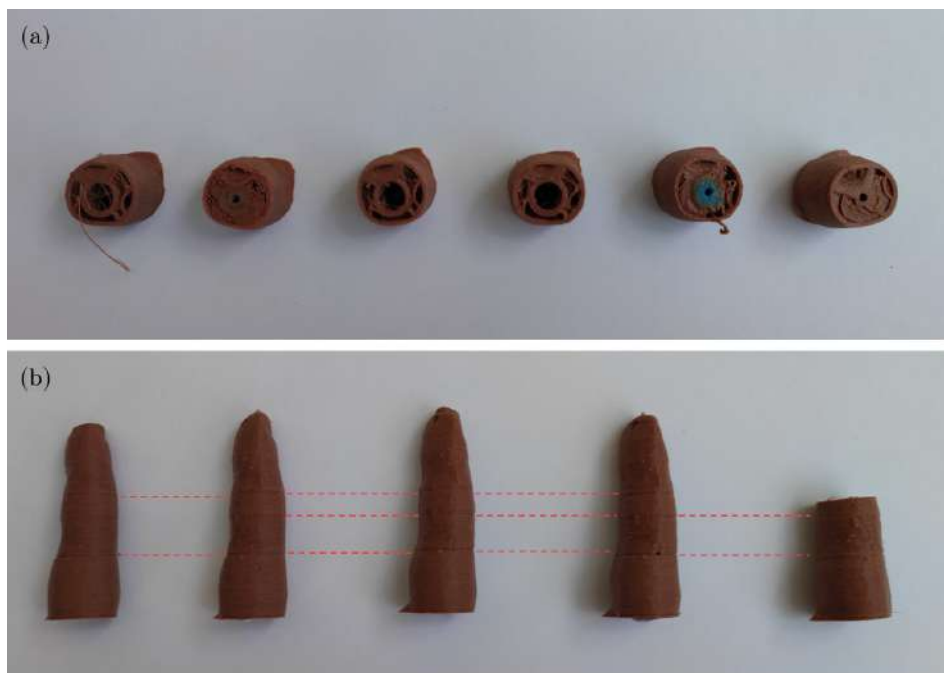


Figure 6.39: Testing of the start-stop method: (a) top view of the *Filaflex* cylinder; (b) lateral view of the *Filaflex* cylinder.



--- Stopping layers marks

Figure 6.40: Printing results of the finger models printed with the start-stop method: (a) top view of broken fingers printed with this method when flexed; (b) lateral view of some of these printed models in which the stopping layers marks are visible.

6.4.2 Printing tests

Throughout the printing tests, two different sets of printing parameters were defined. The set A was previously defined and the set B was the result of several improvements that were performed in the set A. The set B was thought to be the ideal group of printing parameters, since the index models that were printed with these settings revealed to have a good printing quality and did not seem to be too difficult to bend. However, these tests were made using brown *Filaflex* 82A, due to the unavailability of nude *Filaflex* 82A at the time. Printing nude *Filaflex* 82A with those parameters revealed worse quality results. There is a great belief that the filaments' dyes may be the source of these differences, as the filaments' properties and brand are the same. Taking into account the child's physical characteristics, the prosthesis had to be printed using a lighter skin coloured filament. Thus, several printing tests were performed by modifying the set A and B, aiming to reach the ideal printing quality using nude *Filaflex* 82A, as detailed next. The printing settings of these tests are available in Appendix E.

6.4.2.1 Pull tests

In view of the different printing results obtained with the different coloured filaments, some printing tests were made with the aim of improving the printing quality of the models when printing nude *Filaflex*.

These tests were performed by printing the same finger model, namely the last prototype of the index finger. After each printing, a subjective analysis was made in order to assess the quality of the printing, evaluating if there were any defects and how difficult it was to bend the resulting printed finger. The search for the ideal printing parameters was obtained through an iterative process. Considering the results of the previous printing, a new printing test was performed until finding the ideal printing settings. However, after a few tests, no conclusions could be drawn. Evaluating the fingers flexibility became more and more difficult as some fingers were very similar and the human sensibility was not enough to distinguish which was the best model. Thus, with the purpose of choosing the model that would present the best printing quality and that would flex more easily, some of the printing models were exposed to pull tests. The collected data referring to these tests is presented in Appendix F.

Figure 6.41 presents the results of the pull tests that were performed by modifying the set A of printing parameters. The first conclusion that can be drawn is that the more material is present in the the model, the more difficult it is to to bend the finger, but the printing quality is higher. For example, when comparing the model A with the A1, there is no such difference in terms of printing quality. However, the same force, results in a greater displacement in the finger A1, revealing that it is easier to bend this finger. This difference is supported by the smaller amount of material of the second finger, since it has 5% less infill than the A. Finally, the only difference between the A and A2 models

is the number of perimeters (wall width). The model A2 only has one perimeter and it is easier to bend.

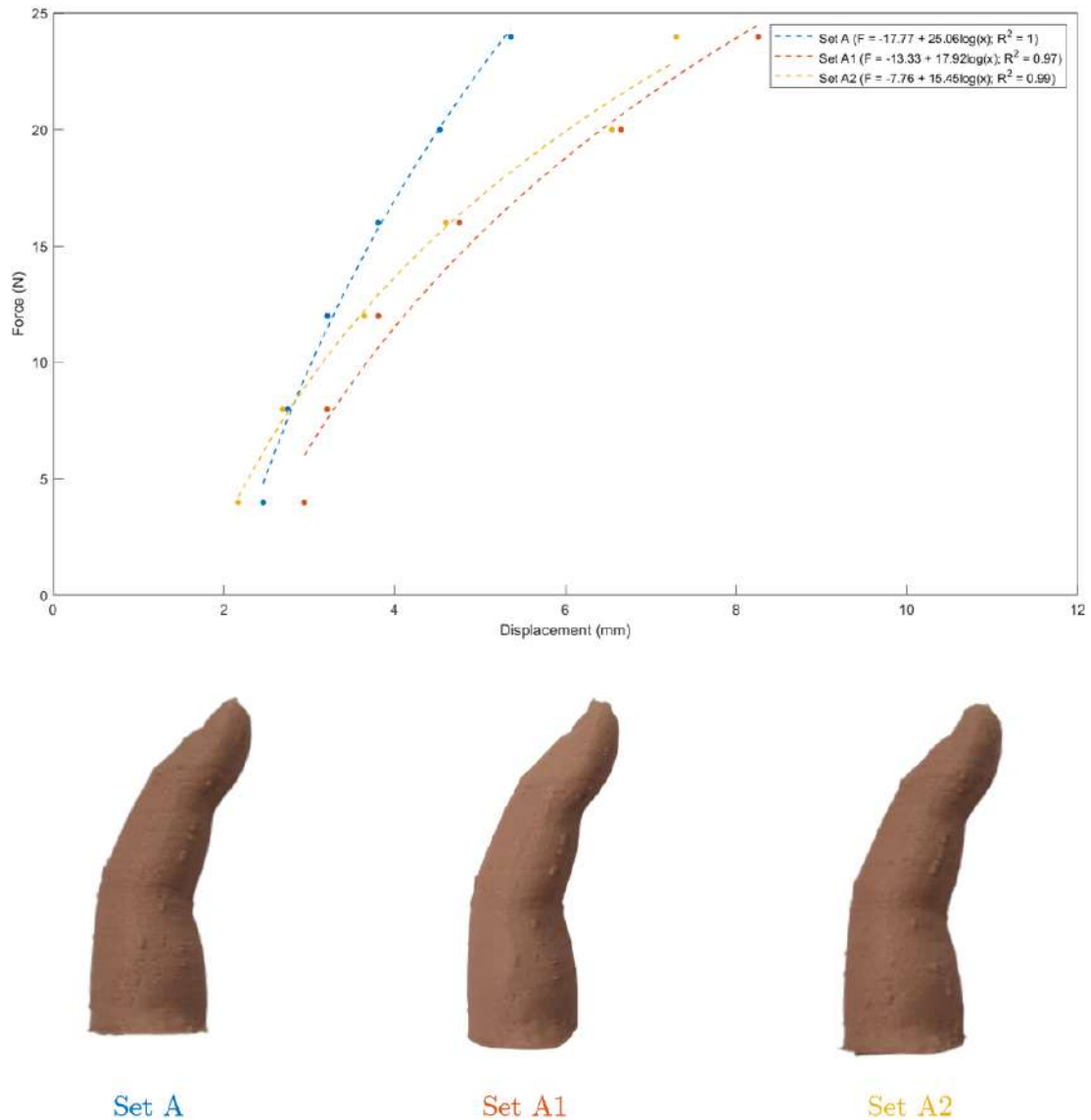


Figure 6.41: Results of the pull tests of the fingers printed by modifying the set A of printing parameters.

The results of the set B also corroborate the hypothesis that less material leads to smaller tensioning forces to bend the fingers, but with poorer printing quality. The major difference between the two sets of printing parameters is the retraction, which was disabled during the tests of the set A. However, although the set B has the retraction on, the amount of extrusion was reduced in comparison with the set A. In light of the previous results, three more tests were made by modifying the set B. These tests consisted of varying the **extrusion multiplier (EM)** value, which controls the amount of material

that is extruded. Figure 6.42 presents the results of these tests, in ascending order of EM values. By analysing these results, it is possible to conclude that as the EM value increases, the force needed to bend the finger also increases and the printing quality improves. When comparing these tests with the previous ones (Figure 6.41), it turns out that most of the fingers printed with modifications made to the set B, for the same vertical displacement, need minor tensioning forces. Nevertheless, besides the improvements that were made, the printing quality is still very poor since there is very poor adhesion between layers.

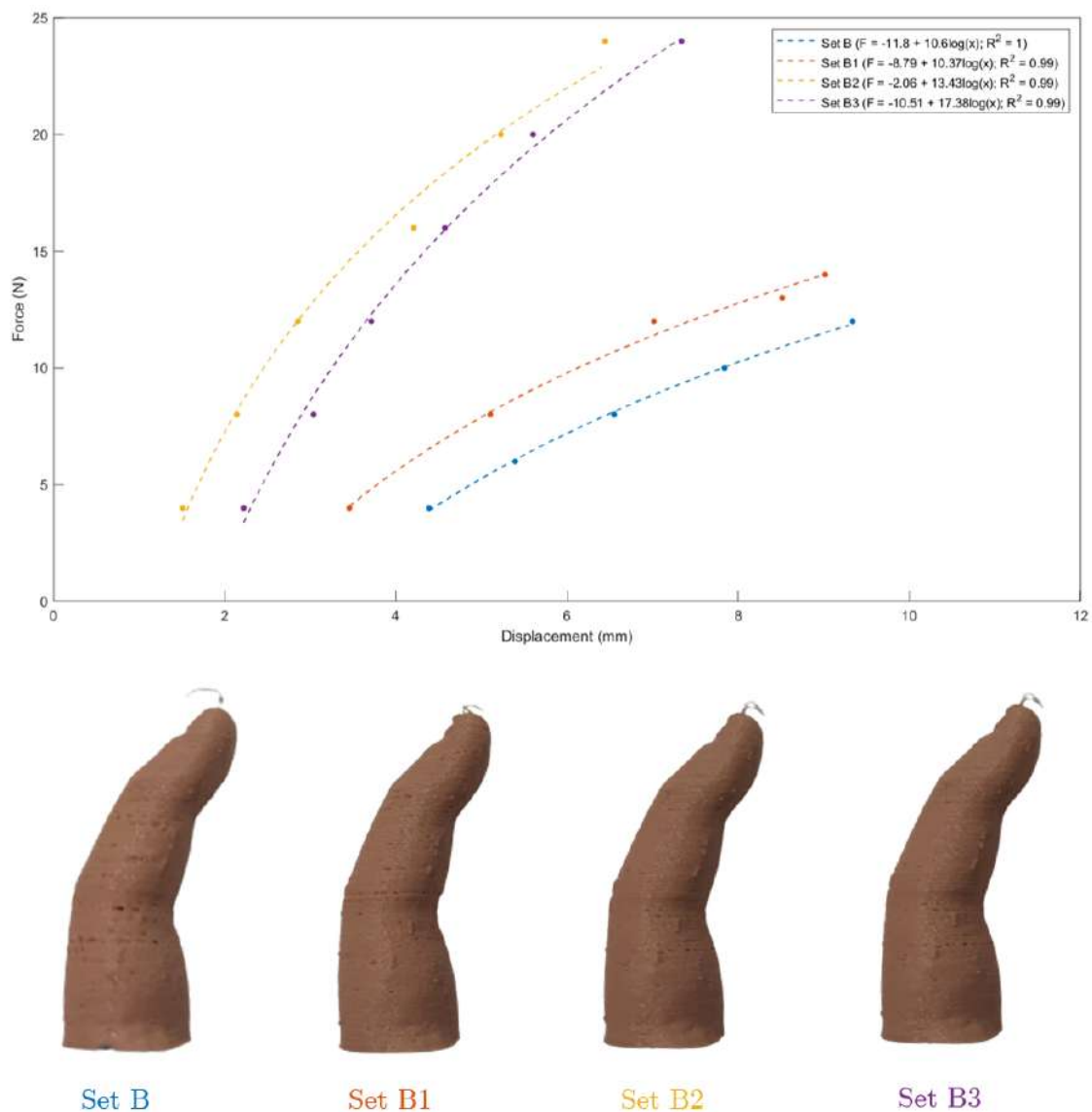


Figure 6.42: Results of the pull tests of the fingers printed by modifying the set B of printing parameters and respective fingers in order of EM value.

Thus, three more tests were performed by modifying the set B of printing parameters for testing the influence of the printing speed. Figure 6.43 presents the results of these

three tests. For the B5 test, the printing speed was reduced to half of the speed of the original printing parameters (set B). Although the quality has improved, there are still some defective layers. For this reason, the speed was increased together with the EM value. This modification resulted in a better adhesion but in high difficulty to bend the finger. Thus, the infill was reduced to 5%. This modification did not change the printing quality and led to smaller tensioning forces. These facts confirm once more that the amount of material that is extruded influences the forces that are needed to flex to fingers and the printing quality.

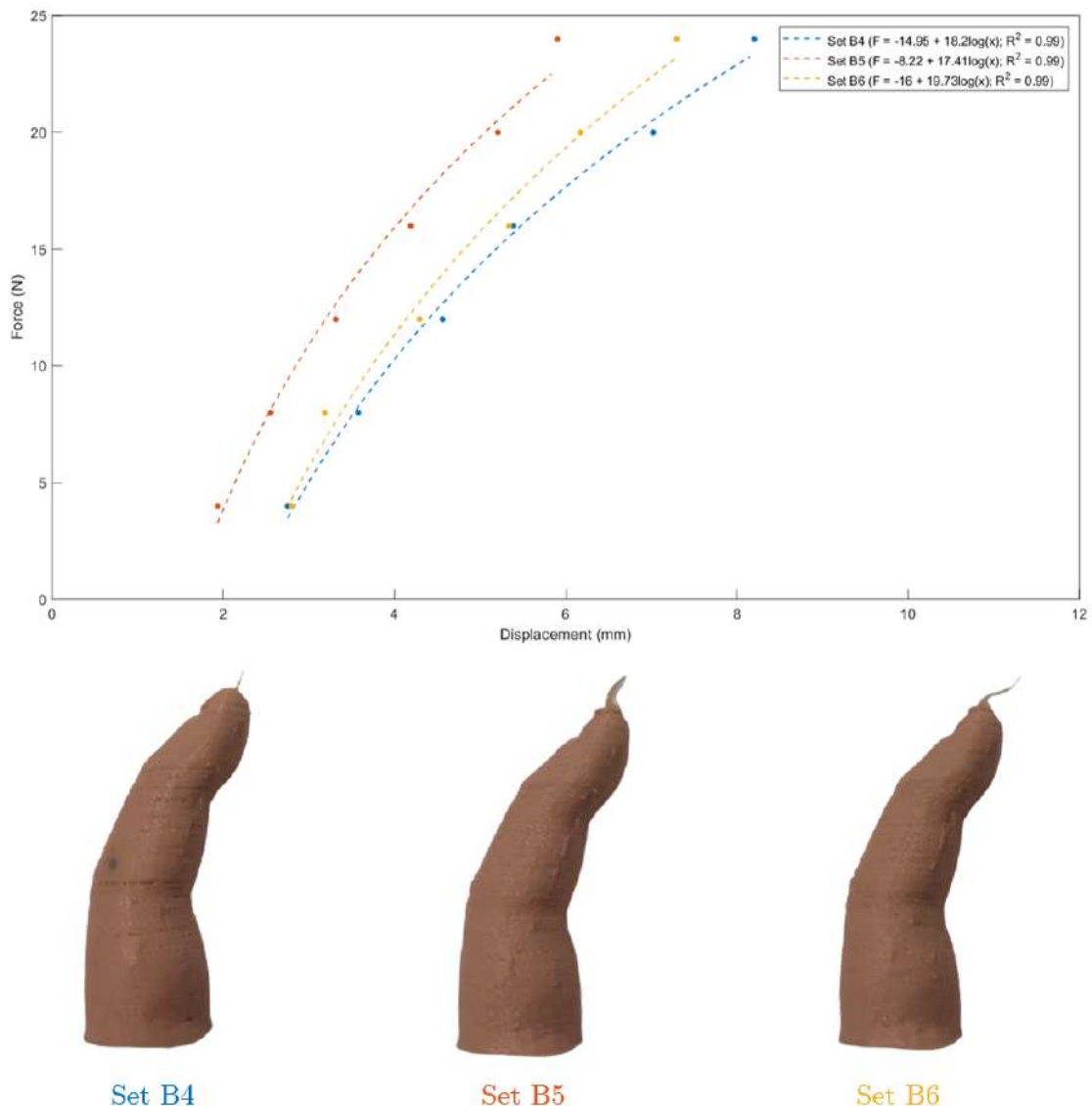


Figure 6.43: Results of the pull tests of the fingers printed by modifying the printing speed of the set B and respective fingers.

Although more printing tests could have been done, the qualitative analysis performed was severely lacking, since no conclusions had been reached. Thus, besides

pointing which were the best printing parameters, the pull tests were also a mean of quantifying the force that was needed to bend a single finger. Some of the printed fingers presented several printing defects that made them invalid for the main goal of this study, which consists of creating a more realistic and appealing upper limb prosthesis. Therefore, only the previously described models were subjected to pull tests. Figure 6.44 presents the other models that were not elected to this evaluation. These fingers were printed horizontally in order to verify if the printing position had some influence. However, the printing quality and the layer orientation would probably compromise the appealing character of the prosthesis and for this reason, these models were excluded.

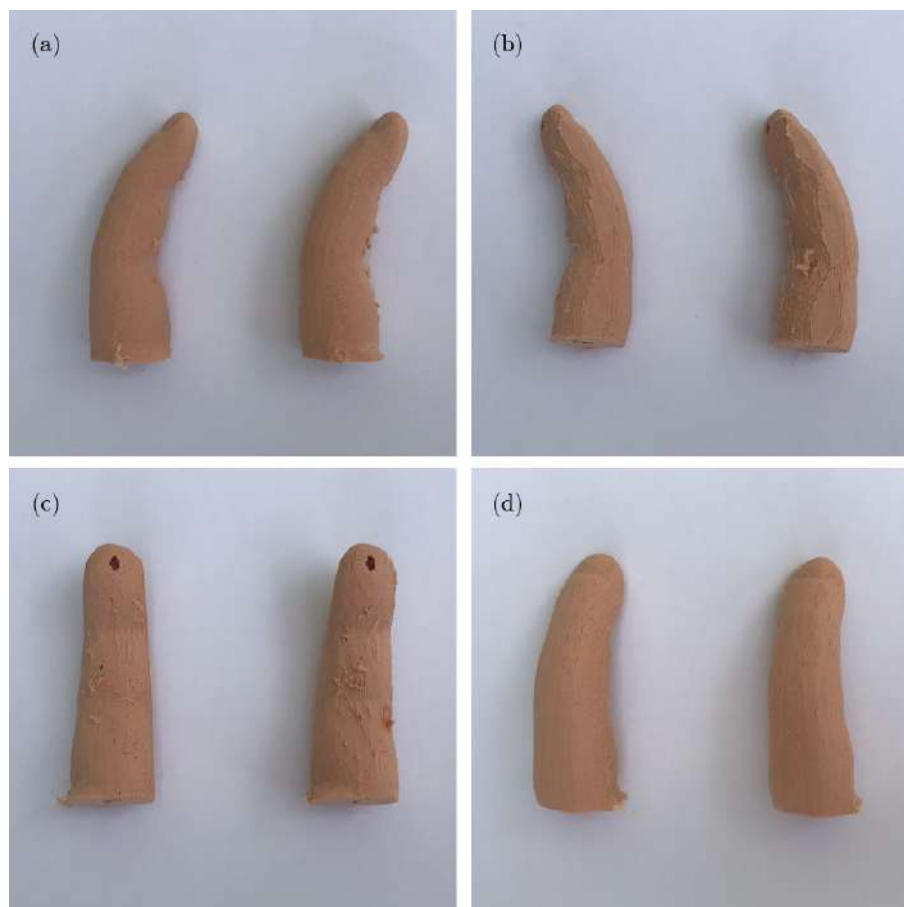


Figure 6.44: Fingers printed horizontally: these fingers were not elected for the pull tests; (a) lateral view (right side); (b) lateral view (left side); (c) posterior view; (d) latero-anterior view.

Thus, in view with these results, the set B was the final choice for printing the whole prosthesis. Although, these printing parameters did not have an ideal printing quality, it was the group of printing settings that required less force to bend. Figure 6.45 compares all the pull tests that were performed, in which is possible to verify that the finger that was printed with the printing parameters of the set B, for the minor value of tensioning force applied, presents the maximum displacement.

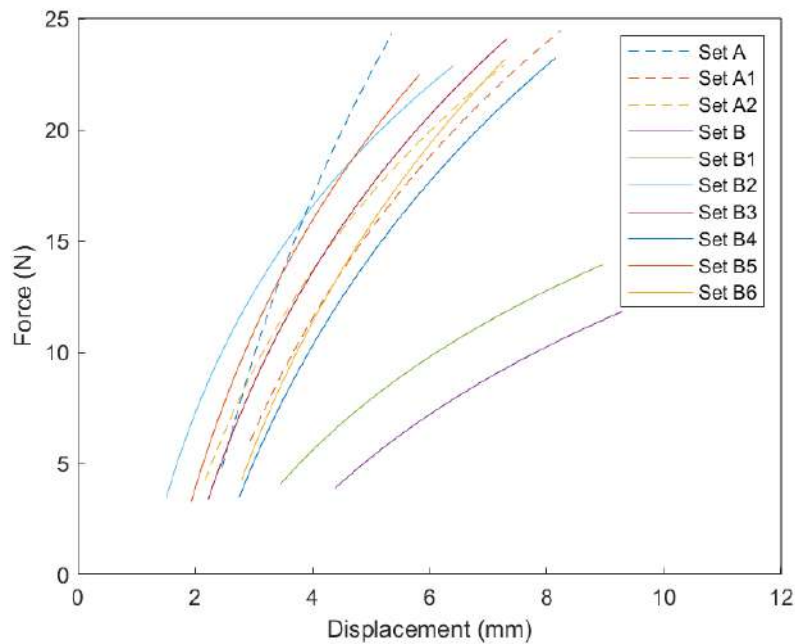


Figure 6.45: Pull tests results of the set A and B experiments with nude *Filaflex 82A*.

In addition to these tests, two more were performed. However, instead of using *Filaflex 82A*, *Filaflex 70A* was used. Although these fingers were not valid to use in the final prosthesis, since the colours available for this filament did not match the child's skin, these tests allowed to evaluate the behaviour of these models when printed with this filament. Considering the high values of the tensioning forces that are needed to bend the fingers printed with *Filaflex 82A*, the study of more flexible filaments may be a first step for further improvements. Figure 6.46 presents the results of these two tests. The first one was printed with the set A of printing parameters and the second one with the set B. Once more, it is possible to notice the difference between extruding a greater or lesser amount of material. The finger that was printed with the set A almost needed double the force of the one printed with the set B to have the same displacement. However, the printing quality is worst in the last one. Nevertheless, the difference of force needed to bend this finger when compared with the finger that was printed with the same settings but with *Filaflex 82A* is notorious. Therefore, it might be interesting to study *Filaflex 70A* for further improvements.

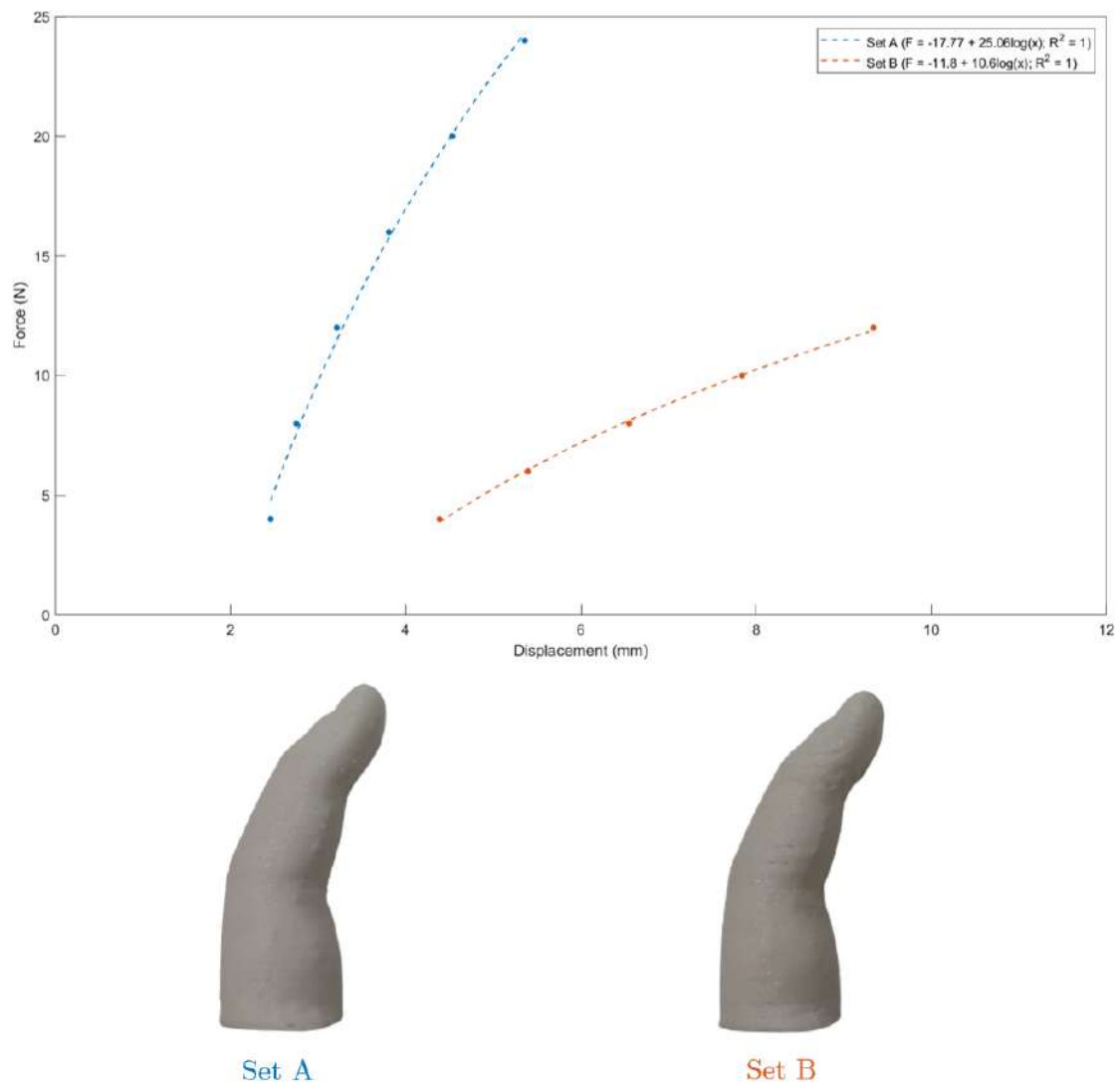


Figure 6.46: Results of the pull tests of the fingers printed with *Filaflex 70A* and respective fingers.

6.4.3 Printing overview

In general, the outcome of the printing tests is quite satisfactory. Although for the purpose of this study, the ideal printing settings have not been found, a huge part of the printed models present a good printing quality. However, due to the mechanic behaviour of the resultant models, the ideal printing settings are still to be defined.

By analysing the resultant plots of the pull tests, all of them (including the tests that were made to assess the best opening angle of the chambers that mimic the interphalangeal joints) present a logarithmic trendline, which reveals the behaviour of the material. This trendline means that the initial displacement is caused by a bigger amount

of force, implying a higher initial energy. Then, after overcoming a certain threshold, a minor amount of force leads to a bigger displacement. In fact, this behaviour is the opposite of what would be desirable, since the ideal behaviour would be a higher facility in flexing the finger initially, followed by the application of higher forces to complete the flexion of the finger.

Although the pull tests were a great method to distinguish objectively which was the best set of printing parameters, there are some key points that need to be discussed. When performing this type of tests in order to assess the materials properties, generally, the tested objects have a uniform geometry so only the material properties will have influence on the objects' behaviour. In this case, the finger's geometry is not uniform and this fact may have influenced the results. Additionally, the force application may also have some influence and these facts could be a possible explanation for the logarithmic behaviour that was obtained. Moreover, even though the pull tests aimed to distinguish which was the best set of printing parameters, it is important to notice that there were other factors that could not be controlled that may have compromised the printing results. The environment temperature during the printing and the portion of filament (the beginning or the end of the coil) that was used to print the model are some of these factors. Finally, it is important to highlight that the mass of the dynamometer, tab and bag was not accounted since no significant displacement was noticed with the application of their weight.

6.5 Prosthesis Assembly

During the course of this study, three similar prostheses were assembled. The differences between the first and second prosthesis are solely the colour of the filaments, as the filaments have the same hardness and are from the same brand. Although only the first prosthesis was needed to match the skin colour of the child, the second one was built to find out if there was any difference in the prosthesis functionality. While performing the printing tests, it was noticed that for the same set of printing parameters, the printing quality was better and the printed components were more malleable when printed with brown *Filaflex 82A* (when compared with to nude *Filaflex 82A*). Therefore, it was decided to assemble these two prostheses. Although the first intention was to use a whippletree mechanism as tensioning system for the main prosthesis, some assembly experiments previously made using this mechanism did not work. Therefore, in order to simplify the model, it was decided to use the tensioning system from the *Raptor Reloaded* prosthesis.

The third prosthesis was developed as a result of the behaviour of the other two prostheses. After being assembled, when these prostheses were flexed, the thermo pins and consequently the gauntlet disconnected from the metacarpal region. This phenomenon occurred due to the difference between the hardness of the *Filaflex* that composes the metacarpal region and the PLA that composes the gauntlet and the remaining wrist components. When these prostheses are flexed, all the energy is absorbed in the interface

between the metacarpal region and the gauntlet, causing the disassembly of the prostheses. Thus, to eliminate this difference of hardness, a third prosthesis was developed to test some of the developed concepts. Unlike the other two prostheses, this one has a metacarpal region printed in PLA without the chamber that simulates the metacarpophalangeal joints. Moreover, instead of two blind holes where the thermo pins fit in, this prosthesis has two through holes in which modified thermo pins are introduced.

Additionally, this prosthesis is composed by fingers printed in *Filaflex 70A* and has a whippletree mechanism from the *Phoenix Hand v2* prosthesis as tensioning system. Since this prosthesis has more flexible fingers and there is no hardness difference between the metacarpal region and the wrist components, it was decided to use this mechanism to test its viability. However, the connection between the fingers is different from the one used in the *Phoenix Hand v2* and is inspired in the *Nazree's Prosthetic Hand*. While the *Phoenix Hand v2* connects the index to the middle finger and the ring finger to the little finger, the *Nazree's Prosthetic Hand* connects the index finger to the little finger and the middle finger to the ring finger. This choice was made based on the human fingers' movements, which rarely move independently [102]. This phenomenon is called enslaving and consists of the involuntary force production by the fingers that were not explicitly involved in a force-production task [103]. The enslaving happens because each finger is actuated by the activity of different muscles, which can act on different fingers. The neighbour fingers are the more affected ones. However, the little finger has some influence on the middle finger. After the thumb, the index is the more independent finger, followed by the little finger. The ring and the middle fingers are the ones who suffer more the enslaving effects [102, 104]. In view of this phenomenon, the middle and ring fingers were connected to each other and the index was connected to the little finger.

Each one of these prostheses takes about four hours to assemble. Generally, they are not difficult to assemble. However, the most difficult task was to tie the guitar strings to the rings and tensioning pins, due to the strings' nature. Regarding the gauntlet, it was decided to mould it without the child's presence so the appointment for the prosthesis' presentation did not take too long.

6.6 Prosthesis Evaluation

Throughout this study, several efforts were made in order to develop a body-powered hand prosthesis that would combine a more real and appealing cosmetic appearance together with a high level of functionality. Figure 6.47 presents the main prosthesis that was developed within the scope of this study.



Figure 6.47: First developed prosthesis: this is the main prosthesis, that was printed with nude filaments to match the skin colour of the child; (a) anterior view; (b) posterior view.

Regarding the cosmetic appearance, it is considered that this goal was met with success. Although the final prosthesis developed during this study consists of a MVP, it presents a high level of anthropomorphism. The presence of some protuberances that simulate the hands creases and knuckles as well as the use of a flexible filament and different infill percentages to mimic the hand's bones contribute to this level of anthropomorphism, creating the idea of a real hand, especially when compared with other 3D-printed prostheses. However, there are some aspects that need to be improved, namely the wrist design. The fact that the tensioning system is external in any of the developed prostheses may be a possible trigger for patients refuse these devices since it compromises their appearance. Nevertheless, one of the goals of this study was to customise the prosthesis in terms of size. Thus, making the tensioning systems internal, as in the *Nazree's Prosthetic Hand*, would have been a challenge in prostheses for children, especially if the size is one of the major concerns as in this study.

Due to the long course of this study, it was decided to scale all the prosthesis components to 110% in order to keep up with the child's growth. Figure 6.48 shows the size difference between the child's healthy hand and the developed prosthesis. In Figure 6.48a it seems that there is a huge difference between the child's hand and the prosthesis. However, in Figure 6.48b it is noticed that this difference is not that significant and it is caused by the stump-prosthesis interface that should be more deep so the prosthesis

could be at the same level of the child's hand. This is a problem that affects most of the wrist-powered prostheses, since they fit in the residual limb, resulting in a bigger hand than desired [10]. In this case, using a lower scaling factor could have eliminated this size difference. Nevertheless, since the children growth is not uniform, predicting these values becomes impossible. Thus, the only solution would have been to repeat the measures and adjust the scaling value.

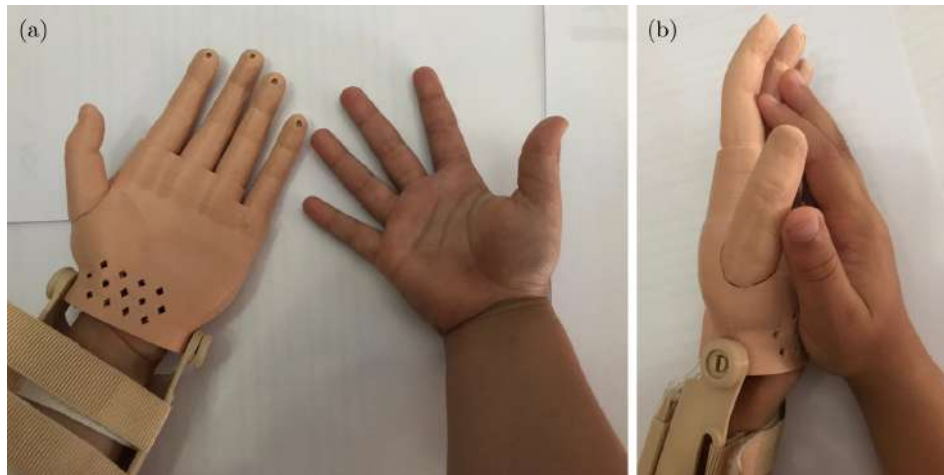


Figure 6.48: Child wearing the prosthesis: even though the prosthesis is not functional, the child was very receptive to the device; (a) size comparison between the prosthesis and sound hand (anterior view); (b) size comparison between the prosthesis and sound hand (lateral view).

Despite all the efforts that were made, unfortunately the final prototype is not functional. Although during the developing and testing stages, some possible errors were expected, nothing predicted the disconnection between the gauntlet and the metacarpal region, which compromises the prosthesis' functionality. However, it is thought that if this problem did not exist, the prosthesis would still not be functional, since a lot of strength is needed to flex the prosthesis. Although it was thought that the *Filaflex* elasticity was enough to substitute the dental bands that compose most of the 3D-printed prostheses to make them flex and return to the initial position, the fingers and the metacarpal region revealed a high resistance to bending. Besides exploring the application of the tensioning forces in order to favour the flexing of the prosthesis, there is a great belief that the materials that compose the prosthesis also influence the prosthesis functionality. Thus, these materials, especially flexible materials, must be explored further in order to make the most of their potential. There is a belief that these improvements must focus first on the materials and then on the prosthesis' mechanisms, since all the mechanisms that were developed were thought to boost the prosthesis functionality. However, mechanisms such as the strings' path in the metacarpal region and the interface between this structure and the gauntlet must be reviewed in order to improve the functionality of the prosthesis.

Despite all the aspects that need to be enhanced, even in terms of appearance or functionality, it is important to refer that the development process was the result of simultaneous, often conflicting, requirements of functionality, resistance, appearance, force needed for flexing and printability. Most of the decisions that were made during the development of the prosthesis were the result of constant trade-offs. For example, a better printing quality would lead to a higher difficulty in flexing the fingers; hiding all the mechanisms inside the metacarpal region would result in huge prosthesis when comparing with child's hand and creating smaller components would probably lead to a lower resistance and durability. However, the resultant prosthesis, which consists of a prototype is considered to be a huge step in the field of flexible 3D-printed prosthesis.

Figure 6.49 presents the second developed prosthesis and Figure 6.50 presents the third prosthesis. The second prosthesis, when compared the first, presented a higher printing quality, especially in the metacarpal region. When handled, the parts printed with brown *Filaflex* 82A revealed to be softer. The third prosthesis was the only one that presented some level of functionality, as it can be seen in Figure 6.51. When flexed, there was a slight bending of the fingers. However, this flexion did not mimic the gripping movement since there is no mechanism that mimics the flexion of the metacarpophalangeal joints. Moreover, a lot of strength was necessary to flex the prosthesis, which is not manageable for a child. Furthermore, the thumb did not move at all when the prosthesis was flexed. The shape of the wire's hole might be one of the reasons for this to happen. Regarding the printing quality, the only present defects in this prosthesis are from the printing with *Filaflex* 70A. It is important to notice that the main objective of this prosthesis was to test some of the developed concepts, especially the functionality of the fingers and the tensioning mechanism. Since it is needed a lot of strength, when the prosthesis is flexed the results of the whiplight are not evident. However, if the movement of one finger is blocked, the finger that is connected has the freedom to continue to move and adapt to the object that is being gripped. Ultimately, each finger of a connected pair moves equally, simulating the enslaving phenomenon. Therefore, this mechanism is a good starting point for enhancing the functionality of further 3D-printed body-powered prostheses.

Finally, if we compare the developed prostheses with other existent prostheses, several improvements can be pointed, especially in aesthetical terms. Aesthetically, the developed prostheses, especially the first and second models, present a high anthropomorphic level, which makes them more appealing. When compared with the prosthesis developed by F. Pinheiro, the improvements are also evident. While the fingers made by F. Pinheiro were made from scratch, the fingers of the present study consist of an adaptation of the replica of the fingers of the child's sound hand [30]. Thus, besides being highly customised prostheses, the developed prostheses become more appealing due to their more natural appearance. Although there are several functionality aspects to improve when compared with other prostheses, there is a great belief that some of the developed concepts could lead to high level of customisation if improved.



Figure 6.49: Second developed prosthesis: this prosthesis was developed in order to find out if the filament colour had some influence in its printing quality and consequently, in the prosthesis functionality; (a) anterior view; (b) posterior view.



Figure 6.50: Third developed prosthesis: this prosthesis was developed in order to evaluate the hypothetical functionality of the third and second prostheses, by eliminating the hardness difference between the metacarpal region and the gauntlet. It also presents a different tensioning mechanism, a whippetree system; (a) anterior view; (b) posterior view.

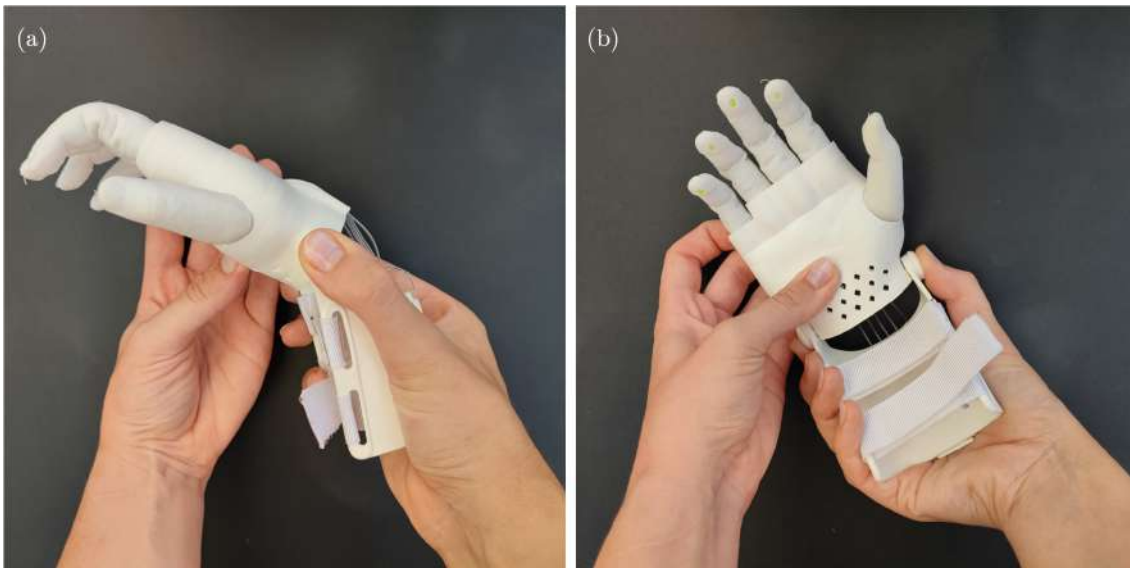


Figure 6.51: Flexion of the third developed prosthesis: (a) lateral view; (b) anterior view.

6.6.1 Prosthesis characteristics

The cosmetic appearance and functionality are two of the main user's need of a prosthesis. However, other aspects such as comfort and price are also important. Table 6.4 presents the materials cost of the three developed prostheses, their mass and printing time. Appendix G presents the discriminate cost of each component that compose these prostheses.

Table 6.4: Materials cost, mass and total printing time of each developed prosthesis.

	1 st Prosthesis (nude)	2 nd Prosthesis (brown)	3 rd Prosthesis (white)
Materials Cost (€)	12.65	12.65	8.77
Mass (g)	105	101	103
Printing Time (h)	26h39	26h39	20h22

By analysing Table 6.4 it is evident how beneficial 3D-printed prostheses are due to their light weight and low costs. According to J. ten Kate *et al.*, most of upper limb prostheses range from 5 to 500 \$ [10]. The obtained costs are within these value and way below the average. However, it is important to refer that only the costs of the materials were considered. Nevertheless, this fact might be quite encouraging for further studies and reveals the promising character of 3D-printed prostheses, especially when printing with flexible materials. The major population benefiting from these values are children (given the frequency which their prostheses' will need replacement) and people from LMICs.

Regarding the weight of the prosthesis, according to J. ten Kate *et al.*, there is record of a single prosthesis that weighs less than 130g. Moreover, the human hand weighs 400

$\pm 90\text{g}$ [10], whereby, for a four-year-old child, the obtained value of the prosthesis' mass is considered to be very satisfactory. In fact, the weight of the developed prostheses was one of the main aspects that was praised by the child's mother. However, this fact would only be proved if there was a constant use of the prosthesis during the daily activities of the child.

Finally, the printing time is also near the common range as most 3D-printed prosthesis take 15 to 20 hours to print. However, the printing time depends on the complexity of the chosen model, the printing settings and on the 3D printer that is being used [10]. This justifies the higher printing time of the first and second prostheses when compared with the third one. Both first and second prostheses have more components printed with *Filaflex*, which requires slower printing speed than PLA.

6.6.2 System Usability Scale assessment

The SUS was the methodology chosen to measure the level of satisfaction of the child and family after presenting the three prostheses. By presenting the three devices it was possible to explain the several concepts that were developed during the whole study. Since SUS is a standard tool, ten additional questions, which follows the SUS logic, were developed in order to obtain a more specific evaluation. The results of these two surveys are 97.5 and 100 (out of 100), respectively, which classifies the prosthesis as "Excellent". However, due to the lack of functionality of the developed prostheses, these results were not expected.

Appendix H presents the answers to the SUS as well as the ones of the ten additional questions. All the answers, except for one, are the extremes of the answer's scale, which leads to these high scores that do not reflect the fact that the prostheses are not totally functional. These extreme answers reveal that, even though the prosthesis is not functional, the progresses, especially in terms of aesthetical appearance, were notorious when compared with other 3D-printed body-powered prostheses. In fact, the aesthetical appearance and the comfort of the prostheses, given by the adhesive foam, were some of the main compliments that were made by the child's mother. However, these extreme answers may have been resultant of some questions that could have been misunderstood.

Nevertheless, the outcome of the child and family was very satisfactory. The child was very receptive to the prosthetic devices. This first impression revealed that a more real appearance might be a possible solution to decrease the rejection of this type of prostheses and be a mean to increase the confidence of children with these type of lesions. However, this fact cannot be proved, since to evaluate this situation, a long-term usability evaluation would be needed. During the whole process, the child's family revealed to be extremely interested, which was very helpful, since the beginning. This fact may be proved by the several attempts to make a plaster replica of the child's limbs extremities. Throughout the study, the child's family was kept in touch so they could be aware of the progresses that were being made.

CONCLUSION

This chapter presents an overview of the present study, in which the final considerations of the developed work are presented, namely the major achievements and suggestions for future work.

7.1 Summary of the Study Achievements

Hands are an essential tool for human beings as they are used in most day-to-day activities. Hence, the absence of this structure, either partial or complete, compromises the quality of life of upper limb amputees. Prosthetic rehabilitation can help revert this scenario since it promotes the reestablishment of the patients' functionality and consequently improves their quality of life. However, not all the patients can afford a prosthesis that answers the most basic user's needs such as comfort, an appealing cosmetic appearance and functionality. Lately, AM has emerged as the solution for the main problems of the prosthetic field since it enables the production of these devices at a low-cost. 3D-printed prostheses have special interest for children since their growth implies to change the device frequently. However, although this type of prostheses has been explored, they seem to present a quite high rejection rate, especially by children, due to their toy-like appearance. Moreover, these prostheses are often rigid devices, which also promotes their rejection. Therefore, there is a need to invest in more flexible and realistic prostheses that also ensure the other essential features such as comfort, low-cost and good functionality.

Although some prostheses with flexible materials have already been proposed, they are mainly cosmetic. Functional prostheses built with this type of materials only use flexible material in some specific parts. There is no complete body-powered solution that uses flexible filaments as main materials. Thus, the main goal of this study was to design a 3D-printed body-powered upper limb prosthesis with flexible materials and improved cosmetic appearance. The hypothesis of this study was that a more realistic, functional, comfortable and tailored hand prosthesis can be developed by using AM and flexible materials, without compromising other features such as lightweightness, ease of repair and low-cost.

Besides these aspects, customisation was also a concern, especially regarding to the size of printed hand when compared to the sound hand. Capturing the anatomical features is crucial to develop customised prosthetic devices and may be the key to reduce the rejection rate of these devices, especially in younger ages. Assessing these features was essential for the course of this study. The methods used to assess these features were simple measurements, photographs, body casting and 3D scanning of the cast. Thus, it was possible to design a highly customised device. However, the measurements and the casting would have been enough since the photos that were taken were not necessary during the whole process of the prosthesis' development.

During the assessment of the anatomical features, communication and transparency with the child and his family were crucial for the good progress of the study. The fact that the family insisted to repeat the body casting procedure after two attempts reveals a high level of interest, which made them an active of part of the whole study. This evidences the importance of both the child and family to have the capacity to deal with expectations. Moreover, the fact that this was not the first experience with a prosthesis of this type also helped the family to actively participate in the whole study.

The usage of DfAM principles for the prosthesis' design, allowed to simplify the whole process. Therefore, it was necessary to previously study the generated concepts in order to get more out of the DfAM principles. During the progress of this study, several prototypes were made in order to test the generated concepts. These prototypes were resultant of simultaneous trade-offs, including printability, functionality, resistance, appearance and force needed for flexing the models.

Although several printing tests using *Filaflex* have been made in order to achieve the best printing quality that led to high level of functionality, the perfect printing settings were not found. Throughout these tests, several issues with this filament were faced and explored. The review of these issues may be a starting point for further improvements, either in prosthetic field or other applications.

During these tests it was discovered that there is a linear relationship between the printing quality and the forces needed to bend the flexible components. Moreover, it was noticed that printing with nude *Filaflex* 82A and brown *Filaflex* 82A leads to different results. This fact might be related with the filament dyes, since the filament and brand were the same. Thus, two different prosthesis were assembled to demonstrate this difference: one in nude and another in brown.

The brown prosthesis was printed with higher quality and revealed to be softer than the original nude prosthesis. Given that the perfect settings were not found, both the prostheses revealed a low level of functionality. Besides the low functionality caused by the high forces needed to flex these prostheses, the difference between the hardness of the *Filaflex* that composes the metacarpal region and the PLA that composes the gauntlet and the remaining wrist components also contributed to this result. When these prostheses are flexed, all the energy is absorbed in the interface between the metacarpal region and the gauntlet, causing the disassembly of the prostheses and leading to their low

functionality.

Therefore, a third prosthesis was developed in order to eliminate this difference of hardness and test some of the developed concepts, namely the usage of the whippletree mechanism as tensioning system. Although it is difficult to flex this prosthesis, this mechanism revealed to be a good option to use in this type of prostheses as it promotes an adaptive grasping, increasing their level of functionality.

Finally, despite the low functionality of the designed prostheses, the final results were very satisfactory, especially when compared with other existent prostheses such as the *Raptor Reloaded* prosthesis:

- The developed prostheses consist of lighter prostheses, which makes the wearing experience more pleasing. Additionally, the fact that they are composed by flexible materials contributes to increase their comfort as the stump-prosthesis can mould to the patient's anatomy.
- These prostheses are aesthetically appealing solutions and consist of a huge cosmetic improvement to the common 3D-printed body-powered prostheses. By enhancing their aesthetical appearance, the acceptance rate of this type of prostheses has a high chance to increase. With more similar features to a real hand, children will stop facing these devices as toys and their rejection might become lower. However, children are not the only ones who benefit from these improvements. Adults may also become more interested in these devices as they have a natural look, instead of a childish unreal appearance. Furthermore, the possibility of customisation with the patients anatomical features has also a huge impact, especially on adults.
- Like other 3D-printed prostheses, the developed devices are low-cost solutions, which makes them perfect for children as they need to replace their prosthetic devices frequently due to their fast growth. In addition, prostheses used by children are more likely to be damaged, whereby cheaper solutions are ideal for children. Furthermore, even if children do not accept well these kind of models, it still consists of a less expensive way to explore children's interest in prostheses. Finally, these low-cost prostheses will also benefit people with lower purchasing power that cannot afford more expensive devices, like people from LMICs.
- These prostheses are composed of several segments, which allows to answer one of the user's needs that are required for children: the easy replacement if any component breaks or if new components are needed due to child's growth. Additionally, this segmentation allows the simplification of the assembly, increasing their user-friendly character, as any patient can assembly their own prosthesis or replace any component if needed.
- Moreover, establishing some kind of sensory feedback was also a key aspect. This feedback is given by the flexibility of the material that composes the terminal device

and by the inner mechanisms that mimic the human bones. The usage of flexible filament simulates the compliance of the hand's skin, allowing to achieve a stronger grip and avoiding the objects to slip. This feature is quite impacting for patients with acquired deficiencies who have a huge need to restore their sensory feedback. Additionally, the different infill percentages that compose the printed parts give the prosthesis a sense of touch similar to a human hand.

The development of the present 3D-printed body-powered hand prostheses has revealed several contributes to the scientific community as it may be one of the first steps for the evolution of prostheses made by AM with flexible materials. This study presents a full methodology to design a customised 3D-printed body prosthesis. This device brings benefits for any patient with an upper limb defect, whether they are children with a congenital disorder that need to have contact with prosthetic devices or traumatic amputees that miss their limbs in the daily activities.

After all, it is important to have in mind that most of these prosthetic devices are made through successive iterations and the present prostheses were no exception. Even though a lot of 3D-printed prostheses have been designed around the world, there is still a huge lack of standard guidelines for this type of prostheses. Further studies must focus on evaluating the existent prostheses, improving them so they can be introduced to the market as the main solution for upper limb amputees [10, 72].

7.2 Future Work

AM has been growing over time and the prosthetic field has been benefiting with this progress. The present study describes a full methodology to develop a 3D-printed body-powered upper limb prosthesis. However, there is still plenty room for improvement. Further work should include:

- **Improvement of the functionality of the designed prostheses:** this might be done by changing the interface between the wrist and the metacarpal region or decreasing the the difference in hardness between these two structures. Reducing the forces needed to flex the prosthesis is also a possible solution to improve the functionality of these devices. This could be done by changing some of the internal designs such as the shape of the wire's holes, especially in the metacarpal region, or by testing other opening angles to simulate the interphalangeal joints of each finger. There is a great belief that exploring even more the behaviour of materials could be the solution for some of the functionality problems. By studying the flexible materials, the elastic behaviour could be improved and the guitar strings could be replaced. Other possible solution to improve these prostheses functionality, could be the design of an articulated device, similar to an *e-NABLE* prosthesis, that simulated the human skeleton. Then, in order to achieve a more appealing appearance, a

flexible glove could cover this device. However, it is possible that this solution would become challenging, especially when printing the glove.

- **Enhancement of the cosmetic appearance:** although significant achievements have been made concerning this topic, there are some features that need to be improved, especially in the metacarpal region and wrist. The level of anthropomorphism of these structures could be increased by reducing the size of the tensioning system, making it internal or creating a new mechanism. Moreover, making the stump-prosthesis interface deeper would also improve the aesthetics of the terminal device since the difference between the size of sound hand and the prosthesis would not be so evident.
- **Evaluation of the prosthesis after increasing its functionality:** one of the first intentions of this study was to evaluate this prosthesis mechanically, after its development. However, due to its low functionality, these tests were not performed. For this evaluation, mechanical resistance and performance tests are suggested. The mechanical resistance measures how much force is needed to withstand a certain weight and what is the maximum payload of the prosthesis before it fails or break. The mechanical performance tests evaluate the grasping capabilities of the prosthesis by measuring its grasping force. This value may be compared with the flexion force of each finger in order to assess what is the contribution of each finger during the grasping activities [105]. The prosthesis may also be evaluated by some stakeholders such the members of rehabilitation teams, elder patients, families, etc., in order to assess possible further improvements. Functionality tests should also be applied.
- **Application of this methodology to other children:** after improving the functionality of this device, it would be important to test this methodology with other children and their families. SUS could be a good tool to evaluate their level of satisfaction. Moreover, by applying this methodology to other children, in a long term, it would be possible to assess if the improvement of the aesthetics of these devices, by making them more similar to a human hand, decreases the rejection rate.

Finally, it is important to highlight that the current study will be continued with the aim of keeping improving the customisation of this type of prostheses, lowering their costs so more people could have access to them.

REFERENCES

- [1] J. M. Lourenço, *The NOVAthesis L^AT_EX Template User's Manual*, NOVA University Lisbon, 2021. [Online]. Available: <https://github.com/joamlourenco/novathesis/raw/master/template.pdf>.
- [2] L. A. Jones and S. J. Lederman, *Human Hand Function*, Oxford University Press, Ed. Oxford University Press, May 2006, ISBN: 9780195173154. DOI: [10.1093/acprof:oso/9780195173154.001.0001](https://doi.org/10.1093/acprof:oso/9780195173154.001.0001).
- [3] D. van der Riet, R. Stopforth, G. Bright, and O. Diegel, "An overview and comparison of upper limb prosthetics", in *2013 Africon*, Pointe-Aux-Piments: IEEE, Sep. 2013, pp. 1–8, ISBN: 978-1-4673-5943-6. DOI: [10.1109/AFRCON.2013.6757590](https://doi.org/10.1109/AFRCON.2013.6757590).
- [4] K. Soyer, B. Unver, S. Tamer, and O. Ulger, "The importance of rehabilitation concerning upper extremity amputees: A Systematic Review", *Pakistan Journal of Medical Sciences*, vol. 32, no. 5, pp. 1312–1319, 2016, ISSN: 1682024X. DOI: [10.12669/pjms.325.9922](https://doi.org/10.12669/pjms.325.9922).
- [5] F. Cordella, A. L. Ciancio, R. Sacchetti, A. Davalli, A. G. Cutti, E. Guglielmelli, and L. Zollo, "Literature Review on Needs of Upper Limb Prosthesis Users", *Frontiers in Neuroscience*, vol. 10, no. 209, May 2016, ISSN: 1662-453X. DOI: [10.3389/fnins.2016.00209](https://doi.org/10.3389/fnins.2016.00209).
- [6] T. R. Dillingham, L. E. Pezzin, and E. J. M. A. C. Kenzie, "Limb Amputation and Limb Deficiency: Epidemiology and Recent Trends in the United States", *Southern Medical Journal*, vol. 95, no. 8, pp. 875–883, 2002.
- [7] K. A. Raichle, M. A. Hanley, I. Molton, N. J. Kadel, K. Campbell, E. Phelps, D. Ehde, and G. Douglas, "Prosthesis use in persons with lower- and upper-limb amputation", *Journal of rehabilitation research and development*, vol. 45, no. 7, pp. 961–972, 2008. DOI: [10.1682/jrrd.2007.09.0151](https://doi.org/10.1682/jrrd.2007.09.0151).
- [8] D. Farina and S. Amsüss, "Reflections on the present and future of upper limb prostheses", *Expert Review of Medical Devices*, vol. 13, no. 4, pp. 321–324, Apr. 2016, ISSN: 1743-4440. DOI: [10.1586/17434440.2016.1159511](https://doi.org/10.1586/17434440.2016.1159511).

REFERENCES

- [9] Enabling The Future, *Enabling The Future – A Global Network Of Passionate Volunteers Using 3D Printing To Give The World A "Helping Hand"*. [Online]. Available: <https://enablingthefuture.org/> (visited on 01/15/2020).
- [10] J. ten Kate, G. Smit, and P. Breedveld, "3D-printed upper limb prostheses: a review", *Disability and Rehabilitation: Assistive Technology*, vol. 12, no. 3, pp. 300–314, Apr. 2017, ISSN: 1748-3107. DOI: [10.1080/17483107.2016.1253117](https://doi.org/10.1080/17483107.2016.1253117).
- [11] K. T. Ulrich and S. D. Eppinger, *Product Design and Development*, 5th Editio. New York: McGraw-Hill Companies, Inc., 2012, ISBN: 978-0-07-340477-6.
- [12] J. M. Zuniga, A. M. Carson, J. M. Peck, T. Kalina, R. M. Srivastava, and K. Peck, "The development of a low-cost three-dimensional printed shoulder, arm, and hand prostheses for children", *Prosthetics and Orthotics International*, vol. 41, no. 2, pp. 205–209, Apr. 2017, ISSN: 0309-3646. DOI: [10.1177/0309364616640947](https://doi.org/10.1177/0309364616640947).
- [13] S. Jain, "Rehabilitation in limb deficiency. 2. The pediatric amputee", *Archives of Physical Medicine and Rehabilitation*, vol. 77, no. 3, S9–S13, 1996, ISSN: 00039993. DOI: [10.1016/s0003-9993\(96\)90237-3](https://doi.org/10.1016/s0003-9993(96)90237-3).
- [14] C. Afonso, I. J. P. Coelho, and I. A. Cadete, "Amputações e Malformações Congénitas do Membro Superior na População Pediátrica - Revisão de 27 Anos Congenital skeletal deficiencies in upper limb in a pediatric population : 27 years Revision", *Revista da Sociedade Portuguesa de Medicina Física e de Reabilitação*, vol. 17, no. 1, pp. 1–4, 2009.
- [15] M. Egermann, P. Kasten, and M. Thomsen, "Myoelectric hand prostheses in very young children", *International Orthopaedics*, vol. 33, no. 4, pp. 1101–1105, Aug. 2009, ISSN: 0341-2695. DOI: [10.1007/s00264-008-0615-y](https://doi.org/10.1007/s00264-008-0615-y).
- [16] S. K. Campbell, D. W. Vander Linden, and R. J. Polzano, *Physical Therapy for Children*, 2nd Editio. W. B. Saunders Co., 1994, pp. 370–372, ISBN: 0-7216-8316-9.
- [17] V. Lopes, "Design and Development of an Upper Limb Prosthesis", Ph.D. dissertation, Instituto Superior Técnico, Universidade de Lisboa, 2017, p. 11.
- [18] W. Gaine, C. Smart, and M. Bransby-Zachary, "Upper Limb Traumatic Amputees: Review of prosthetic use", *Journal of Hand Surgery*, vol. 22, no. 1, pp. 73–76, Feb. 1997, ISSN: 0266-7681. DOI: [10.1016/S0266-7681\(97\)80023-X](https://doi.org/10.1016/S0266-7681(97)80023-X).
- [19] B. Phillips, G. Zingalis, S. Ritter, and K. Mehta, "A Review of Current Upper-limb Prostheses for Resource Constrained Settings", in *2015 IEEE Global Humanitarian Technology Conference (GHTC)*, IEEE, Oct. 2015, pp. 52–58, ISBN: 978-1-4673-6561-1. DOI: [10.1109/GHTC.2015.7343954](https://doi.org/10.1109/GHTC.2015.7343954).

- [20] N. B. Gold, M.-N. Westgate, and L. B. Holmes, “Anatomic and Etiological Classification of Congenital Limb Deficiencies”, *American Journal of Medical Genetics Part A*, vol. 155, no. 6, pp. 1225–1235, Jun. 2011, ISSN: 15524825. DOI: [10.1002/ajmg.a.33999](https://doi.org/10.1002/ajmg.a.33999).
- [21] V. S. Nelson, K. M. Flood, P. R. Bryant, M. E. Huang, P. F. Pasquina, and T. L. Roberts, “Limb Deficiency and Prosthetic Management. 1. Decision Making in Prosthetic Prescription and Management”, *Archives of Physical Medicine and Rehabilitation*, vol. 87, no. 3, pp. 3–9, Mar. 2006, ISSN: 00039993. DOI: [10.1016/j.apmr.2005.11.022](https://doi.org/10.1016/j.apmr.2005.11.022).
- [22] A. Watts and G. Hooper, “(iii) Congenital hand anomalies”, *Current Orthopaedics*, vol. 20, no. 4, pp. 266–273, Aug. 2006, ISSN: 02680890. DOI: [10.1016/j.cuor.2006.06.013](https://doi.org/10.1016/j.cuor.2006.06.013).
- [23] A. Agrawal, H. Sakale, and S. Kumar, “Transverse terminal upper limb deficiency through the arm: The problem and management”, *Journal of Orthopedics, Traumatology and Rehabilitation*, vol. 10, no. 2, p. 145, 2018, ISSN: 0975-7341. DOI: [10.4103/jotr.jotr_39_18](https://doi.org/10.4103/jotr.jotr_39_18).
- [24] I. R. Makhoul, I. Goldstein, T. Smolkin, R. Avrahami, and P. Sujov, “Congenital limb deficiencies in newborn infants: prevalence, characteristics and prenatal diagnosis”, *Prenatal Diagnosis*, vol. 23, no. 3, pp. 198–200, Mar. 2003, ISSN: 0197-3851. DOI: [10.1002/pd.550](https://doi.org/10.1002/pd.550).
- [25] H. J. Day, “The ISO/ISPO classification of congenital limb deficiency”, *Prosthetics and Orthotics International*, vol. 15, no. 2, pp. 67–69, 1991, ISSN: 17461553. DOI: [10.3109/03093649109164635](https://doi.org/10.3109/03093649109164635).
- [26] A. Saikia, S. Mazumdar, N. Sahai, S. Paul, D. Bhatia, S. Verma, and P. K. Rohilla, “Recent advancements in prosthetic hand technology”, *Journal of Medical Engineering & Technology*, vol. 40, no. 5, pp. 255–264, Jul. 2016, ISSN: 0309-1902. DOI: [10.3109/03091902.2016.1167971](https://doi.org/10.3109/03091902.2016.1167971).
- [27] A. J. Thurston, “Paré and Prosthetics: the early history of artificial limbs”, *ANZ Journal of Surgery*, vol. 77, no. 12, pp. 1114–1119, Dec. 2007, ISSN: 1445-1433. DOI: [10.1111/j.1445-2197.2007.04330.x](https://doi.org/10.1111/j.1445-2197.2007.04330.x).
- [28] S. Watve, G. Dodd, R. MacDonald, and E. R. Stoppard, “Upper limb prosthetic rehabilitation”, *Orthopaedics and Trauma*, vol. 25, no. 2, pp. 135–142, Apr. 2011, ISSN: 18771327. DOI: [10.1016/j.mporth.2010.10.003](https://doi.org/10.1016/j.mporth.2010.10.003).
- [29] B. Maat, G. Smit, D. Plettenburg, and P. Breedveld, “Passive prosthetic hands and tools: A literature review”, *Prosthetics and Orthotics International*, vol. 42, no. 1, pp. 66–74, Feb. 2018, ISSN: 0309-3646. DOI: [10.1177/0309364617691622](https://doi.org/10.1177/0309364617691622).
- [30] F. C. B. Dias Pinheiro, “Development of a Functional Upper Limb Prosthesis”, Ph.D. dissertation, Instituto Superior Técnico, Universidade de Lisboa, 2018, p. 8.

REFERENCES

- [31] G. McGimpsey and T. Bradford, “Limb Prosthetics Services and Devices: Critical Unmet Need: Market Analysis”, *Bioengineering Institute Center for Neuroprosthetics*, pp. 1–35, 2008.
- [32] *Ottobock North America Consumer Home | Ottobock US*. [Online]. Available: <https://www.ottobockus.com/> (visited on 03/09/2021).
- [33] Ottobock, *Cosmetic upper limb solutions | Ottobock US*. [Online]. Available: <https://www.ottobockus.com/prosthetics/upper-limb-prosthetics/solution-overview/cosmetic-solutions/> (visited on 01/26/2020).
- [34] —, *Custom silicone finger and hand prosthetics | Ottobock US*. [Online]. Available: <https://www.ottobockus.com/prosthetics/upper-limb-prosthetics/solution-overview/custom-silicone-prosthetics/> (visited on 01/23/2020).
- [35] J. W. Sensinger, J. Lipsey, A. Thomas, and K. Turner, “Design and evaluation of voluntary opening and voluntary closing prosthetic terminal device”, *Journal of Rehabilitation Research and Development*, vol. 52, no. 1, pp. 63–76, 2015, ISSN: 0748-7711. DOI: 10.1682/JRRD.2014.03.0087.
- [36] K. Berning, S. Cohick, R. Johnson, L. A. Miller, and J. W. Sensinger, “Comparison of body-powered voluntary opening and voluntary closing prehensor for activities of daily life”, *Journal of Rehabilitation Research and Development*, vol. 51, no. 2, pp. 253–262, 2014, ISSN: 0748-7711. DOI: 10.1682/JRRD.2013.05.0123.
- [37] M. B. Burn, A. Ta, and G. R. Gogola, “Three-Dimensional Printing of Prosthetic Hands for Children”, *The Journal of Hand Surgery*, vol. 41, no. 5, e103–e109, May 2016, ISSN: 03635023. DOI: 10.1016/j.jhsa.2016.02.008.
- [38] J. Zuniga, D. Katsavelis, J. Peck, J. Stollberg, M. Petrykowski, A. Carson, and C. Fernandez, “Cyborg beast: a low-cost 3d-printed prosthetic hand for children with upper-limb differences”, *BMC Research Notes*, vol. 8, no. 1, p. 10, 2015, ISSN: 1756-0500. DOI: 10.1186/s13104-015-0971-9.
- [39] C. Behrend, W. Reizner, J. A. Marchessault, and W. C. Hammert, “Update on Advances in Upper Extremity Prosthetics”, *The Journal of Hand Surgery*, vol. 36, no. 10, pp. 1711–1717, Oct. 2011, ISSN: 03635023. DOI: 10.1016/j.jhsa.2011.07.024.
- [40] *Didrick Medical*, 2013. [Online]. Available: <https://www.x-finger.com/index.html> (visited on 03/02/2021).
- [41] *Everyday Prosthetic Fingers - ASME*. [Online]. Available: <https://www.asme.org/topics-resources/content/everyday-prosthetic-fingers> (visited on 03/02/2021).

- [42] M. A. Kelley, H. Benz, S. Engdahl, and J. F. Bridges, “Identifying the benefits and risks of emerging integration methods for upper limb prosthetic devices in the United States: an environmental scan”, *Expert Review of Medical Devices*, vol. 16, no. 7, pp. 631–641, 2019, ISSN: 17452422. DOI: [10.1080/17434440.2019.1626231](https://doi.org/10.1080/17434440.2019.1626231).
- [43] Ottobock, *bebionic hand - Ottobock USA*, 2017. [Online]. Available: <https://www.ottobockus.com/prosthetics/upper-limb-prosthetics/solution-overview/bebionic-hand/> (visited on 01/24/2020).
- [44] H. Mano, S. Fujiwara, and N. Haga, “Adaptive behaviour and motor skills in children with upper limb deficiency”, *Prosthetics and Orthotics International*, vol. 42, no. 2, pp. 236–240, Apr. 2018, ISSN: 0309-3646. DOI: [10.1177/0309364617718411](https://doi.org/10.1177/0309364617718411).
- [45] M. A. James, A. M. Bagley, K. Brasington, C. Lutz, S. McConnell, and F. Molitor, “Impact of Prostheses on Function and Quality of Life for Children with Unilateral Congenital Below-the-Elbow Deficiency”, *The Journal of Bone & Joint Surgery*, vol. 88, no. 11, pp. 2356–2365, Nov. 2006, ISSN: 0021-9355. DOI: [10.2106/JBJS.E.01146](https://doi.org/10.2106/JBJS.E.01146).
- [46] L. C. Smail, C. Neal, C. Wilkins, and T. L. Packham, “Comfort and function remain key factors in upper limb prosthetic abandonment: findings of a scoping review”, *Disability and Rehabilitation: Assistive Technology*, pp. 1–10, Mar. 2020, ISSN: 1748-3107. DOI: [10.1080/17483107.2020.1738567](https://doi.org/10.1080/17483107.2020.1738567).
- [47] E. A. Biddiss and T. T. Chau, “Upper limb prosthesis use and abandonment: A survey of the last 25 years”, *Prosthetics and Orthotics International*, vol. 31, no. 3, pp. 236–257, Sep. 2007, ISSN: 0309-3646. DOI: [10.1080/03093640600994581](https://doi.org/10.1080/03093640600994581).
- [48] S. Salminger, H. Stino, L. H. Pichler, C. Gstoettner, A. Sturma, J. A. Mayer, M. Szivak, and O. C. Aszmann, “Current rates of prosthetic usage in upper-limb amputees – have innovations had an impact on device acceptance?”, *Disability and Rehabilitation*, pp. 1–12, Dec. 2020, ISSN: 0963-8288. DOI: [10.1080/09638288.2020.1866684](https://doi.org/10.1080/09638288.2020.1866684).
- [49] R. C. Crandall and W. Tomhave, “Pediatric Unilateral Below-Elbow Amputees: Retrospective Analysis of 34 Patients Given Multiple Prosthetic Options”, *Journal of Pediatric Orthopaedics*, vol. 22, no. 3, pp. 380–383, May 2002, ISSN: 0271-6798. DOI: [10.1097/01241398-200205000-00023](https://doi.org/10.1097/01241398-200205000-00023).
- [50] L. E. Diment, M. S. Thompson, and J. H. Bergmann, “Three-dimensional printed upper-limb prostheses lack randomised controlled trials: A systematic review”, *Prosthetics and Orthotics International*, vol. 42, no. 1, pp. 7–13, Feb. 2018, ISSN: 0309-3646. DOI: [10.1177/0309364617704803](https://doi.org/10.1177/0309364617704803).

REFERENCES

- [51] I-SCOOP, *Additive manufacturing and 3D printing in manufacturing*. [Online]. Available: <https://www.i-scoop.eu/additive-manufacturing-3d-printing/> (visited on 01/26/2020).
- [52] I. Gibson, D. W. Rosen, and B. Stucker, *Additive Manufacturing Technologies*. Boston, MA: Springer US, 2010, pp. 20–35, ISBN: 978-1-4419-1119-3. DOI: 10.1007/978-1-4419-1120-9. [Online]. Available: <http://link.springer.com/10.1007/978-1-4419-1120-9>.
- [53] E. Tempelman, H. Shercliff, and B. N. van Eyben, “Additive Manufacturing”, in *Manufacturing and Design*, 11, Elsevier, 2014, pp. 187–200, ISBN: 978-0-08-099922-7. DOI: 10.1016/B978-0-08-099922-7.00011-1.
- [54] S. Vyavahare, S. Teraiya, D. Panghal, and S. Kumar, “Fused deposition modelling: a review”, *Rapid Prototyping Journal*, vol. 26, no. 1, pp. 176–201, Jan. 2020, ISSN: 1355-2546. DOI: 10.1108/RPJ-04-2019-0106.
- [55] V. Dhinakaran, K. Manoj Kumar, P. Bupathi Ram, M. Ravichandran, and M. Vinayagamorthy, “A review on recent advancements in fused deposition modeling”, *Materials Today: Proceedings*, vol. 27, pp. 752–756, 2020, ISSN: 22147853. DOI: 10.1016/j.matpr.2019.12.036. [Online]. Available: <https://linkinghub.elsevier.com/retrieve/pii/S2214785319340477>.
- [56] F. P. Melchels, J. Feijen, and D. W. Grijpma, “A review on stereolithography and its applications in biomedical engineering”, *Biomaterials*, vol. 31, no. 24, pp. 6121–6130, 2010, ISSN: 01429612. DOI: 10.1016/j.biomaterials.2010.04.050.
- [57] L. Novakova-Marcincinova and J. Novak-Marcincin, “Applications of rapid prototyping fused deposition modeling materials”, *23rd DAAAM International Symposium on Intelligent Manufacturing and Automation 2012*, vol. 1, no. 1, pp. 57–60, 2012.
- [58] T. D. Ngo, A. Kashani, G. Imbalzano, K. T. Nguyen, and D. Hui, “Additive manufacturing (3D printing): A review of materials, methods, applications and challenges”, *Composites Part B: Engineering*, vol. 143, no. February, pp. 172–196, Jun. 2018, ISSN: 13598368. DOI: 10.1016/j.compositesb.2018.02.012.
- [59] L. Mertz, “Dream It, Design It, Print It in 3-D: What Can 3-D Printing Do for You?”, *IEEE Pulse*, vol. 4, no. 6, pp. 15–21, Nov. 2013, ISSN: 2154-2287. DOI: 10.1109/MPUL.2013.2279616.
- [60] Hybrid Manufacturing Technologies, *Hybrid Manufacturing Resources*, 2018. [Online]. Available: <http://www.hybridmanutech.com/resources.html> (visited on 01/17/2020).
- [61] M. Javaid and A. Haleem, “Additive manufacturing applications in orthopaedics: A review”, *Journal of Clinical Orthopaedics and Trauma*, vol. 9, no. 3, pp. 202–206, Jul. 2018, ISSN: 09765662. DOI: 10.1016/j.jcot.2018.04.008.

- [62] Prusa3D - Open-Source 3D printers by Josef Prusa. [Online]. Available: <https://www.prusa3d.com/> (visited on 05/18/2021).
- [63] Z. Liu, Y. Wang, B. Wu, C. Cui, Y. Guo, and C. Yan, "A critical review of fused deposition modeling 3D printing technology in manufacturing polylactic acid parts", *The International Journal of Advanced Manufacturing Technology*, vol. 102, no. 9-12, pp. 2877–2889, Jun. 2019, ISSN: 0268-3768. DOI: 10.1007/s00170-019-03332-x.
- [64] Recreus Filaflex | Impresión 3D | Venta de filamento 3D. [Online]. Available: <https://recreus.com/gb/> (visited on 09/05/2021).
- [65] NinjaTek, *NinjaTek | NinjaFlex*, 2016. [Online]. Available: <https://ninjatek.com/ninjaflex/> (visited on 03/06/2021).
- [66] 82A FILAFLEX 250 GR - Recreus Filaflex | Filamento 3d | Impresión 3d. [Online]. Available: <https://recreus.com/en/producto/82a-filaflex-250-gr/nude-en/1-75-mm-en/> (visited on 03/06/2021).
- [67] H. J. Qi, K. Joyce, and M. C. Boyce, "Durometer Hardness and the Stress-Strain Behavior of Elastomeric Materials", *Rubber Chemistry and Technology*, vol. 76, no. 2, pp. 419–435, May 2003, ISSN: 1943-4804. DOI: 10.5254/1.3547752.
- [68] Smooth On, *Durometer Shore Hardness Scale*, 2019. [Online]. Available: <https://www.smooth-on.com/page/durometer-shore-hardness-scale/> (visited on 03/06/2021).
- [69] *7 Design for Additive Manufacturing (DfAM) Principles*. [Online]. Available: <https://www.cati.com/blog/2018/12/7-design-additive-manufacturing-dfam-principles/> (visited on 03/07/2021).
- [70] I. Gibson, D. Rosen, B. Stucker, and M. Khorasani, "Design for Additive Manufacturing", in *Additive Manufacturing Technologies*, Cham: Springer International Publishing, 2021, pp. 555–607. DOI: 10.1007/978-3-030-56127-7_19.
- [71] *Design for Additive Manufacturing 3D Printing Strategies*. [Online]. Available: <https://markforged.com/resources/blog/design-for-additive-manufacturing-dfam> (visited on 09/18/2021).
- [72] K. S. Tanaka and N. Lightdale-Miric, "Advances in 3D-Printed Pediatric Prostheses for Upper Extremity Differences", *Journal of Bone and Joint Surgery*, vol. 98, no. 15, pp. 1320–1326, Aug. 2016, ISSN: 0021-9355. DOI: 10.2106/JBJS.15.01212.
- [73] G. Xu, L. Gao, K. Tao, S. Wan, Y. Lin, A. Xiong, B. Kang, and H. Zeng, "Three-dimensional-printed upper limb prosthesis for a child with traumatic amputation of right wrist", *Medicine (United States)*, vol. 96, no. 52, e9426, Dec. 2017, ISSN: 15365964. DOI: 10.1097/MD.0000000000009426.

REFERENCES

- [74] Enabling The Future, *The Cyborg Beast – Enabling The Future*. [Online]. Available: <http://enablingthefuture.org/upper-limb-prosthetics/cyborg-beast/> (visited on 01/24/2020).
- [75] —, *The Raptor Hand*. [Online]. Available: <http://enablingthefuture.org/upper-limb-prosthetics/the-raptor-hand/> (visited on 01/24/2020).
- [76] J. S. Cuellar, G. Smit, A. A. Zadpoor, and P. Breedveld, “Ten guidelines for the design of non-assembly mechanisms: The case of 3D-printed prosthetic hands”, *Proceedings of the Institution of Mechanical Engineers, Part H: Journal of Engineering in Medicine*, vol. 232, no. 9, pp. 962–971, Sep. 2018, ISSN: 0954-4119. DOI: [10.1177/0954411918794734](https://doi.org/10.1177/0954411918794734).
- [77] *Phoenix Hand – Enabling The Future*. [Online]. Available: <http://enablingthefuture.org/phoenix-hand/> (visited on 03/16/2021).
- [78] A. Nazree, *Nazree’s Prosthetic Hand | 3D CAD Model Library | GrabCAD*, 2016. [Online]. Available: <https://grabcad.com/library/nazree-s-prosthetic-hand-1> (visited on 05/31/2021).
- [79] J. A. d. A. Corveira, “Design and development of a Soft Body-Actuated 3D printed prosthetic hand”, Ph.D. dissertation, Faculdade de Ciências e Tecnologia da Universidade de Coimbra, 2017.
- [80] Autodesk | *Software de projeção, engenharia e entretenimento 3D*. [Online]. Available: <https://www.autodesk.pt/> (visited on 09/06/2021).
- [81] R. Alturkistani, K. A. S. Devasahayam, R. Thomas, E. L. Colombini, C. A. Cifuentes, S. Homer-Vanniasinkam, H. A. Wurdemann, and M. Moazen, “Affordable passive 3D-printed prosthesis for persons with partial hand amputation”, *Prosthetics and Orthotics International*, vol. 44, no. 2, pp. 92–98, Apr. 2020, ISSN: 0309-3646. DOI: [10.1177/0309364620905220](https://doi.org/10.1177/0309364620905220).
- [82] A. Mohammadi, J. Lavranos, H. Zhou, R. Mutlu, G. Alici, Y. Tan, P. Choong, and D. Oetomo, “A practical 3D-printed soft robotic prosthetic hand with multi-articulating capabilities”, *PLOS ONE*, vol. 15, no. 5, L. Connal, Ed., e0232766, May 2020, ISSN: 1932-6203. DOI: [10.1371/journal.pone.0232766](https://doi.org/10.1371/journal.pone.0232766).
- [83] Patient Innovation, *Patient Innovation - Sharing Solutions, Improving Life*, 2018. [Online]. Available: <https://patient-innovation.com/?language=pt-pt%20https://patient-innovation.com/> (visited on 09/15/2021).
- [84] J. W. Seeds, R. C. Cefalo, and W. N. Herbert, “Amniotic band syndrome”, *American Journal of Obstetrics and Gynecology*, vol. 144, no. 3, pp. 243–248, Oct. 1982, ISSN: 00029378. DOI: [10.1016/0002-9378\(82\)90574-9](https://doi.org/10.1016/0002-9378(82)90574-9). [Online]. Available: [http://dx.doi.org/10.1016/0002-9378\(82\)90574-9](http://dx.doi.org/10.1016/0002-9378(82)90574-9).
- [85] *e-NABLE Device Sizing – Google Drive*. [Online]. Available: <https://drive.google.com/drive/folders/OB7IZ4iPA1DJZMC1EXy1id3NjMzQ> (visited on 03/08/2021).

- [86] J. M. Müller, R. L. dos Santos, and R. V. Brigido, “Produção de alginato por microrganismos”, *Polímeros*, vol. 21, no. 4, pp. 305–310, Oct. 2011, ISSN: 1678-5169. DOI: 10.1590/S0104-14282011005000051.
- [87] *Innovative practice solutions for the dental practice - Zhermack*. [Online]. Available: https://www.zhermack.com/en/product%7B%5C_%7Dcategory/dental/ (visited on 09/06/2021).
- [88] *3D Digitizing – Intelligent Design – Additive Manufacturing | SHINING 3D*. [Online]. Available: <https://www.shining3d.com/> (visited on 09/06/2021).
- [89] K.-s. Lee and M.-c. Jung, “Flexion and Extension Angles of Resting Fingers and Wrist”, *International Journal of Occupational Safety and Ergonomics*, vol. 20, no. 1, pp. 91–101, Jan. 2014, ISSN: 1080-3548. DOI: 10.1080/10803548.2014.11077038. [Online]. Available: <http://www.tandfonline.com/doi/full/10.1080/10803548.2014.11077038>.
- [90] A. Buryanov and V. Kotiuk, “Proportions of Hand Segments”, *International Journal of Morphology*, vol. 28, no. 3, pp. 755–758, Sep. 2010, ISSN: 0717-9502. DOI: 10.4067/S0717-95022010000300015.
- [91] F. P. Schuller-Ellis and G. T. Lazar, “Internal morphology of human phalanges”, *The Journal of Hand Surgery*, vol. 9, no. 4, pp. 490–495, Jul. 1984, ISSN: 03635023. DOI: 10.1016/S0363-5023(84)80099-4.
- [92] *ImageJ*. [Online]. Available: <https://imagej.nih.gov/ij/> (visited on 09/06/2021).
- [93] J. M. Six and R. Macefield, *System Usability Scale (SUS) | Usability.gov*, 2016. [Online]. Available: <https://www.usability.gov/how-to-and-tools/methods/system-usability-scale.html> (visited on 05/26/2021).
- [94] UX Research, *Measuring and Interpreting System Usability Scale (SUS) - UIUX Trend*, 2017. [Online]. Available: <https://uiuxtrend.com/measuring-system-usability-scale-sus/> (visited on 05/26/2021).
- [95] Team UnLimbited, *Unlimbited Phoenix Hand by Team UnLimbited - Thingiverse*, 2017. [Online]. Available: <https://www.thingiverse.com/thing:1674320> (visited on 08/11/2021).
- [96] W. Linder, *Digital photogrammetry: A practical course*. Berlin, Heidelberg: Springer Berlin Heidelberg, 2009, pp. 1–2, ISBN: 9783540927242. DOI: 10.1007/978-3-540-92725-9.
- [97] *3DF Zephyr - photogrammetry software - 3d models from photos*. [Online]. Available: <https://www.3dflow.net/3df-zephyr-photogrammetry-software/> (visited on 09/15/2021).
- [98] K. Y. Lee and D. J. Mooney, “Alginate: Properties and biomedical applications”, *Progress in Polymer Science*, vol. 37, no. 1, pp. 106–126, Jan. 2012, ISSN: 00796700. DOI: 10.1016/j.progpolymsci.2011.06.003.

REFERENCES

- [99] A. H. Dewi, I. D. Ana, J. Wolke, and J. Jansen, “Behavior of plaster of Paris-calcium carbonate composite as bone substitute. A study in rats”, *Journal of Biomedical Materials Research Part A*, vol. 101A, no. 8, pp. 2143–2150, Aug. 2013, ISSN: 15493296. DOI: [10.1002/jbm.a.34513](https://doi.org/10.1002/jbm.a.34513).
- [100] WANHAO is the global leading manufacturer of desktop 3D printer. [Online]. Available: <https://wanhao.store/> (visited on 09/15/2021).
- [101] R. Srinivasan, K. Nirmal Kumar, A. Jenish Ibrahim, K. Anandu, and R. Gurudhevan, “Impact of fused deposition process parameter (infill pattern) on the strength of PETG part”, *Materials Today: Proceedings*, vol. 27, pp. 1801–1805, 2020, ISSN: 22147853. DOI: [10.1016/j.matpr.2020.03.777](https://doi.org/10.1016/j.matpr.2020.03.777).
- [102] C. Häger-Ross and M. H. Schieber, “Quantifying the Independence of Human Finger Movements: Comparisons of Digits, Hands, and Movement Frequencies”, *The Journal of Neuroscience*, vol. 20, no. 22, pp. 8542–8550, Nov. 2000, ISSN: 0270-6474. DOI: [10.1523/JNEUROSCI.20-22-08542.2000](https://doi.org/10.1523/JNEUROSCI.20-22-08542.2000).
- [103] V. M. Zatsiorsky, Z.-M. Li, and M. L. Latash, “Enslaving effects in multi-finger force production”, *Experimental Brain Research*, vol. 131, no. 2, pp. 187–195, Mar. 2000, ISSN: 00144819. DOI: [10.1007/s002219900261](https://doi.org/10.1007/s002219900261).
- [104] Z.-M. Li, S. Dun, D. A. Harkness, and T. L. Brininger, “Motion Enslaving among Multiple Fingers of the Human Hand”, *Motor Control*, vol. 8, no. 1, pp. 1–15, Jan. 2004, ISSN: 1087-1640. DOI: [10.1123/mcj.8.1.1](https://doi.org/10.1123/mcj.8.1.1).
- [105] R. Mio, M. Sanchez, and Q. Valverde, “Mechanical Testing Methods for Body-Powered Upper-Limb Prostheses: A Review”, in *2018 IEEE 18th International Conference on Bioinformatics and Bioengineering (BIBE)*, IEEE, Oct. 2018, pp. 170–176, ISBN: 978-1-5386-6217-5. DOI: [10.1109/BIBE.2018.00040](https://doi.org/10.1109/BIBE.2018.00040).

THOROUGH DESCRIPTION OF ADDITIVE MANUFACTURING METHODS

This Appendix presents a more detailed description of the seven methods of Additive Manufacturing.

Power bed fusion consists in depositing thin layers of material powder on a working plate in a walled operating volume. Then, a laser or electron beam is used to sinter or melt the particles together, by heating them where it is desired, layer-by-layer. Heated particles will be fixed and after the first layer is over, the procedure is repeated. The powder that was not sintered is only removed after the whole process is finished, to help to sustain consolidated parts. The unsintered powder can be reused, but the particles partially sintered should be eliminated to avoid compromising the next produced object. Although they cannot be combined, this technique can use different materials. Power bed fusion is a slow and expensive process that results in porous products that may need posterior processing. This technique is often used for advanced applications such as tissue engineering, aerospace and electronics [53, 58, 60].

Vat photopolymerization is very similar to power bed fusion, but it uses an **ultraviolet (UV)** light to cure the powder particles, instead of laser or electron beams. This procedure occurs in a vat with a controlled environment. Support structures may exist, but they need to be mechanically eliminated afterwards. Heating or photo-curing may be used as posterior treatment in order to achieve a better results. Vat photopolymerization offers a better surface quality than powder bed fusion but is slower and the range of materials available is limited. This technique allows to obtain bigger pieces and its equipment is commonly cheaper [10, 53, 58, 60]

Material jetting prints physical objects by depositing individual droplets, layer-by-layer where it is desired. During the procedure, the printed material, is cured by high intensity UV light. However, thermally molten materials can also be used and then solidify at room temperature. Usually, this printing machines have more than one extruder: one for printing supports and the remaining ones to print the object itself, allowing the combination of different materials. Final products also benefit from smooth surfaces [53, 60]

Sheet lamination uses a roll of adhesive sheet materials. Layers are continuously cut from this roll in the desired shape by using a mechanical cutter or a laser and are then assembled to form the object. The excess material after the cut is left for support and removed in the end. Although a lot of waste is generated due to this partial subtracting character, the remaining material can be recycled. This technique origins lower quality surfaces and poorer dimensional accuracy when compared with other AM techniques. Post-processing treatment, dependent on the materials, such high temperature may be applied to achieve better properties. Sheet lamination is applied in fields like paper manufacturing, foundry industries and electronics [53].

Binder jetting uses an organic or inorganic adhesive liquid to link powder materials. Like powder bed fusion, this technique deposits powder materials in thin layers. Binder jetting is usually used to build mock-ups as it enables the use of a combination of different colours [53, 60].

Direct energy deposition uses an energy source, usually a laser beam, that is directed onto a surface where powder particles are simultaneously being projected. This procedure does not use a horizontal printing plate and therefore printing layers might not be horizontal. This enables printing onto existing parts. The resulting objects are not porous and have a controlled microstructure which leads to excellent mechanical properties. However, direct energy deposition has low accuracy, low surface quality and produces less complex designs. The manufacturing costs and time are low and it is mainly used in the automotive and aerospace industry [53, 58].

ADDITIONAL DETAILS ON THE CONCEPT DEVELOPMENT

This Appendix presents a more detailed description of the used methodology used in this study, which was inspired in the Product Design and Development methodology [11]. Figure B.1 presents the long version of the flowchart that illustrates the development process of the prosthesis.

APPENDIX B. ADDITIONAL DETAILS ON THE CONCEPT DEVELOPMENT

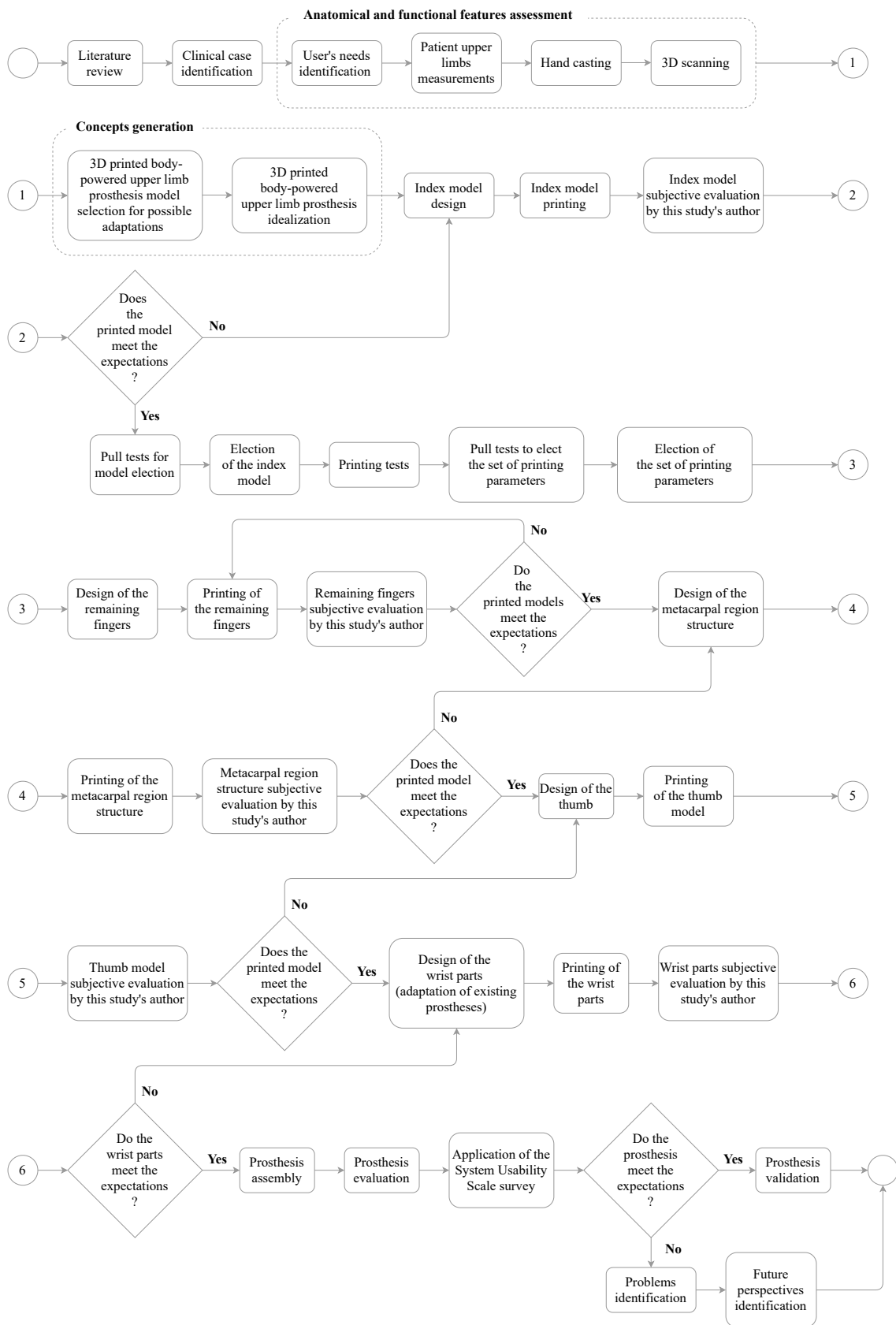


Figure B.1: Extended methodology flowchart.

DOCUMENTATION OF THE ANATOMICAL AND FUNCTIONAL FEATURES ASSESSMENT

This Appendix presents the documents used to assess the anatomical and functional features of the child.

The first document consists of the protocol used to assess these features.

The second document is the form that was used within the scope of this protocol. The last file is the informed consent that was presented to child's carer.

All these documents were translated to Portuguese so the child's family and carer could be aware of all the procedures.



Data Collection Protocol

Study Description:

This protocol was established within the scope of a Biomedical Engineering Master Thesis aiming to develop a body-powered hand prosthesis with flexible materials by Additive Manufacturing. This study is taking place on NOVA School of Science and Technology in partnership with *Patient Innovation*.

The main goal of this study is to improve the cosmetic appearance of 3D-printed body-powered prostheses through the replacement of the stiff material that composes *e-NABLE* prostheses. This material will be replaced by a combination of rigid and flexible materials in order to give these prostheses a more real-life appearance.

For this purpose, it was necessary to determine the optimal combination of materials combination as well as to analyse some of the existent prostheses. The identification of the user's needs is crucial to determine the prosthesis specifications and therefore create some concepts aiming to identify the best model to develop. Concerning concepts generation and selection, it is desired a high level of customization, especially regarding to the size of printed hand when compared to the sound hand. Establishing sensory feedback was also a concern.

Finally, as a result of the created concepts, several prototypes for testing and concept validation will be designed, according to Product Design and Development methodology.



Data Collection Goals:

The present protocol describes the data collection methodology for this study. It is composed of two methods and presents an explanation for each method as well as the listing of all necessary materials.

To simplify the progress of this study, it will be based on a single clinical case of a child with an upper limb disorder, selected from the *Patient Innovation's* program "*Dar a mão*". However, this protocol can be reproduced in other patients with similar disorders for further work.

The main goal of this protocol is to collect biometric data in order to maximize the customization of this study's resulting prosthesis. Hand casting and simple measurements will be providing different types of information, from single to three-dimensional data. Furthermore, the redundancy between these two methods will prevent the necessity of a second appointment with the patient to collect further data.



Part I – Measurements

This protocol's procedure is partly inspired on the measurement form used on Patients Innovation's program "*Dar a mão*". Besides the measurement's information, some personal data will also be taken as well as several photos of both limbs in specific positions.

Material:

- Pen;
- Printed form;
- Measuring tape;
- 40 cm ruler;
- 1 € coin;
- Camera;
- Sheets of paper;
- A3 graph paper.

Procedure:

1. Fill the form with personal information and limbs' measurements.
2. Ask the child to place the two limbs resting on the graph paper with the ruler placed between the two arms, parallel to them.
3. Repeat the exemplified positions from Figure 1 and take a photo of each one. Each photo should:
 - Include the whole forearm, including the elbow;
 - Be taken directly from above the forearms and not from another angle;
 - Include a coin as an additional measurement reference.



Development of a Body-powered
Hand Prosthesis with Flexible
Materials by Additive Manufacturing

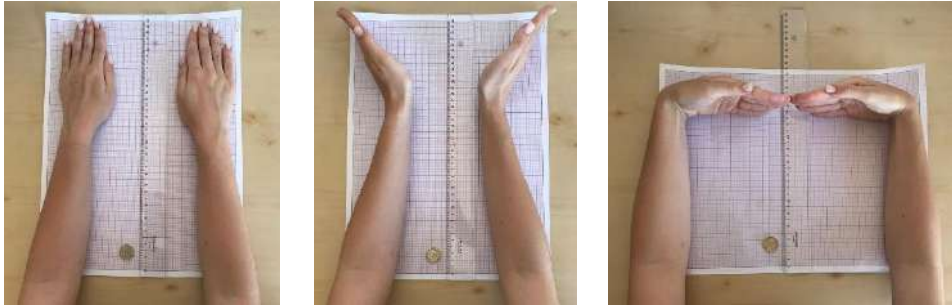


Figure 1: Positions to repeat.



Part II – Hand Casting

This final procedure aims to build a three-dimensional replica of the child's limbs and avoid future meetings. Therefore, measurements that were not taken in sequence of this protocol can be done without the child's presence. Moreover, the hand's replica could be scanned instead of exposing the child to a long-time consuming procedure.

The hand's impression is made with alginate and then filled with Plaster of Paris. After the plaster is set, the alginate can be removed and the hand replica is finished.

Material:

- 2 buckets or other containers tall enough to cover the limb up about 10 cm above the limbs extremities;
- 0,5 L measuring cup;
- Alginate;
- Water;
- Plaster of Paris;
- 2 Whisks;
- Cup;
- Vaseline or baby oil;
- Balance;
- Baby wipes;
- Knife.

Procedure:

1. Grease the child's healthy limb with baby oil.



Development of a Body-powered Hand Prosthesis with Flexible Materials by Additive Manufacturing



2. Mix one-part alginate (cup) with two-parts water using the whisk's help until filling the bucket up to two thirds of its height. Don't stop mixing until the mixture is ready to make the limb's impression.
3. Dip the child's healthy limb with an open hand in the alginate and wait 3 minutes until it solidifies. It is important to keep the child as still as possible. If the child starts to feel uncomfortable, try to distract the child by chatting, singing a song or telling a short story.
4. Remove the child's limb and clean it with baby wipes.
5. Repeat the process for the other limb.
6. Dissolve the Plaster of Paris in water in the measuring cup with the whisk's help.
7. Fill the alginate with the plaster solution up to the top and let it rest.
8. After a few hours, when the plaster is set and dry, remove the alginate from the two replicas using the knife.

Note: The alginate and plaster solutions are prepared according to the instructions recommended by the materials producer.

Data Collection Form

Personal Data

Name _____

Birthday: _____ Sex: Male Female

Height: _____ Weight: _____

Clinical Background

Condition's Cause:

Congenital disorder Which one? _____

Amputation When? _____

Affected Limb: Right Left

Previous Prostheses:

Yes Which one(s)? _____ Prescription Date: _____

_____ Prescription Date: _____

No

Existing Joints:

Wrist Does the child present wrist flexion? Yes No

Does the child present wrist rotation? Yes No

Elbow Does the child present elbow flexion? Yes No

Does the child present elbow rotation? Yes No

Injury's Classification: _____

Activities with higher level of difficulty: _____

Limbs' Measurements

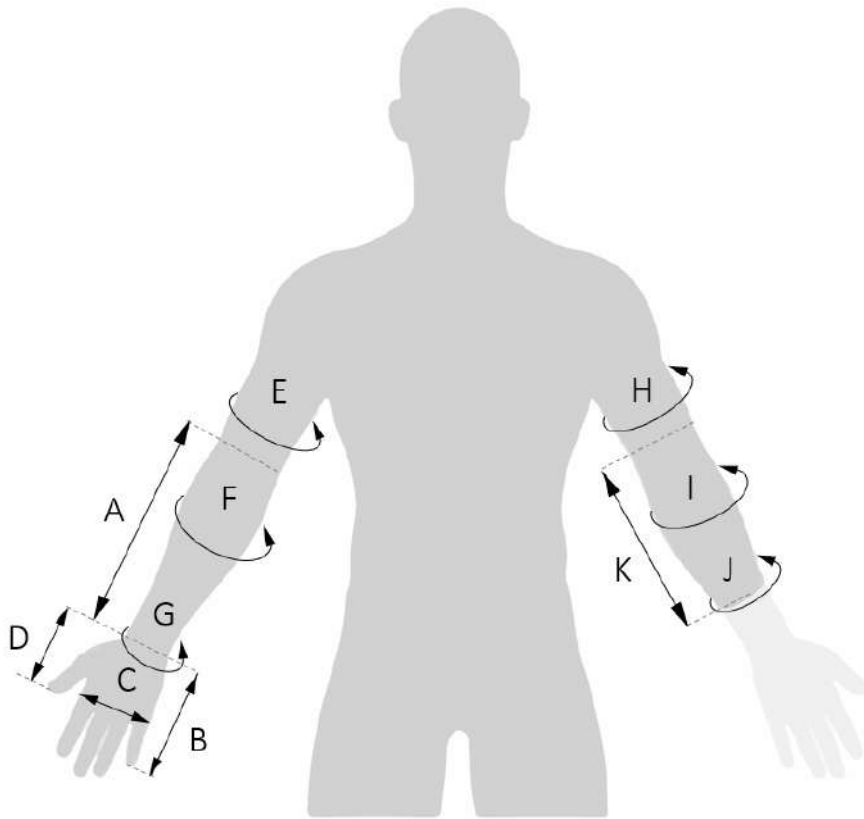


Figure 1: Measurements' guide.

Table 1: Measurements' record.

Measurement identification	1st Measurement	2nd Measurement	3rd Measurement
A			
B			
C			
D			
E			
F			
G			
H			
I			
J			
K			

Uncertainty: _____

Parental Informed Consent

Dear Child Carer,

I, Ana Maria Gomes Oliveira, am finishing my Master Degree in Biomedical Engineering at NOVA School of Science and Technology and I would like to request your child's collaboration in this study to support my Master Thesis titled "*Development of a Body-powered Hand Prosthesis with Flexible Materials by Additive Manufacturing*".

This study is taking place at NOVA School of Science and Technology in partnership with *Patient Innovation* and aims to develop a body-powered hand prosthesis with flexible materials by Additive Manufacturing, commonly known as 3D printing.

The main goal of this study is to improve the cosmetic appearance of 3D-printed body-powered prostheses through the replacement of the stiff material that composes *e-NABLE* prostheses. This material will be replaced by a combination of rigid and flexible materials in order to give these prostheses a more real-life appearance.

For this purpose, it was necessary to determine the optimal combination of materials combination as well as to analyse some of the existent prostheses. The identification of the user's needs is crucial to determine the prosthesis specifications and therefore create some concepts aiming to identify the best model to develop. Concerning concepts generation and selection, it was desired a high level of customization, especially regarding to the size of printed hand when compared to the sound hand. Establishing sensory feedback was also a concern.

Finally, as a result of the created concepts, several prototypes for testing and concept validation will be designed, according to Product Design and Development methodology.

The data collection process will be composed of two methods: simple anatomic measurements and hand casting. These procedures will enable the acquisition of biometric data to maximize the customization of this study's resulting prosthesis

To simplify the progress of this study, it will be based on a single clinical case of a child with an upper limb disorder selected from *Patient Innovation's* program "*Dar a mão*". However, you are free to quit the study anytime if you so desire. Please be aware that your child's collaboration is voluntary and that this is a non-profit study.

All collected data will be confidentially protected and any of your child's photos allowing your child's identification will not be shared.

If you have any doubts or concerns about the present study or protocol, do not hesitate to contact me at the following number xxx xxx xxx or e-mail: amg.oliveira@campus.fct.unl.pt.

I confirm that I have clearly explained and disclosed all the necessary procedures relative to the study referred in this document. I answered to all the asked questions and assured that was enough lead time for the Child Carer to reflect and make an informed decision.

Date: __/__/____ _____

(Ana Maria Gomes Oliveira)

Dear Child Carer,

Please, read this document carefully. Do not hesitate to ask for more information if you require further clarifications.

Check that all information is correct. If everything is as you expect, then, sign this document.

I declare I have understood the goals that were purposed and explained to me. I had the opportunity to present all my doubts and concerns related to this issue and for each one I received a clear answer. I had enough time to reflect my proposal so I declare that I authorize/do not authorize (*delete as appropriate*) the referred study as well as the directly related procedures that may be necessary to my own interest and supported by reasonable arguments.

Date: __/__/____ _____

(Child Carer)

PHALANGES MEASUREMENTS

The diameter of the phalanges was defined by crossing two studies: F. P. A. Buryanov and V. Kotiuk [90] as well as Schulter-Ellis and G. T. Lazar [91], which performed analyses about the morphologies of the human phalanges. In order to obtain the diameter of each phalanx, the midshaft of each phalanx was measured ten times in Figure D.1 by using *ImageJ* software [92]. The mean of these ten measurements (D), was then confronted with the values from the F. P. Schulter-Ellis and G. T. Lazar's study [91] to validate the performed measurements. The measurements of all fingers (except for the thumb) were performed using the frontal plane. The thumb was measured using the sagittal plane. Finally, after validated, the considered diameter of each phalanx for the present prosthesis was $0.63D$. Table D.1 presents the ten measurements of each phalanx made with *ImageJ*, as well as their mean and SD.



Figure D.1: Antero-posterior X-ray of a human hand [90].

Table D.1: Phalanges measurements (mm).

Phalanges Label	Fingers					
	Little	Ring	Middle	Index	Thumb	
Proximal	1	8.64	9.96	11.10	10.48	7.45
	2	8.80	9.82	10.73	10.79	7.10
	3	8.64	9.98	11.04	10.48	7.19
	4	8.32	10.31	10.73	10.41	7.31
	5	8.97	10.16	10.79	10.55	7.66
	6	8.49	10.00	11.10	10.48	7.16
	7	8.32	10.47	11.10	10.55	7.25
	8	8.80	10.00	10.73	10.48	7.30
	9	8.33	10.16	10.99	10.41	7.10
	10	8.81	10.30	11.04	10.41	7.60
	Mean	8.61	10.11	10.96	10.50	7.31
SD	0.24	0.20	0.17	0.11	0.20	
Middle	1	7.70	9.54	9.16	8.91	-
	2	7.70	9.05	9.10	8.94	-
	3	7.88	9.17	9.68	8.94	-
	4	7.70	9.20	9.41	8.89	-
	5	7.40	9.05	9.16	8.89	-
	6	7.74	9.54	9.47	9.07	-
	7	7.86	9.36	9.41	9.10	-
	8	7.42	9.03	9.05	8.97	-
	9	7.86	9.05	9.36	9.10	-
	10	7.53	9.01	9.23	9.07	-
	Mean	7.68	9.20	9.30	8.99	-
SD	0.18	0.21	0.20	0.09	-	
Distal	1	4.93	5.28	5.84	6.31	5.59
	2	4.84	5.21	5.67	6.18	5.52
	3	5.25	5.36	5.90	6.15	5.59
	4	5.32	5.39	6.25	6.34	5.73
	5	4.77	5.43	5.43	6.13	5.82
	6	5.04	5.21	6.25	6.31	5.47
	7	5.09	4.93	6.18	6.18	5.67
	8	5.10	5.36	5.93	6.15	5.65
	9	4.77	5.18	5.74	6.29	5.59
	10	4.91	5.16	5.90	6.15	5.80
	Mean	5.00	5.25	5.91	6.22	5.64
SD	0.19	0.15	0.26	0.08	0.12	

PRINTING PARAMETERS TESTS

This appendix presents the printing parameters that were used during the main printing tests that were performed during this study. The printing parameters that remained the same are based on the the printing settings recommendations. Tables [E.1](#) to [E.3](#) present the printing settings that were changed during the printing tests. These tests were performed with the aim to asses which was the best set of parameters that combined a good printing quality with low forces needed to flex the prosthesis.

Table E.1: Print settings of the main printing tests: "-" means the parameter is disabled.

Parameters	Set A	Set A1	Set A2	Set B	Set B1	Set B2	Set B3	Set B4	Set B5	Set B6
	Layers and perimeters									
Vertical shells	2	2	1	2	2	2	2	2	2	2
Quality (slower slicing)	-	-	-	-	-	-	-	-	-	-
Infill										
Infill	15	10	15	15	15	15	15	15	15	5
Speed										
Perimeters (mm/s)	20	20	20	20	20	20	20	20	20	15
Small Perimeters (mm/s or %)	20	20	20	20	20	20	20	20	20	15
External Perimeters (mm/s or %)	20	20	20	20	20	20	20	20	20	15
Infill (mm/s)	20	20	20	20	20	20	20	20	20	15
Top solid infill (mm/s or %)	15	15	15	15	15	15	15	15	15	15
Solid Infill (mm/s or %)	20	20	20	20	20	20	20	20	20	15
Support material (mm/s)	20	20	20	20	20	20	20	20	20	15
Bridges (mm/s)	20	20	20	20	20	20	20	20	20	15
Gap fill (mm/s)	20	20	20	20	20	20	20	20	20	15

Table E.2: Printer settings of the main printing tests.

Parameters	Set A	Set A1	Set A2	Set B	Set B1	Set B2	Set B3	Set B4	Set B5	Set B6
Extruder 1										
Length (mm)	0.8	0.8	0.8	3.5	3.5	3.5	3.5	3.5	3.5	3.5
Lift Z (mm)	0.6	0.6	0.6	0.04	0.04	0.04	0.04	0.04	0.04	0.04
Deretraction Speed (mm/s)	0	0	0	35	35	35	35	35	35	35

Table E.3: Filament settings of the main printing tests: "(x)" means that the parameter is selected, while "(-)" means the parameter is disabled.

Parameters		Set A	Set A1	Set A2	Filament							
Filament	Extrusion multiplier	1.25	1.25	1.25	1.1	1.15	1.2	1.25	1.1	1.25	1.25	1.25
Filament Overrides												
	Length (mm)	(-)	N/A	(-)	N/A	(-)	(x)	(x)	(x)	(x)	(x)	(x)
	Lift Z (mm)	(-)	N/A	(-)	N/A	(-)	0	0.04	(x)	0.04	(x)	0.04
	Only lift Z above (mm)	(-)	N/A	(-)	N/A	(-)	0	0	(x)	0	(x)	0
	Only lift Z below (mm)	(-)	N/A	(-)	N/A	(-)	209	209	(x)	209	(x)	209
	Retraction Speed (mm/s)	(-)	N/A	(-)	N/A	(-)	35	35	(x)	35	(x)	35
Retraction	Deretraction Speed (mm/s)	(-)	N/A	(-)	N/A	(-)	35	35	(x)	35	(x)	35
	Extra length on restart (mm)	(-)	N/A	(-)	N/A	(-)	0	0	(x)	0	(x)	0
	Minimum travel after retraction (mm)	(-)	N/A	(-)	N/A	(-)	1	1	(x)	1	(x)	1
	Retract on layer change	(-)	-	(-)	-	(-)	x	x	(x)	x	(x)	x
	Wipe while retracting	(-)	-	(-)	-	(-)	x	x	(x)	x	(x)	x
	Retract amount before wipe (%)	(-)	N/A	(-)	N/A	(-)	0	0	(x)	0	(x)	0

PULL TESTS

This Appendix presents the protocol defined to evaluate some of the developed prototypes of the fingers. This protocol was developed with the aim of testing the functionality of different designs as well as to assess the best printing parameters that would lead to a higher level of functionality. This Appendix also presents the drawings of the finger support and horizontal tab designed for the pull tests protocol as well as the values of the several pull tests that were made. These values can be consulted in Tables F.1 to F.15. u_c correspond to combined standard uncertainty and c_v to the variation coefficient.



Pull Tests Protocol

Study Description:

This protocol was established within the scope of a Biomedical Engineering Master Thesis aiming to develop a body-powered hand prosthesis with flexible materials by Additive Manufacturing. This study is taking place on NOVA School of Science and Technology in partnership with *Patient Innovation*.

The main goal of this study is to improve the cosmetic appearance of 3D-printed body-powered prostheses through the replacement of the stiff material that composes *e-NABLE* prostheses. This material will be replaced by a combination of rigid and flexible materials in order to give these prostheses a more real-life appearance.

For this purpose, it was necessary to determine the optimal materials combination as well as to analyse some of the existent prostheses. The identification of the user's needs is crucial to determine the prosthesis specifications and therefore create some concepts aiming to identify the best model to develop. Concerning concepts generation and selection, it was desired a high level of customization, especially regarding to the size of printed hand when compared to the sound hand. Establishing sensory feedback was also a concern.

Finally, as a result of the created concepts, several prototypes for testing and concept validation were designed, according to Product Design and Development methodology.



Data Collection Goals:

The present protocol describes the methodology for the pull tests used to evaluate the printed fingers in terms of force needed to bend each finger model.

The prosthesis development was divided into three main design stages. Fingers were the first components to be addressed as there were previous studies about them. During this stage, only the index was designed. After validating the index design, its design could be used in the other fingers. During this study, several different models were developed. However, only some of them were subjected to pull tests.

These tests had the goal of selecting the opening angle of the chambers that mimic the interphalangeal joints and lead to lower bending forces. Besides selecting the opening angle, these tests were also used to select the best printing parameters. During the design of the fingers, several printing tests were also performed in order to find the best printing quality. However, despite all efforts, it was quite difficult to determine the best printing parameters, which combine a good printing quality and low bending forces.

Thus, the main goal of this protocol is to determine which will be index model as the printing parameters which will be used, by measuring the necessary force to bend the fingers. Following this methodology allows to evaluate the fingers objectively, avoiding possible errors from a subjective assessment.



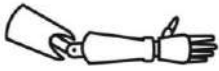
Methodology principle:

This protocol measures the force needed to bend each finger model. Metallic cylinders with different masses will be applied to the fingers, generating different forces and causing the finger to bend. Consequently, the fingertip suffers an approximately vertical displacement that is measured with a dial gauge. The measures stop when each finger bending reaches the desired displacement of 10 mm.

The dynamometer weight as well as the weight of the tissue bag used to place the weights will increase the applied force. Both the dynamometer and the tissue bag must be weighed, so the real applied force is known. This force is given by the following equation, where m_{bag} , m_{din} and m are the masses of the tissue bag, dynamometer and metallic cylinders, respectively, and g ; the gravitational constant:

$$W = (m_{bag} + m_{din} + m) \cdot g$$

However, it is expected that the W value and the value measured from the dynamometer do not present significant differences.



Methodology

The present protocol was developed considering the laboratory environment and conditions. Regarding the main goals of this protocol, the methodology does not need to be very strict or use expensive equipment.

The only requirement needed to test the fingers was an elevated structure where the fingers could be fixed, and its wire could be pulled vertically. For the present study, a support that can be fixed by screws to the available elevated structure was designed as well as an horizontal tab, so the contact point of the dial gauge was in contact with the tab fitted into the top of the dynamometer. The fingers are then fixed to a fitting hole. Figure 1 shows the 3D-printed designed support and the horizontal tab, also 3D-printed with PET.



Figure 1: Designed structures for the present protocol: (a) finger's support; (b) horizontal tab.



Development of a Body-powered Hand Prosthesis with Flexible Materials by Additive Manufacturing



Material:

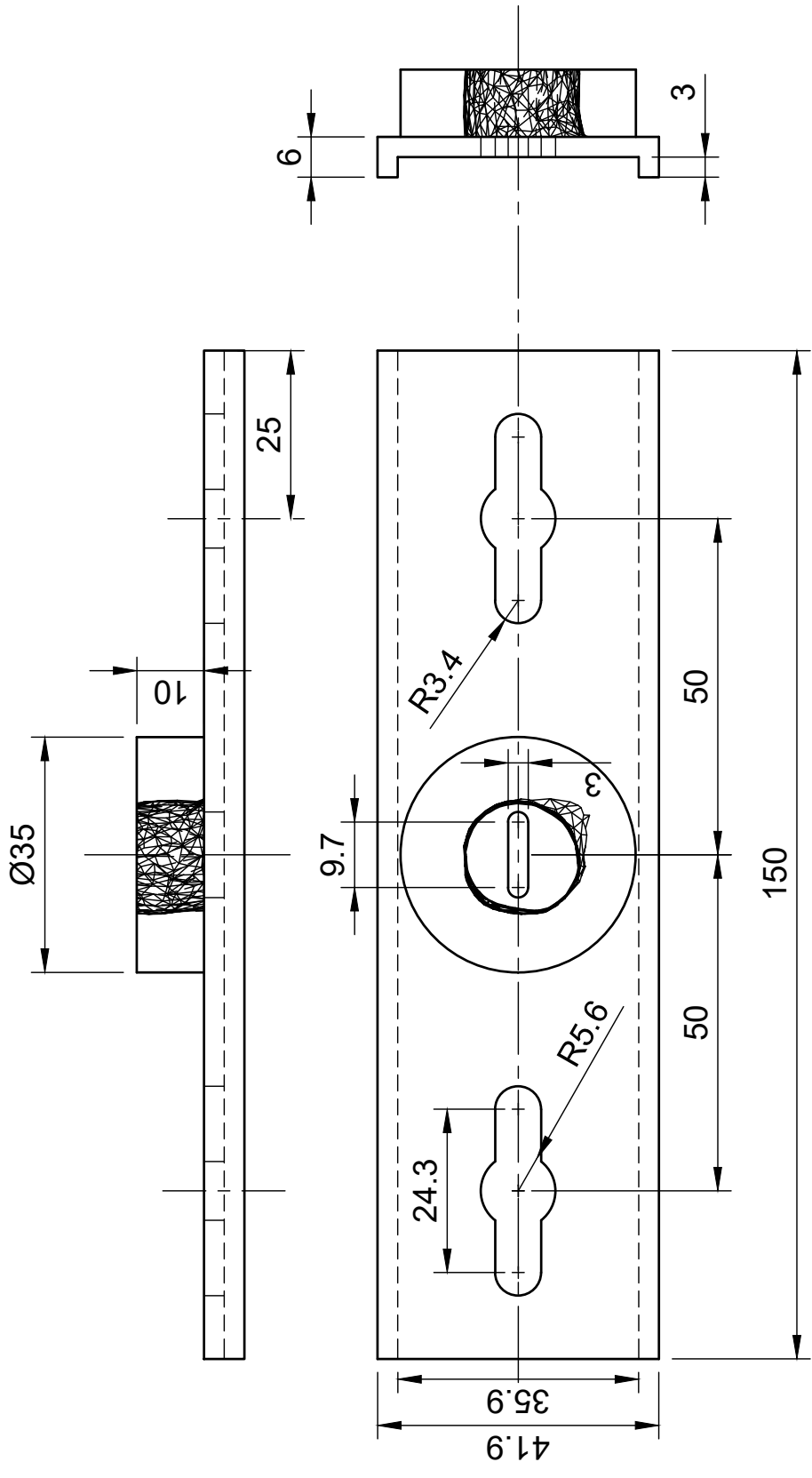
- Fingers support;
- Acoustic guitar strings, E and B (40 cm for each finger);
- 2 screws and respective nuts and washers;
- Small nuts;
- Dial gauge;
- Dynamometer;
- Light tissue bag;
- Pliers;
- Weights.

Procedures:

1. Weight the tissue's bag and dynamometer and register their values. Repeat this step two more times and calculate the mean value of their weights.
2. Fix the fingers' support to the elevated structure using the screws and the respective nuts. For this study M8×50 screws were used.
3. Pass the metal wire through the finger and lock it at the top by wrapping the wire's tip around the small nut with the pliers' help.
4. Insert the finger at the finger's support, making sure the wire passes through the support's hole.
5. Fix the horizontal tab at the top of the dynamometer.
6. Fix the dynamometer at the other end of the wire. If necessary, use the pliers once more.
7. Tie the tissue bag at the dynamometer's far end.
8. Fix the dial gauge at the elevated structure. Its pointer must be placed at its maximum displacement and simultaneously touching the horizontal tab. Make sure the dial gauge is calibrated.



9. Place the weights inside the tissues bag, starting at 400g and then adding 400g at a time. For the present study, the available metallic cylinders had masses between 100 and 800g. Higher mass values were obtained by combining cylinders. If between two values the finger reaches the maximum bending capacity, measure the medium value between the last two values.
10. Read the dynamometer's value as well as the marked value in the dial gauge for each added weight and register the read values. Repeat this step twice more.
11. When the finger reaches its maximum vertical displacement, stop adding weight.
12. Remove the tested finger and repeat steps 2 to 11 for the next finger to test.



Projectou	AM0	Dec. 2020
Desenhou		
Copiou		
Verificou		



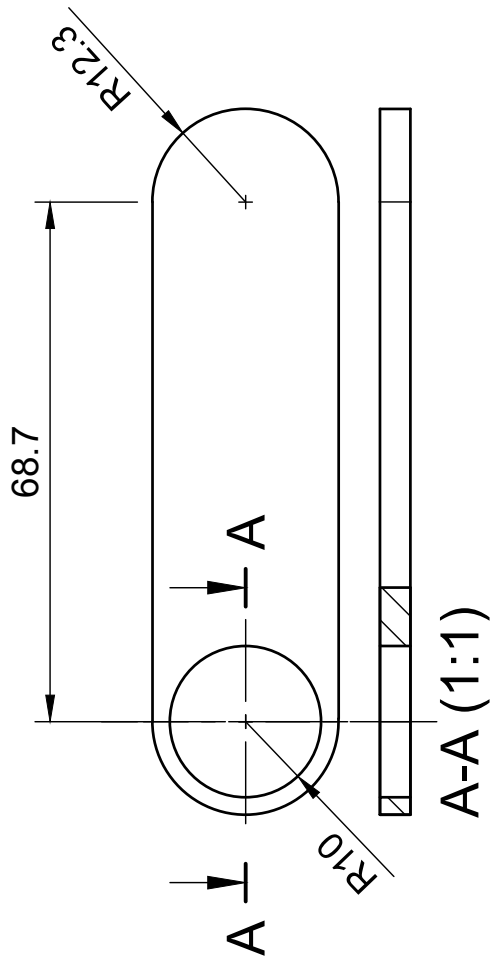
Ana Maria Oliveira

Biomedical Engineering

Finger's Support

1:1

ISO 2768
m-K



Projectou	AM0	Dec. 2020
Desenhou		
Copiou		
Verificou		



Ana Maria Oliveira

Biomedical Engineering

Horizontal Tab

1:1

ISO 2768
m-K

Table F.1: Pull tests results of the model with 55° chambers.

Force (N)	Measurements			Mean	u_c	c_v
	1st	2nd	3rd			
4	2.54	2.60	2.63	2.59	0.03	0.02
8	4.15	4.13	4.16	4.15	0.01	0.00
12	6.33	6.25	6.30	6.29	0.02	0.01
16	8.15	8.21	8.27	8.21	0.03	0.01
18	9.15	9.13	9.18	9.15	0.01	0.00

Table F.2: Pull tests results of the model with 60° chambers.

Force (N)	Measurements			Mean	u_c	c_v
	1st	2nd	3rd			
4	4.45	4.41	4.30	4.39	0.04	0.02
6	5.36	5.45	5.38	5.40	0.03	0.01
8	6.55	6.48	6.62	6.55	0.04	0.01
10	7.81	7.90	7.81	7.84	0.03	0.01
12	9.35	9.34	9.32	9.34	0.01	0.00

Table F.3: Pull tests results of the model with 65° chambers.

Force (N)	Measurements			Mean	u_c	c_v
	1st	2nd	3rd			
4	4.90	4.93	4.90	4.31	0.01	0.00
6	5.58	5.56	5.50	5.55	0.02	0.01
8	6.47	6.55	6.57	6.53	0.03	0.01
10	7.78	7.74	7.81	7.78	0.02	0.00
12	9.34	9.33	9.30	9.32	0.01	0.00

Table F.4: Pull tests results of the model printed with the set A parameters.

Force (N)	Measurements			Mean	u_c	c_v
	1st	2nd	3rd			
4	2.43	2.45	2.50	2.46	0.02	0.01
8	2.79	2.75	2.71	2.75	0.02	0.01
12	3.32	3.27	3.15	3.21	0.03	0.02
16	3.81	3.77	3.84	3.81	0.02	0.01
20	4.49	4.56	4.54	4.53	0.02	0.01
24	5.39	5.35	5.34	5.36	0.02	0.00

Table F.5: Pull tests results of the model printed with the set A1 parameters.

Force (N)	Measurements			Mean	u_c	c_v
	1st	2nd	3rd			
4	2.97	2.97	2.89	2.94	0.03	0.02
8	3.27	3.16	3.20	3.21	0.03	0.02
12	3.77	3.78	3.88	3.81	0.04	0.02
16	4.81	4.78	4.68	4.76	0.04	0.01
20	6.70	6.63	6.64	6.66	0.02	0.01
24	8.25	8.31	8.22	8.26	0.03	0.01

Table F.6: Pull tests results of the model printed with the set A2 parameters.

Force (N)	Measurements			Mean	u_c	c_v
	1st	2nd	3rd			
4	2.18	2.18	2.15	2.17	0.01	0.01
8	2.75	2.64	2.68	2.69	0.03	0.02
12	3.62	3.62	3.70	3.65	0.03	0.01
16	4.64	4.52	4.64	4.60	0.04	0.02
20	6.57	6.51	6.56	6.55	0.02	0.00
24	7.25	7.30	7.34	7.30	0.03	0.01

Table F.7: Pull tests results of the model printed with the set B parameters.

Force (N)	Measurements			Mean	u_c	c_v
	1st	2nd	3rd			
4	4.45	4.41	4.30	4.39	0.04	0.02
6	5.36	5.45	5.38	5.40	0.03	0.01
8	6.55	6.48	6.62	6.55	0.04	0.01
10	7.81	7.90	7.81	7.84	0.03	0.01
12	9.35	9.34	9.32	9.34	0.01	0.00

Table F.8: Pull tests results of the model printed with the set B1 parameters.

Force (N)	Measurements			Mean	u_c	c_v
	1st	2nd	3rd			
4	3.46	3.43	3.48	3.46	0.01	0.01
8	5.07	5.10	5.14	5.10	0.02	0.01
12	6.96	7.04	7.04	7.01	0.03	0.01
13	8.48	8.55	8.51	8.51	0.02	0.00
14	9.05	8.98	9.02	9.02	0.02	0.00

Table F.9: Pull tests results of the model printed with the set B2 parameters.

Force (N)	Measurements			Mean	u_c	c_v
	1st	2nd	3rd			
4	1.50	1.50	1.53	1.51	0.01	0.01
8	2.14	2.17	2.12	2.14	0.01	0.01
12	2.82	2.85	2.95	2.86	0.02	0.01
16	4.15	4.24	4.24	4.21	0.03	0.01
20	5.24	5.17	5.27	5.23	0.03	0.01
24	6.39	6.44	6.50	6.44	0.03	0.01

Table F.10: Pull tests results of the model printed with the set B3 parameters.

Force (N)	Measurements			Mean	u_c	c_v
	1st	2nd	3rd			
4	2.25	2.18	2.24	2.22	0.02	0.02
8	3.07	3.03	3.02	3.04	0.02	0.01
12	3.68	3.73	3.73	3.71	0.02	0.01
16	4.57	4.55	4.60	4.57	0.01	0.01
20	5.59	5.57	5.65	5.60	0.02	0.01
24	7.33	7.31	7.37	7.34	0.02	0.00

Table F.11: Pull tests results of the model printed with the set B4 parameters.

Force (N)	Measurements			Mean	u_c	c_v
	1st	2nd	3rd			
4	2.75	2.81	2.70	2.75	0.03	0.02
8	3.53	3.63	3.57	3.58	0.03	0.01
12	4.51	4.58	4.60	4.56	0.03	0.01
16	5.40	5.34	5.43	5.39	0.03	0.01
20	7.04	6.96	7.07	7.02	0.03	0.01
24	8.25	8.18	8.18	8.20	0.02	0.00

Table F.12: Pull tests results of the model printed with the set B5 parameters.

Force (N)	Measurements			Mean	u_c	c_v
	1st	2nd	3rd			
4	1.99	1.91	1.91	1.94	0.03	0.02
8	2.61	2.56	2.50	2.56	0.03	0.02
12	3.25	3.27	3.32	3.31	0.03	0.01
16	4.20	4.17	4.20	4.19	0.01	0.00
20	5.17	5.26	5.20	5.21	0.03	0.01
24	5.92	5.89	5.90	5.90	0.01	0.00

Table F.13: Pull tests results of the model printed with the set B6 parameters.

Force (N)	Measurements			Mean	u_c	c_v
	1st	2nd	3rd			
4	2.79	2.75	2.84	2.79	0.03	0.02
8	3.19	3.19	3.18	3.19	0.00	0.00
12	4.29	4.26	4.33	4.29	0.02	0.01
16	5.40	5.32	5.30	5.34	0.03	0.01
20	6.00	6.32	6.20	6.17	0.09	0.03
24	7.20	7.35	7.35	7.30	0.05	0.01

Table F.14: Pull tests results of the model printed with *Filaflex 70A* and the set A parameters.

Force (N)	Measurements			Mean	u_c	c_v
	1st	2nd	3rd			
4	4.40	4.42	4.45	4.42	0.01	0.01
8	5.85	5.80	5.83	5.83	0.01	0.00
12	7.05	7.10	7.00	7.05	0.03	0.01
13	7.80	7.75	7.77	7.77	0.01	0.00
14	8.25	8.15	8.08	8.16	0.05	0.01

Table F.15: Pull tests results of the model printed with *Filaflex 70A* and the set B parameters.

Force (N)	Measurements			Mean	u_c	c_v
	1st	2nd	3rd			
3	4.50	4.35	4.46	4.44	0.04	0.02
4	5.60	5.62	5.70	5.64	0.03	0.01
6	6.50	6.30	6.44	6.41	0.06	0.02
7	7.35	7.45	7.60	7.47	0.07	0.02
8	8.55	8.85	8.68	8.69	0.09	0.02

PROSTHESES COSTS

The present appendix presents the discriminated cost of the developed prostheses' material. The total values include the cost of all the components needed to construct the prostheses, including the printing supports. The costs of all prototypes made during the present study were not considered. Tables G.1 and G.2 present the costs of the first, second and third prostheses, respectively.

Table G.1: Discriminated cost of the first and second prostheses

Components	Quantity	Unit	Cost (€)
<i>Filaflex</i>	97.10		0.69
PLA	30.74	g	1.53
PET-G	0.08		0.00
Velcro	0.22		0.51
Grosgrain ribbons	0.40	m	0.32
Guitar strings	2		1.10
Screws	5	u.a.	0.08
Adhesive foam	1		0.75
		Total	12.65

Table G.2: Discriminated third prosthesis.

Components	Quantity	Unit	Cost (€)
<i>Filaflex</i>	41.98		3.85
PLA	88.24	g	1.94
PET-G	0.08		0.00
Velcro	0.22		0.51
Grosgrain ribbons	0.4	m	0.32
Guitar strings	2		1.10
Screws	3	u.a.	0.3
Adhesive foam	1		0.75
		Total	8.77

SYSTEM USABILITY SCALE

The following document presents the surveys that were used to obtain the feedback of the child and his family, as well as the corresponding results.



System Usability Scale

Study Description:

This survey is being applied within the scope of a Biomedical Engineering Master Thesis aiming to develop a body-powered hand prosthesis with flexible materials by Additive Manufacturing. This study is taking place on NOVA School of Science and Technology in partnership with *Patient Innovation*.

The main goal of this study was to improve the cosmetic appearance of 3D-printed body-powered prostheses through the replacement of the stiff material that composes *e-NABLE* prostheses. This material was replaced by a combination of rigid and flexible materials in order to give these prostheses a more real-life appearance.

For this purpose, it was necessary to determine the optimal materials combination as well as to analyse some of the existent prostheses. The identification of the user's needs was crucial to determine the prosthesis specifications and therefore create some concepts aiming to identify the best model to develop. Concerning concepts generation and selection, it was desired a high level of customization, especially regarding to the size of printed hand when compared to the sound hand. Establishing sensory feedback was also a concern.

Finally, as a result of the created concepts, several prototypes for testing and concept validation were designed, according to Product Design and Development methodology.



Data Collection Goals:

The prosthetic device developed during this study was based on a single clinical case, a child selected from the *Patient Innovation* program “*Dar a mão*” in order to simplify the course of this research. However, this survey may be applied to other patients with similar lesions in further studies with a similar methodology.

The present survey has the main goal of evaluating the usability of the prosthesis developed during this study, whereby it is pretended to obtain the feedback of the child and his family. Additionally, the prosthesis functionality as well as their aesthetic appearance, the production costs, weight and the total printing time will also be evaluated.

Thus, in order to assess the level of satisfaction of the child and family, it will be used a survey with an usability scale, the *System Usability Scale* (SUS). This is a standard tool that allows to measure the usability of a wide variety of products or even services. It is composed by ten questions with five response options that goes from “Strongly agree” to “Strongly disagree”, which correspond to 5 and 1 scores, respectively. These responses are then converted to a score that will correspond to the evaluation of the child and family in terms of usability.

Finally, an additional survey with ten questions that follow the SUS logic will be presented. However, those questions were adapted to the features of the designed prosthesis, which can be used in further identical studies.



System Usability Scale

1 – Strongly disagree | 5 – Strongly agree

1. I think that I would like to use this device frequently.

				×
1	2	3	4	5

2. I found the device unnecessarily complex.

×				
1	2	3	4	5

3. I thought the device was easy to use.

				×
1	2	3	4	5

4. I think that I would need the support of a technical person to be able to use this device.

×				
1	2	3	4	5

5. I found the various functions in this device were well integrated.

				×
1	2	3	4	5

6. I thought there was too much inconsistency in this system.

×				
1	2	3	4	5

7. I would imagine that most people would learn to use this system very quickly.

			×	
1	2	3	4	5

8. I found the system very cumbersome to use.

×				
1	2	3	4	5

9. I felt very confident using the system.

				×
1	2	3	4	5

10. I needed to learn a lot of things before I could get going with this system.

×				
---	--	--	--	--



Additional Questions

1 – Strongly disagree | 5 – Strongly agree

1. I found the aesthetic appearance of the prosthesis appealing to its daily use.

				×
--	--	--	--	---

1 2 3 4 5

2. The prosthesis is quite similar to a toy.

×				
---	--	--	--	--

1 2 3 4 5

3. The prosthesis is quite similar, in aesthetical terms, to a human hand.

				×
--	--	--	--	---

1 2 3 4 5

4. I think that the prosthesis is easily breakable.

×				
---	--	--	--	--

1 2 3 4 5

5. I think that the fitting of the prosthesis is very intuitive.

				×
--	--	--	--	---

1 2 3 4 5

6. I think that the fitting of the prosthesis is uncomfortable.

×				
---	--	--	--	--

1 2 3 4 5

7. I found the prosthesis' operating mode complicated.

			×	
--	--	--	---	--

1 2 3 4 5

8. I found the system very cumbersome to use.

×				
---	--	--	--	--

1 2 3 4 5

9. I think that the prosthesis would be a good complement for the daily living activities.

				×
--	--	--	--	---

1 2 3 4 5

10. This prosthesis might consist of a restriction for the daily living activities.

×				
---	--	--	--	--

